Delayed gadolinium-enhanced magnetic resonance imaging and T2 mapping of cartilage of the distal metacarpus3/metatarsus3 of the normal Thoroughbred horse

by

Ann Carstens

BVSc, University of Pretoria, RSA
MS(Vet Physiol) Texas A&M University, USA
MMedVet(Chir), University of Pretoria, RSA
MMedVet(Diag Im), University of Pretoria, RSA

Submitted in fulfilment of the requirements for the degree of Doctor of Philosophy in the Faculty of Veterinary Science, University of Pretoria

Pretoria, July 2013

DECLARATION

I, Ann Carstens, do hereby declare that this thesis, which I hereby submit for the degree Doctor of Philosophy at the University of Pretoria, is my own work and has not previously been submitted by me for a degree at this or any other institution.

The published articles within are submitted with the permission of the copyright holders of the publications.

Signed this day of in the year of our Lord

Ann Carstens

SUPERVISOR

Dr Eveliina Lammentausta, PhD

Department of Diagnostic Radiology

Oulu University Hospital

Oulu, Finland

and

Joint and Soft Tissue Unit

Department of Clinical Sciences, Malmö

University of Lund

Lund, Sweden

CO-SUPERVISORS

Prof Robert M Kirberger, BVSc, MMedVet(Rad)

Diagnostic Imaging Section

Department of Companion Animal Clinical Studies

Faculty of Veterinary Science

University of Pretoria, Pretoria, South Africa

Prof Leif E Dahlberg, MD, PhD

Head of Department of Orthopaedics

Clinical Sciences, Lund

Lund University

Skåne University Hospital

SE-221 85 Lund, SWEDEN

to John

Wisdom is the principle thing, therefore get wisdom and with all thy getting get understanding

Prov.4:7

ACKNOWLEDGEMENTS

Thank you to Eveliina Lammentausta, my promoter, for bearing with me for the past 4 years, for your insight, advice and patience in assisting me to tackle this project – it was a case of my jumping in “where angels fear to tread!”

Robert Kirberger was the “man-behind-the-scenes” co-promoter. Without his encouragement and organisational expertise this project would have taken longer and may possibly not even have seen the light of day. Thank you Rob.

I first heard of dGEMRIC at a congress of the European Association of Veterinary Diagnostic imaging in Svolvaer, Norway in 2008, where the keynote address describing dGEMRIC was presented by Leif Dahlberg. I am grateful to him for introducing this fascinating technique to me, giving the flash of inspiration that triggered this project and treating me with such hospitality on my visits to Sweden. Carl Tiderius, thank you for a lovely evening in your home.

Lizelle Fletcher, a co-author, thanks for keeping tabs on me, so that our stats could be above reproach. Joyce Jordaan, the ever patient, non-wearying data analyst, who unerringly ran “yet another” SPSS or SAS run for me. Thank you for your open door and positive encouragement every time something went wrong.

Thanks to Mark Velleman, a co-author, who opened the doors of the Pretoria MR trust of the Faery Glen Hospital and provided the scans free of charge even though this was a veterinary project, and for supporting me the few times things got a bit hot!

Radiography sisters Annetjie Bester, Alma Halberg, Isabel Martin and Sumari Torentina, from the Pretoria MR trust; your willingness and professionality were very much appreciated. The radiography sisters Beverley Olivier, Melanie McClean and Lizette Neethling, from the Onderstepoort Veterinary Academic Hospital, who did the radiography and helped with the CT on the 48 plus limbs! Thank you.

Antoinette Lourens who always assisted at the drop of a hat, Estelle Mayhew who repeatedly changed figures into tiff format and Petro Bester, for the detailed editing and appearance of the manuscript. Thank you!

The entire staff of the Highveld Horsecare Unit, but particularly Nadia who did the logistics and helped with the clinical examinations of the horses, and Johan, who had the unenviable task of shooting the horses. Thank you also to the grooms who helped with the handling of the horses and the amputation of the specimens. Beverley Seaborne, thank you for allowing me to utilize the horses!

Dave and Lilly Hughes, and Oom Ben du Toit of the Randfontein abattoir, providing me, and helping me with the specimens to perform the pilot studies! It was good to meet you and work with you.

Leon Prozesky, a co-author, thank you for your advice and assistance and the use of the post mortem facilities as well as the no-cost histological slides! A big thank you to all the staff in the Pathology section, Department of Paraclinical Sciences, Faculty of Veterinary Science, particularly Peter and Joey, for the assistance in preparation of the histological slides and teaching me how to section cartilage and bone.

Prof Sybrand van den Berg whose lecture on lameness in 1980 inspired me to become a surgeon and from there on a radiologist. He was my mentor.

Johan Schoeman, head of the Department of Companion Animal Clinical Studies for fascilitating and approving my study leave, without which I would not have even embarked on this project. I am very grateful to the University of Pretoria Veterinary Faculty Research Fund, the Department of Companion Animal Clinical Studies, and for Prof RM Kirberger's National Research Foundation of South Africa fund for financing the bulk of the research costs.

My ouers, dankie dat julle met liefde alles ondersteun het wat ek aangepak het.

John, vir jou liefde, geduld en ondersteuning. Dis nou verby. Die naweke en aande is weer ons s'n!

Jesus Christus. Vir alles.

LIST OF ABBREVIATIONS

BC	distance between articular cartilage surface and bone-cartilage interface
FOV	field of view
dGEMRIC	delayed Gadolinium Enhanced Magnetic Resonance Imaging of Cartilage
FCD	Fixed Charge Density
FT	Friedman test: non-parametric statistical test for dependent variables
Gd-DTPA^{2-}	Gadolinium contrast agent, N- methylglucamine salt of the gadolinium complex of diethylenetriamine pentaacetic acid
GrA	Group A – control horses
GrBchill	Group B – limbs chilled
GrBfrozen	Group B – limbs frozen
Hz	Hertz
IR	inversion recovery
ICC	intraclass correlation coefficient
K-W	Kruskall-Wallis test: non-parametric statistical test for independent variables
M-W	Mann-Whitney test: non-parametric statistical test for independent variables
Mc3	metacarpus3
MRI	Magnetic Resonance Imaging
mmol	millimol
ms	millisecond/s
Mt3	metatarsus3
OARSI	OsteoArthritis Research Society International
OVAH	Onderstepoort Veterinary Academic Hospital
pix	pixel
PDw	Proton Density weighted
ROI	Region Of Interest
S	site
SD	standard deviation
STIR	short tau inversion recovery
T	Tesla
T1	spin-lattice relaxation time
T2	spin-spin relaxation time
T2*	T2 star relaxation time
TI	inversion recovery time
TE	time to echo
TM	tide mark: distance between articular cartilage surface and mineralized cartilage interface
TR	time to repeat
TSE	turbo spin echo
W-SRT	Wilcoxon signed rank test: non-parametric statistical test for dependent variables
α	level of significance

TABLE OF CONTENTS

LIST OF FIGURES

LIST OF TABLES

SUMMARY

Osteoarthritis of the metacarpo/metatarsophalangeal joint is a major cause of lameness in the horse. Magnetic resonance imaging and particularly delayed gadolinium enhanced imaging of cartilage (dGEMRIC) and T2 cartilage mapping in humans has been shown to visualize cartilage matrix changes in osteoarthritis early in the disease process. T2 mapping is a non-invasive technique characterizing hyaline articular cartilage and repair tissue. In dGEMRIC, the negatively charged administered Gd-DTPA^{2-}, penetrates hyaline cartilage in an inverse relationship to the proteoglycan concentration thereof. In osteoarthritis, proteoglycan concentration is decreased with increased penetration of Gd-DTPA^{2-} due to a relative decrease in negative charge of the proteoglycan-depleted cartilage.

This study was performed on normal cadaver limbs of twelve euthanized racing Thoroughbreds. Six horses' midcondylar distal third metacarpals/metatarsals (Mc3s/Mt3s) underwent six precontrast inversion recovery (IR) sequences for dGEMRIC T1 relaxation time calculation, as well as T2 mapping sequences using a 1.5T machine. Gd-DTPA^{2-} was injected intra-articularly and the same six IR sequences repeated at 30, 60, 120, and 180 minutes post-injection at the same midcondylar sites. The distal Mc3/Mt3 cartilage thickness was measured histologically and compared to selected images of the T1 and T2 weighted sequences. T1 and T2 maps were created by fitting the respective data into mono-exponential relaxation equations for each pixel, and mean values of certain regions of interest were calculated. A second group of six horses' fore and hind limbs were randomly assigned to two groups and the limbs either chilled or frozen, allowed to return to room temperature and scanned similarly to the first control group. Chilling and freezing effects on dGEMRIC and T2 mapping results were evaluated.

The main conclusions from this study are that IR and proton density weighted (T2 mapping) sequences can measure distal Mc3/Mt3 cartilage thickness where the cartilage doesn't overlap with that of the proximal phalanx. However, accurate measurement was hampered by the thin cartilage in this region. dGEMRIC mapping, using intra-articular Gd-DTPA^{2-} is a

feasible technique and T1 relaxation times decrease in a similar fashion to that of the human, with the optimal time of scanning after intra-articular Gd-DTPA^{2-} injection being 60-120 minutes. There is little effect on T1 or T2 relaxation time and mapping images after chilling and freezing of the limbs except where the magic angle effect predominates in the T2 mapping sequences.

Limitations of this study include relatively coarse spatial resolution of the thin cartilage, the overlap of the distal Mc3/Mt3 cartilage with the adjacent phalanx and the relatively low number of limbs used, resulting in low statistical power, particularly in the frozen limbs' study. In spite of these limitations, this study provides technical information and reference values of dGEMRIC and T2 mapping in the cadaver distal Mc3/Mt3 of the normal Thoroughbred horse of value for forthcoming studies.

Future studies need to evaluate intravenous administration of Gd-DTPA^{2-} and cartilage mapping in live exercised *vs.* non-exercised horses. Ultimately, dGEMRIC and T2 mapping of horse metacarpo/metatarso-phalangeal joints with differing degrees of osteoarthritis should be used to attempt to diagnose early cartilage degeneration to endeavour to halt or delay its progression.

CHAPTER 1

GENERAL INTRODUCTION

Osteoarthritis in the horse is one of the major causes of lameness, and is particularly common in the metacarpo/metatarsophalangeal (fetlock) joint. Clinical hands-on evaluation with additional perineural and intra-articular local anaesthesia usually results in localization of the cause of pain. Diagnostic imaging and particularly radiography and ultrasonography have been the mainstay of the next step in confirming the cause of lameness until a few decades ago. Computed tomography and scintigraphy have added great additional diagnostic value in the past twenty years and more recently magnetic resonance imaging (MRI). Since cartilage degeneration does not always result in pain or lameness *per se* it is important to use modalities that can identify early cartilage and bone injury to address the condition before it has progressed into irreversible matrix damage.

Magnetic resonance imaging has changed the face of musculoskeletal imaging in humans and in horses in the past twenty years. Daily, MRI sequences and sophisticated physiological MRI tests are adapted to visualize increasing detail of bones, joints, ligaments and tendons. Higher field magnets are also available enabling even higher imaging resolution.

Although there is much funding available in many equine disciplines, the use of MRI in diagnosing horse lameness is limited to the larger practices and institutions and even then, the far greater knowledge and research in MRI is nearly limited to man. It is in the best interests of the equine world that osteoarthritis research focussing on lameness remains a priority. The pathophysiology of osteoarthritis in the fetlock joint is currently the focus of much research with cartilage, subchondral bone, biomechanics of the joint, and biomarkers being the most topical. It is still debatable whether subchondral bone injury precedes cartilage injury or *vice versa*, or if changes occur simultaneously, and what the interaction between these tissues are to ultimately result in degeneration of the joint.

Magnetic resonance imaging has been used to evaluate most articular and peri-articular structures both of normal and osteoarthritic joints, with certain sequences having being identified to be superior to others for specific tissues and injuries. MRI utilizing mapping techniques such as T2 and delayed gadolinium enhanced magnetic resonance imaging of cartilage (dGEMRIC) has been shown to be a reliable indicator of early cartilage degeneration and osteoarthritis in human and animal models. If this type of information can be made available early in the life of the equine athlete, attempts can be made to decrease the progression of the disease, thereby resulting in less pain and morbidity, increased athletic abilities and prolongation of the horse's career. This should also result in decreased loss of earnings and more confidence in the equine industry.

The two most common MRI machines currently in use in equine veterinary medicine are the standing low-field units and the 1.5T machine that requires the animal to be under general anaesthesia. The current standing unit can detect cartilage lesions in fetlock joints, but has the disadvantage of long acquisition times and movement artefacts since the horse is awake and tends to sway even though sedated. The resolution needed for adequate signal information in dGEMRIC may make the use of the standing machine less desirable but this still needs to be determined.

The 1.5T unit has decidedly superior resolution, but is more costly and requires more maintenance. A few equine veterinary institutions have 3T machines with even better resolution, but it is unlikely that use of this machine will become the norm in the nearby future. The question arises, whether the owner of the superior equine athlete will allow his/her animal to be placed under general anaesthesia, although complications with general anaesthesia for elective procedures are very low. Another solution would be to use a high field standing unit with relatively fast scanning sequences and optimal software to minimize movement artefacts. The condition of the horse's joint cartilage could be assessed with standard MRI sequences and mapping techniques, appropriate therapy instigated and progression of the condition and/or effect of the therapy monitored in the same way. It is highly unlikely, however, to be available for the equine world in the foreseeable future.

This study lays the foundation of T2 and dGEMRIC mapping in the cadaver equine fetlock joint. Studies building on this need to evaluate intravenous administration of Gd-DTPA^{2-} and cartilage mapping in live exercised *vs.* non-exercised horses. Ultimately, horse metacarpo/metatarso-phalangeal joints with differing degrees of osteoarthritis should be evaluated using these techniques. It is hoped that findings will result in earlier diagnosis of the disease and ultimately a healthier horse.

CHAPTER 2

LITERATURE REVIEW

The horse is utilized for multiple disciplines in the modern world, both for recreational and working purposes. When it is unable perform, emotional and financial implications arise. [1] Lameness is the primary cause of poor performance in horses, [2-7] with the most common source of lameness being the distal limb. [6, 8-13] Since racing is a large source of internal revenue and employment in many countries, lameness in the Thoroughbred race horse is often studied. Twenty five percent of racing Thoroughbreds experience metacarpo/metatarsophalangeal joint pain, [6] with this joint being the most commonly affected by traumatic and degenerative lesions of the appendicular skeleton, often referred to as overload arthrosis, resulting in osteoarthritis. [7, 9, 14-17]

Lesions in the articular cartilage generally show no signs of pain due to the lack of nociceptive receptors, with osteoarthritic pain thought to be caused by intra-articular factors released from the synovium or bone and other associated structures. [18] This implies that cartilage damage can and does progress while no clinical signs such as lameness are yet apparent. [19] For this reason it is important to find modalities which can identify early cartilage damage enabling timeous therapy to be instigated. It has been suggested that early diagnosis of pre-osteoarthritic conditions could improve outcome and reduce disability in humans and that pre-osteoarthritis indeed is a modifiable disease process. [20]

Two thirds of adult human articular cartilage by dry weight is collagen, [21] of which the majority is type II collagen, as well as types III, IX, X, XI. The articular hyaline cartilage collagen fibrils, overlying the subchondral bone are organized into a structural framework important for normal cartilage biomechanics. The collagen fibres adjacent to the subchondral bone are arranged perpendicularly to the joint surface (70-90% of the total thickness), the intermediate layer randomly arranged (1-15% of the total cartilage thickness) and the most superficial layer parallel to the joint surface (5-15% of

the cartilage thickness). [22] Between this framework of fibrils are interposed proteoglycans, of which, in normal articular cartilage, the content is higher in the deeper layer decreasing superficially.

Proteoglycans are mainly composed of a central core protein with multiple glycosylated side chains, primarily keratin sulfate and chondroitin sulfate. Aggrecan, secreted from the chondrocyte, binds to hyaluronan to form large proteoglycan aggregates. The negatively charged proteoglycan aggregates exhibiting a fixed charge density (FCD), bind positively charged cations, mostly sodium, which increases the osmolarity of the extracellular matrix, causing water to be drawn into the cartilage and the hydrated proteoglycan to swell. This swelling is constrained because of the intermingled collagen framework, thus putting this network under tension and giving the cartilage its compressive stiffness, vital for normal cartilage function. [23]

The articular cartilage consists of four functionally and structurally divided zones, namely the zone of calcified cartilage, the deep zone, the middle or transitional (radial) zone and the superficial (articular or tangential) zone. [23] This stratification is well visualized on T2 mapping images of normal human cartilage and correlates well with histological zones, where the shorter T2 relaxation values are in the radial zone, due to the highly organized radially orientated fibrils resulting in increased internuclear dipolar relaxations and relative restriction of water motion. The longer T2 relaxation values in the transitional zone are as result of the more haphazard organization of collagen. [24, 25] Clinically this has also been utilized in humans. [26] This typical visible layered pattern with increasing T2 values from the subchondral bone to the articular surface, has been seen in the distal femur of the horse. [27] The T2 measurement technique has been reported to show good intra- and inter repeatability in human articular cartilage [28-30] and is likely to be the same in the horse. It has been shown that T2 values are sensitive to mechanical cartilage stress in humans. [31] A 0.65 mm decrease in cartilage thickness has been seen in weight-bearing cartilage, [32] and signal intensity of superficial cartilage layers is decreased with increasing levels of compression. [33] Another report specifically ascribes the increase in signal intensity in T2 mapped cartilage of humeral femoral condyles to cartilage compression. [34] The

typical mean T2 values for different ROIs of human cartilage is between 15 and 60 ms, varying slightly with the magnetic field strength used, [35] and can vary up to between 10 and 80 ms.

The mechanical properties of cartilage have been assessed by means of quantitative magnetic resonance imaging (MRI). These techniques could be used to identify biomechanical changes in cartilage undergoing early degenerative changes. The orientation and amount of collagen fibrils can be illustrated by means of T2 relaxation times, [24, 36, 37] and has been suggested to be a possible marker for acute and chronic osteoarthritis. [38] Delayed gadolinium enhanced MRI of cartilage (dGEMRIC) has been shown to be able to predict a high percentage of the variation in the ability of articular cartilage to bear load [39] as well as to reflect spatial changes in cartilage proteoglycan concentration. [40] Both T2 and dGEMRIC may therefore be able to shed more light on the biomechanical properties of articular cartilage. [37]

Osteoarthritis (or degenerative joint disease) is a chronic degenerative disease characterized by a degeneration of articular cartilage, subchondral bone loss and or thickening, and soft tissue changes in the synovium. Matrix fibrillation, fissure appearance, gross ulceration and full thickness loss of the cartilage occurs. The synovial membrane is also often affected. [41] The progression of the disease in humans is generally divided into three phases. Stage 1 is defined as proteolytic breakdown of the cartilage matrix, followed by Stage 2 where fibrillation and erosion of the cartilage surface occurs accompanied by the release of cartilage breakdown products into the synovial fluid. This is followed by Stage 3 where synovitis occurs, the synoviocytes phagocytose these breakdown products and proteases and pro-inflammatory cytokines are produced. The activity of proteases, such as metalloproteases, collagenase, stromelysin, aggrecanase and other inflammatory products such as plasminogen activator, plasmin and cathepsin B, cytokines, interleukin-1β and tissue necrosis factor-β, interacting with one another, result in a cascade of events ultimately resulting in collagen degradation which is an irreversible step in osteoarthritis. [41] Disruption of the proteoglycans may lead to swelling as result of increased oncotic pressure, followed by the loss of the degraded proteoglycans and therefore loss of cartilage volume. [42]

Subchondral bone, which absorbs stress and maintains joint shape,

shows a variation of density and thickness across the joint surface. [43] Subchondral bone changes in osteoarthritis have been postulated to have three different mechanisms, namely excessive bone deposition leading to a stiffer more brittle bone, secondly excessive bone resorption leading to bone weakening and thirdly, reactivation of the ossification at the tidemark resulting in thinning of the cartilage. [44-46] Excessive stress may result in buckling of the trabeculae which may result in microdamage. In this respect it is important to remember that impaired biomechanical cartilage properties, e.g. by glycosaminoglycan loss, may alter subchondral bone load and trigger bone changes. Adaptation remodelling of the distal Mc3/Mt3 occurs to strengthen the bone which becomes denser. [47, 48] Overload arthrosis in the palmar region of the distal Mc3 condyle has been reported to result in "subchondral bone sclerosis, devitalization and mechanical failure leading to collapse of the overlying cartilage". [15] It is still not known whether osteoarthritis starts in the cartilage, in the subchondral bone or whether the changes occur simultaneously as well as when the changes become pathological and/or irreversible. [43] Subchondral osteophytes have also been reported in the horse metacarpo/metatarsophalangeal joints. [49]

In an *in vitro* study of horse metacarpo/metatarsophalangeal joints, utilizing a cartilage degradation index technique, it was found that initial cartilage degeneration tends to commence at the dorsal articular margin of proximal phalanx one. In the metacarpophalangeal joint this then spreads to the central and palmar parts of proximal articular cartilage of phalanx one, whereas in the metatarsophalangeal joint the most degeneration occurs in the plantar aspect of proximal phalanx one and much less so centrally, indicating differences in biokinematics between fore- and hindlimb fetlock joints. [50] It has been reported that cartilage from the palmar aspect of joints with osteoarthritis had the highest histological scores of osteoarthritic sites. [51]

The causes of osteoarthritis in the metacarpo/metatarsophalangeal joints are multifactorial, including conformation, type of athletic discipline, rate of training, nature of the ground surface, genetic predisposition, fatigue, and others. [52] Biomechanical factors are believed to be of importance and the high succeptibility to injury has been related to the relatively small surface area, large range of motion and the high impact of full body mass during the weight-

bearing phase. [16] Common sites for injury in the fetlock joint are the proximodorsal phalanx one (osteochondral fragments), palmar/plantar metacarpal/metatarsal condyles with "wear-lines" across the opposing condylar surfaces, often with associated maladaptive bone remodelling and sclerosis, [53] the sagittal ridge of the distal metacarpus/metatarsus (osteochondritis dissecans) and the distal metacarpal/metatarsal and proximal phalanx one condyles (degenerative joint disease and osteochondritis dissecans). [54]

The use of MRI in equine arthrology and lameness has been reported and researched quite extensively in the past years, [55-96] and has been hailed as the gold standard for soft tissue evaluation of joints and associated tendons and ligaments. [19]

In a recent study evaluating the reliability of high-(1.5T) and low-field standing (0.27T) MRI systems to detect cartilage and bone changes in horse cadaver fetlocks with pain localised to the fetlocks, T1-weighted spoiled gradient echo, T2*-weighted gradient echo and STIR sequences (high-field) and T1-weighted gradient echo, T2*-weighted gradient echo, T2 –weighted-fast spin echo and STIR (low-field) sequences were acquired. [97] The authors concluded that all the pulse sequences showed high sensitivity for detection of subchondral bone lesions and moderate sensitivity for the detection of trabecular lesions. Cartilage lesions were well-detected by high-field T2*-weighted gradient echo and low-field T2-weighted fast spin echo sequences, but the chance of false positive results of detecting cartilage lesions was high in both high- and low-field MRI units, and moderate for detecting subchondral bone pathology. [97] There is therefore a place to investigate other MRI techniques such as dGEMRIC and T2 mapping to determine the presence of early cartilage damage possibly even earlier than when using non-mapping MRI techniques. To simultaneously evaluate the condition of the subchondral and trabecular bone would also add value to the understanding of the pathogenesis of the disease.

T2-weighted sequences, which are sensitive to tissue hydration, due to its strong influence on T2 relaxation, provide good tissue contrast. [98] Generally subchondral bone and ligamentous and tendinous structures are hypo-intense and cartilage, synovial fluid and fat are relatively hyperintense.

Early degradative changes in the extracellular matrix affect tissue hydration, by increasing overall water content via osmosis and by increasing mobility of water. T2 relaxation time has been shown to be inversely correlated with collagen concentration and the integrity of the collagen network [99, 100] and mechanical properties of articular cartilage. [38, 101] Clinically, T2 relaxation time has been shown to be inversely correlated to cartilage volume and thickness and with severity of the disease. [102] Degradation of the cartilage matrix, can be seen with T2-weighted images as clefts and fibrillation. [42] Focal areas of increased T2 correspond to arthroscopically visualized cartilage lesions. [103]

When cartilage is damaged or degraded, T2 relaxation time increases. [102, 104, 105] This is mostly due to disintegration of the collagen network, [35, 102] but also due to an increase in free extracellular fluid, [106, 107] and to a lesser extent due to a loss of proteoglycans [105] and has also been postulated to be as result of a combination of changes in cartilage molecular conformation. [106]

In T1-weighted sequences, generally cartilage, subchondral bone and ligamentous and tendinous structures are hypo-intense and fat relatively hyperintense. However, in T1-weighted contrast-enhanced sequences all structures containing contrast are hyperintense. T1 relaxation time without gadolinium has been shown to correlate with water content of the cartilage. [108]

Magnetic resonance imaging including the use of the contrast agent gadolinium (Gd-DTPA^{2-}) has been used in human studies to visualize cartilage damage and osteoarthritis early in the disease process. [109-114]

A quantitative method of evaluating the cartilage entails parametric mapping of cartilage utilizing post-processing of the images to give relaxation time-associated colour-maps that provide a visual interpretation of the specific area's relaxation times. This has been described in T2, T2*, T1rho, delayed gadolinium enhancement of MR in cartilage and other techniques. [42, 103, 115-119] T2 mapping is a non-invasive technique that can characterize collagen network and water content of hyaline articular cartilage and repair tissue. [98] In dGEMRIC, the negatively charged Gd-DTPA^{2-}, injected either intra-articularly or intravenously, penetrates hyaline cartilage in an inverse relationship to the proteoglycan concentration of the cartilage. This takes a while to occur, in contrast to normal arthrography where the contrast is immediately visible within the joint, *ergo* "delayed". dGEMRIC in humans is optimally evaluated

between 30 and 100 mins. [120] When proteoglycan concentration is decreased due to cartilage degradation, as seen in osteoarthritis, the penetration of Gd-DTPA^{2-} is increased due to a relative decrease in negative charge of the proteoglycan-depleted cartilage. Delayed gadolinium enhanced MRI of cartilage has been shown to be an excellent indicator of early degenerative cartilaginous changes in humans. [113]

To create a relaxation time map, several images are acquired by varying only a certain sequence parameter, characterizing each relaxation time behaviour. The sequence parameter modulating signal intensity is inversion time (TI) for T1 mapping (dGEMRIC), and time to echo (TE) for T2 mapping. The change of image intensity as a function of this sequence parameter is fitted pixel by pixel into mono-exponential relaxation equations. Results of these calculations yield a relaxation time value for each pixel. The characterization of smaller regions of the articulating surfaces using T2 and dGEMRIC can be made by freehand drawing of cartilage regions of interest (ROIs). A mean of the relaxation time values for pixels within a ROI can be then used to characterize the cartilage within each ROI. T2 weighted images of cartilage in the presence of Gd-DTPA show similar contrast with and without contrast, implying it is possible to perform T2 and dGEMRIC studies in the same scanning session. [100]

Only a handful of quantitative MRI techniques has been reported in horses. T2 mapping of experimentally made defects in the articular cartilage of the equine stifle using a 1.5T machine, revealed that T2 mapping helped differentiate hyaline cartilage from reparative fibrocartilage. Mean T2 values from the deep to middle to superficial layers of normal cartilage, respectively, were 40.7, 53.6, and 61.6 ms, whereas T2 values were 53.3, 58.6, and 54.9 ms at reparative fibrous tissue sites. [27]

The use of dGEMRIC using a 3T machine has been reported once in a group of ponies, where it was used to test effects of administered bone morphogenic protein in experimentally-created femoral condyle lesions. [121] The adjacent non-injured cartilage had significantly lower dGEMRIC T1 relaxation times than lesion repair tissue at 12 weeks post lesion creation. At 52 weeks, dGEMRIC T1 relaxation times were lower in both the lesion and the adjacent cartilage. Authors proposed that these findings could have been

due to early osteoarthritis or because the bone morphogenic protein caused cartilage degeneration. Other proposed theories were that changes were caused by immobilization and un-loading of the cartilage because of pain. A review of the advances in biochemical evaluation of horse cartilage reports dGEMRIC and T2 and T1rho mapping as techniques which need further investigation. [19]

This study was performed to determine the feasibility of performing dGEMRIC and T2 mapping in the distal metacarpus3/metatarsus3 (Mc3/Mt3) of normal horse cadaver limbs and to identify potential pitfalls and limitations. The aim was to provide normal dGEMRIC and T2 mapping reference values and therefore provide a platform on which to base later studies of horses with osteoarthritis.

Since much human and animal MRI research is performed on cadaver tissues, and these studies are often conducted at times when convenience dictates, necessitating preservation of the specimen by means of cooling or freezing, it was deemed necessary to determine the effects of this type of cryopreservation on the distal Mc3/Mt3. The effects of chilling and freezing on cartilage in certain MRI sequences have been described in the horse, [57, 122, 123] but not the effect on dGEMRIC or T2 mapping.

Other questions concerning dGEMRIC and T2 mapping that have been addressed in humans but as yet not in the horse include the comparison between intra-articular and intravenous delivery of Gd-DTPA^{2-}, [124-127] the effect of exercise [128] on gadolinium uptake in cartilage and in exercise patterns in individuals [129] and the appearance of dGEMRIC and T2 mapping images in horses with different degrees of osteoarthritis. [103, 109, 112-114, 130]

The effect of osteoarthritis on the biomechanical properties of the cartilage should also be investigated as has been, and is being done in humans. [37, 101, 131] These are questions that can be addressed in the horse in future, based on the results of this current study.

This study was performed on normal cadaver limbs of twelve racing Thoroughbreds which were humanely euthanized post retirement. The first six horses' metacarpo/metatarsophalangeal joints', mid condylar distal Mc3s/Mt3s underwent six precontrast inversion recovery (IR) sequences for dGEMRIC T1 relaxation time calculation as well as T2 relaxation sequence

scans using a 1.5T machine. Thereafter Gd-DTPA^{2-} was injected intraarticularly and the same six IR T1 sequences were repeated at 30, 60, 120, and 180 minutes post injection at the same midcondylar areas. The distal Mc3/Mt3 cartilage thickness was measured histologically and on selected IR and proton density weighted (PDw) images of the dGEMRIC and T2 weighted sequences respectively, and these compared to validate the technique for dGEMRIC and T2 mapping. T1 maps were created by fitting the respective data into mono-exponential relaxation equations and mean values of certain regions of interest were calculated. The effect of intra-articular Gd-DTPA^{2-} on T1 relaxation time from pre-Gd to 180 minutes post injection was determined. A second group of six horses' fore and hindlimbs were randomly assigned to 2 groups, one where the limbs were chilled for 48 hours and the second where the limbs were frozen for up to 90 days. The limbs were then allowed to return to room temperature and scanned similarly to the first fresh limb control group. The effect of chilling and freezing on the dGEMRIC and T2 mapping results were evaluated.

It is important that the dGEMRIC and T2 mapping techniques be repeated in live animals to determine whether these techniques are feasible for early prediction of osteoarthritis in the athlete.

REFERENCES

1. Anonymous. A comparison of the economic costs of equine lameness, colic, and equine protozoal myeloencephalitis (EPM) in the United States. Animal and Plant Health Inspection service. 2001. Available at http://www.aphis.usda.gov/animal_health/nahms/equine/downloads/equine98/Equine98_is_Colic.pdf. (accessed May 2011).

2. Dyson PK, Jackson BF, Pfeiffer DU, Price JS. Days lost from training by two- and three-year-old thoroughbred horses: A survey of seven UK training yards. Equine Vet J 2008;40:650-657.

3. Perkins NR, Reid SW, Morris RS. Profiling the New Zealand Thoroughbred racing industry. 2. conditions interfering with training and racing. N Z Vet J 2005;53:69-76.

4. Parente EJ, Russau AL, Birks EK. Effects of mild forelimb lameness on exercise performance. Equine Vet J Suppl 2002;252-256.

5. Hernandez J, Hawkins DL. Training failure among yearling horses. Am J Vet Res 2001;62:1418-1422.

6. Bailey CJ, Reid SW, Hodgson DR, Bourke JM, Rose RJ. Flat, hurdle and steeple racing: Risk factors for musculoskeletal injury. Equine Vet J 1998;30:498-503.

7. Olivier A, Nurton JP, Guthrie AJ. An epizoological study of wastage in thoroughbred racehorses in Gauteng, South Africa. J S Afr Vet Assoc 1997;68:125-129.

8. Rossdale PD, Hopes R, Digby NJ, Offord K. Epidemiological study of wastage among racehorses 1982 and 1983. Vet Rec 1985;116:66-69.

9. Wilsher S, Allen WR, Wood JL. Factors associated with failure of thoroughbred horses to train and race. Equine Vet J 2006;38:113-118.

10. Broster CE, Burn CC, Barr AR, Whay HR. The range and prevalence of pathological abnormalities associated with lameness in working horses from developing countries. Equine Vet J 2009;41:474-481.

11. de Grauw JC, van de Lest CH, van Weeren R, Brommer H, Brama PA. Arthrogenic lameness of the fetlock: Synovial fluid markers of inflammation and cartilage turnover in relation to clinical joint pain. Equine Vet J 2006;38:305-311.

12. Dabareiner RM, Cohen ND, Carter GK, Nunn S, Moyer W. Musculoskeletal problems associated with lameness and poor performance among horses used for barrel racing: 118 cases (2000-2003). J Am Vet Med Assoc 2005;227:1646-1650.

13. Bailey CJ, Reid SW, Hodgson DR, Rose RJ. Impact of injuries and disease on a cohort of two- and three-year-old Thoroughbreds in training. Vet Rec 1999;145:487-493.

14. Brommer H, van Weeren PR, Brama PA, Barneveld A. Quantification and age-related distribution of articular cartilage degeneration in the equine fetlock joint. Equine Vet J 2003;35:697-201.

15. Norrdin RW, Bay BK, Drews MJ, Martin RB, Stover SM. Overload arthrosis: Strain patterns in the equine metacarpal condyle. J Musculoskelet Neuronal Interact 2001;1:357-362.

16. Pool RR. Pathologic manifestations of joint disease in the athletic horse, In: McIlwraith CW, Trotter GW, editors. Joint disease in the horse. Philadelphia: WB Saunders; 2006. p. 87-104.

17. McIlwraith CW. General pathology of the joint and response to injury. In: McIlwraith CW, Trotter GW, editors. Joint disease in the horse. Philadelphia: WB Saunders; 2006. p. 40-70.

18. Bekkers JEJ, Creemers LB, Dhert WJA, Saris DBF. Diagnostic modalities for diseased articular Cartilage—From defect to degeneration: A review. Cartilage 2010;1:157-164.

19. Pease A. Biochemical evaluation of equine articular cartilage through imaging. Vet Clin North Am Equine Pract 2012;28:637-646.

20. Chu CR, Williams AA, Coyle CH, Bowers ME. Early diagnosis to enable early treatment of pre-osteoarthritis. Arthritis Res Ther 2012;14:212.

21. Eyre DR, Weis MA, Wu JJ. Articular cartilage collagen: An irreplaceable framework? Equine Vet J 2006;12:57-63.

22. Garcia-Lopez JM, Kirker-Head CA. Occult subchondral osseous cyst-like lesions of the equine tarsocrural joint. Vet Surg 2004;33:557-564.

23. Pearle AD, Warren RF, Rodeo SA. Basic science of articular cartilage and osteoarthritis. Clin Sports Med 2005;24:1-12.

24. Nieminen MT, Rieppo J, Toyras J, Hakumaki JM, Silvennoinen J, Hyttinen MM, et al. T2 relaxation reveals spatial collagen architecture in articular cartilage: A comparative quantitative MRI and polarized light microscopic study. Magn Reson Med 2001;46:487-493.

25. Xia Y, Moody JB, Burton-Wurster N, Lust G. Quantitative in situ correlation between microscopic MRI and polarized light microscopy studies of articular cartilage. Osteoarthritis Cartilage 2001;9:393-406.

26. Maier CF, Tan SG, Hariharan H, Potter HG. T2 quantitation of articular cartilage at 1.5 T. J Magn Reson Imaging 2003;17:358-364.

27. White LM, Sussman MS, Hurtig M, Probyn L, Tomlinson G, Kandel R. Cartilage T2 assessment: Differentiation of normal hyaline cartilage and reparative tissue after arthroscopic cartilage repair in equine subjects. Radiology 241:407-14, 2006.

28. Koff MF, Parratte S, Amrami KK, Kaufman KR. Examiner repeatability of patellar cartilage T2 values. Magn Reson Imaging 2009;27:131-136.

29. Glaser C, Horng A, Mendlik T, Weckbach S, Hoffmann RT, Wagner S, et al. T2 relaxation time in patellar cartilage--global and regional reproducibility at 1.5 Tesla and 3 Tesla. Rofo 2007;179:146-152.

30. Glaser C, Mendlik T, Dinges J, Weber J, Stahl R, Trumm C, et al. Global and regional reproducibility of T2 relaxation time measurements in human patellar cartilage. Magn Reson Med 2006;56:527-534.

31. Nishii T, Kuroda K, Matsuoka Y, Sahara T, Yoshikawa H. Change in knee cartilage T2 in response to mechanical loading. J Magn Reson Imaging 2008;28:175-180.

32. Waterton JC, Solloway S, Foster JE, Keen MC, Gandy S, Middleton BJ, et al. Diurnal variation in the femoral articular cartilage of the knee in young adult humans. Magn Reson Med 2000;43:126-132.

33. Rubenstein JD, Kim JK, Henkelman RM. Effects of compression and recovery on bovine articular cartilage: Appearance on MR images. Radiology 1996;201:843-850.

34. Mosher TJ, Smith H, Dardzinski BJ, Schmithorst VJ, Smith MB. MR imaging and T2 mapping of femoral cartilage: In vivo determination of the magic angle effect. Am J Roentgenol 2001;177:665-669.

35. Mosher TJ, Dardzinski BJ. Cartilage MRI T2 relaxation time mapping: Overview and applications. Semin Musculoskelet Radiol 2004;8:355-368.

36. Xia Y. Relaxation anisotropy in cartilage by NMR microscopy (mu MRI) at 14-mu m resolution. Magn Reson Med 1998;39:941-949.

37. Lammentausta E, Kiviranta P, Nissi MJ, Laasanen MS, Kiviranta I, Nieminen MT, et al. T2 relaxation time and delayed gadolinium-enhanced MRI of cartilage (dGEMRIC) of human patellar cartilage at 1.5 T and 9.4 T:

Relationships with tissue mechanical properties. J Orthop Res 2006;24:366-374.

38. Lammentausta E, Kiviranta P, Toyras J, Hyttinen MM, Kiviranta I, Nieminen MT, et al. Quantitative MRI of parallel changes of articular cartilage and underlying trabecular bone in degeneration. Osteoarthritis Cartilage 2007;15:1149-1157.

39. Nieminen MT, Toyras J, Laasanen MS, Silvennoinen J, Helminen HJ, Jurvelin JS. Prediction of biomechanical properties of articular cartilage with quantitative magnetic resonance imaging. J Biomech 2004;37:321-328.

40. Nieminen MT, Rieppo J, Silvennoinen J, Toyras J, Hakumaki JM, Hyttinen MM, et al. Spatial assessment of articular cartilage proteoglycans with gd-DTPA-enhanced T1 imaging. Magn Reson Med 2002;48:640-648.

41. Martel-Pelletier J. Pathophysiology of osteoarthritis. Osteoarthritis Cartilage 2004;12 Suppl A:S31-3.

42. Taylor C, Carballido-Gamio J, Majumdar S, Li X. Comparison of quantitative imaging of cartilage for osteoarthritis: T2, T1rho, dGEMRIC and contrast-enhanced computed tomography. Magn Reson Imaging 2009;27:779-784.

43. Kawcak CE, McIlwraith CW, Norrdin RW, Park RD, James SP. The role of subchondral bone in joint disease: A review. Equine Vet J 2001;33:120-126.

44. Cruz AM, Hurtig MB. Multiple pathways to osteoarthritis and articular fractures: Is subchondral bone the culprit? Vet Clin North Am Equine Pract 2008;24:101-116.

45. Henrotin Y, Pesesse L, Sanchez C. Subchondral bone in osteoarthritis physiopathology: State-of-the art and perspectives. Biomed Mater Eng 2009;19:311-316.

46. Pastoureau PC, Hunziker EB, Pelletier JP. Cartilage, bone and synovial histomorphometry in animal models of osteoarthritis. Osteoarthritis Cartilage 2010;18 Suppl 3:S106-12.

47. O'Brien TR, Hornof WJ, Meagher DM. Radiographic detection and characterization of palmar lesions in the equine fetlock joint. J Am Vet Med Assoc 1981;178:231-237.

48. Pool RR, Meagher DM. Pathologic findings and pathogenesis of racetrack injuries. Vet Clin North Am Equine Pract 1990;6:1-30.

49. Olive J, D'Anjou MA, Girard C, Laverty S, Theoret CL. Imaging and histological features of central subchondral osteophytes in racehorses with metacarpophalangeal joint osteoarthritis. Equine Vet J 2009;41:859-864.

50. Brommer H, Brama PA, Barneveld A, van Weeren PR. Differences in the topographical distribution of articular cartilage degeneration between equine metacarpo- and metatarsophalangeal joints. Equine Vet J 2004;36:506-510.

51. Smith KJ, Bertone AL, Weisbrode SE, Radmacher M. Gross, histologic, and gene expression characteristics of osteoarthritic articular cartilage of the metacarpal condyle of horses. Am J Vet Res 67:1299-30.

52. Butler JA, Colles CM, Dyson SJ, Kold SE, Poulos PW. General principles. In: Clinical radiology of the horse. 3rd ed. Chichester, United Kingdom: Wiley-Blackwell; 2009. p. 1-36.

53. Rubio-Martinez LM, Cruz AM, Gordon K, Hurtig MB. Structural characterization of subchondral bone in the distal aspect of third metacarpal bones from thoroughbred racehorses via micro-computed tomography. Am J Vet Res 2008;69:1413-1422.

54. Martinelli MJ, Baker GJ, Clarkson RB, Eurell JC, Pijanowski GJ, Kuriashkin IV. Magnetic resonance imaging of degenerative joint disease in a horse: A comparison to other diagnostic techniques. Equine Vet J 1996;28:410-415.

55. Anastasiou A, Skioldebrand E, Ekman S, Hall LD. Ex vivo magnetic resonance imaging of the distal row of equine carpal bones: Assessment of bone sclerosis and cartilage damage. Vet Radiol Ultrasound 2003;44:501-12.

56. Bolen G, Audigie F, Spriet M, Vandenberghe F, Busoni V. Qualitative comparison of 0.27T, 1.5T, and 3T magnetic resonance images of the normal equine foot. J Equine Vet Sci 2010;30:9-20.

57. Bolen G, Haye D, Dondelinger R, Busoni V. Magnetic resonance signal changes during time in equine limbs refrigerated at 4 degrees C. Vet Radiol Ultrasound 2010;51:19-24.

58. Barrett MF, Frisbie DD. The role of MRI in selected equine case management. Vet Clin North Am Equine Pract 2012;28:647-658.

59. Daniel AJ, Judy CE, Rick MC, Saveraid TC, Herthel DJ. Comparison of radiography, nuclear scintigraphy, and magnetic resonance imaging for detection of specific conditions of the distal tarsal bones of horses: 20 cases (2006-2010). J Am Vet Med Assoc 2012;240:1109-1114.

60. Declercq J, Martens A, Maes D, Boussauw B, Forsyth R, Boening KJ. Dorsoproximal proximal phalanx osteochondral fragmentation in 117 warmblood horses. Vet Comp Orthop Traumatol 2009;22:1-6.

61. Dyson S, Pool R, Blunden T, Murray R. The distal sesamoidean impar ligament: Comparison between its appearance on magnetic resonance imaging and histology of the axial third of the ligament. Equine Vet J 2010;42:332-339.

62. Dyson S, Murray R, Schramme M, Branch M. Magnetic resonance imaging of the equine foot: 15 horses. Equine Vet J 2003;35:18-26.

63. Gaschen L, Burba DJ. Musculoskeletal injury in Thoroughbred racehorses correlation of findings using multiple imaging modalities. Vet Clin North Am Equine Pract 2012;28:539-561.

64. Gaschen L, LeRoux A, Trichel J, Riggs L, Bragulla HH, Rademacher N, et al. Magnetic resonance imaging in foals with infectious arthritis. Vet Radiol Ultrasound 2011;52:627-633.

65. Gonzalez LM, Schramme MC, Robertson ID, Thrall DE, Redding RW. MRI features of metacarpo(tarso)phalangeal region lameness in 40 horses. Vet Radiol Ultrasound 2010;51:404-414.

66. Gutierrez-Nibeyro SD, White NA,2nd, Werpy NM, Tyrrell L, Allen KA, Sullins KE, et al. Magnetic resonance imaging findings of desmopathy of the collateral ligaments of the equine distal interphalangeal joint. Vet Radiol Ultrasound 2009;50:21-31.

67. Gutierrez-Nibeyro SD, Werpy NM, White NA,II, McCutcheon LJ, Weng H, Christopher JM. Standing low-field magnetic resonance imaging appearance of normal collateral ligaments of the equine distal interphalangeal joint. Vet Radiol Ultrasound 2011;52:521-533.

68. Gutierrez-Nibeyro SD, Werpy NM, White NA,II. Standing low-field magnetic resonance imaging in horses with chronic foot pain. Aust Vet J 2012;90:75-83.

69. Getman LM, McKnight AL, Richardson DW. Comparison of magnetic resonance contrast arthrography and arthroscopic anatomy of the equine palmar lateral outpouching of the middle carpal joint. Vet Radiol Ultrasound 2007;48:493-500.

70. Janssen I, Swagemakers J, Koene M, Lischer C. Development of an increased signal intensity in fat-suppressed images into a navicular cyst of an 11-year-old warmblood horse evidenced by six follow-up standing low-field magnetic resonance imaging examinations over 2 years. J Equine Vet Sci 2013;33:136-141.

71. Judy CE, Saveraid TC, Rick MC, Herthel DJ. Magnetic resonance imagning of the equine stifle in a clinical setting. Proceedings, 3rd World

Veterinary Orthopaedic Congress, ESVOT-VOS, 15th ESVOT Congress, Bologna, Italy, 15-18 September, 2010:210-212.

72. Kamm JL, Goodrich LR, Werpy NM, McIlwraith CW. A descriptive study of the equine proximal interphalangeal joint using magnetic resonance imaging, contrast arthrography, and arthroscopy. Vet Surg 2012;41:677-684.

73. King JN, Zubrod CJ, Schneider RK, Sampson SN, Roberts G. Mri findings in 232 horses with lameness localized to the metacarpo(tarso)phalangeal region and without a radiographic diagnosis. Vet Radiol Ultrasound 2013;54:36-47.

74. Labens R, Schramme MC, Robertson ID, Thrall DE, Redding WR. Clinical, magnetic resonance, and sonographic imaging findings in horses with proximal plantar metatarsal pain. Vet Radiol Ultrasound 2010;51:11-18.

75. Latorre R, Arencibia A, Gil F, Rivero M, Henry RW, Ramirez G, et al. Correlation of magnetic resonance images with anatomic features of the equine tarsus. Am J Vet Res 67:756-61, 2006.

76. Murray RC, Mair TS, Sherlock CE, Blunden AS. Comparison of high-field and low-field magnetic resonance images of cadaver limbs of horses. Vet Rec 2009;165:281-288.

77. Murray RC, Blunden TS, Schramme MC, Dyson SJ. How does magnetic resonance imaging represent histologic findings in the equine digit? Vet Radiol Ultrasound 2006;47:17-31.

78. Smith M, Dyson S. The fetlock region. In: Murray RC (ed). Equine MRI, 1st ed. Chichester, United Kingdom: Wiley-Blackwell, 2011. p.173-189.

79. Nagy A, Dyson SJ. Magnetic resonance findings in the carpus and proximal metacarpal region of non-lame horses. In: Proceedings of the 55th Annual Convention of the American Association of Equine Practitioners, Las Vegas, Nevada, USA, 5-9 December 2009;55:408-17.

80. Nagy A, Dyson S. Magnetic resonance anatomy of the carpus of the horse described from images acquired from low-field and high-field magnets. Vet Radiol Ultrasound 2011;52:273-283.

81. Powell SE. Low-field standing magnetic resonance imaging findings of the metacarpo/metatarsophalangeal joint of racing thoroughbreds with lameness localised to the region: A retrospective study of 131 horses. Equine Vet J 2012;44:169-177.

82. Rodriguez MJ, Agut A, Soler M, Lopez-Albors O, Arredondo J, Querol M, et al. Magnetic resonance imaging of the equine temporomandibular joint anatomy. Equine Vet J 2010;42:200-207.

83. Saveraid TC, Judy CE. Use of intravenous gadolinium contrast in equine magnetic resonance imaging. Vet Clin North Am Equine Pract 2012;28:617-636.

84. Schramme MC. MRI features of subchondral bone injury in the metacarpophalangeal and metatarsophalangeal joints of horses. Proceedings, 3rd World Veterinary Orthopaedic Congress, ESVOT-VOS, 15th ESVOT Congress, Bologna, Italy, 15-18 September, 2010;15:244-246.

85. Schramme MC. Relationship between histopathological lesions and magnetic resonance imaging (mri) in diseases of the foot of the horse. Bulletin De L Academie Veterinaire De France 2012;165:243-248.

86. Sherlock C, Mair T, Blunden T. Deep erosions of the palmar aspect of the navicular bone diagnosed by standing magnetic resonance imaging. Equine Vet J 2008;40:684-692.

87. Sherlock CE, Mair TS, Ter Braake F. Osseous lesions in the metacarpo(tarso)phalangeal joint diagnosed using low-field magnetic resonance imaging in standing horses. Vet Radiol Ultrasound 2009;50:13-20.

88. Smith MA, Dyson SJ, Murray RC. The appearance of the equine metacarpophalangeal region on high-field vs. standing low-field magnetic resonance imaging. Vet Radiol Ultrasound 2011;52:61-70.

89. Selberg K, Werpy N. Fractures of the distal phalanx and associated soft tissue and osseous abnormalities in 22 horses with ossified sclerotic ungual cartilages diagnosed with magnetic resonance imaging. Vet Radiol Ultrasound 2011;52:394-401.

90. Spriet M, Mai W, McKnight A. Asymmetric signal intensity in normal collateral ligaments of the distal interphalangeal joint in horses with a low-field MRI system due to the magic angle effect. Vet Radiol Ultrasound 2007;48:95-100.

91. Tranquille CA, Parkin TDH, Murray RC. Magnetic resonance imaging-detected adaptation and pathology in the distal condyles of the third metacarpus, associated with lateral condylar fracture in Thoroughbred racehorses. Equine Vet J 2012;44:699-706.

92. Vallance SA, Bell RJW, Spriet M, Kass PH, Puchalski SM. Comparisons of computed tomography, contrast enhanced computed tomography and standing low-field magnetic resonance imaging in horses with lameness localised to the foot. part 1: Anatomic visualisation scores. Equine Vet J 2012;44:51-56.

93. Werpy NM, Ho CP, Pease A, Kawcak CE. Preliminary study on detection of osteochondral defects in the fetlock joint using low and high field strength magnetic resonance imaging. Proceedings of the 54th Annual Convention of the American Association of Equine Practitioners, San Diego, California, USA, 6-10 December 2008;54:447-451.

94. Werpy NM, Ho CP, Pease AP, Kawcak CE. The effect of sequence selection and field strength on detection of osteochondral defects in the metacarpophalangeal joint. Vet Radiol Ultrasound 2011;52:154-160.

95. Werpy NM, Ho CP, Garcia EB, Kawcak CE. The effect of varying echo time using T2-weighted fse sequences on the magic angle effect in the collateral ligaments of the distal interphalangeal joint in horses. Vet Radiol Ultrasound 2013;54:31-35.

96. Young AC, Dimock AN, Puchalski SM, Murphy B, Spriet M. Magnetic resonance and radiographic diagnosis of osseous resorption of the flexor surface of the distal phalanx in the horse. Equine Vet J 2012;44:3-7.

97. Smith MA, Dyson SJ, Murray RC. Reliability of high- and low-field magnetic resonance imaging systems for detection of cartilage and bone lesions in the equine cadaver fetlock. Equine Vet J 2012;44:684-691.

98. Goodwin DW. Visualization of the macroscopic structure of hyaline cartilage with MR imaging. Semin Musculoskelet Radiol 2001;5:305-312.

99. Xia Y, Zheng S, Bidthanapally A. Depth-dependent profiles of glycosaminoglycans in articular cartilage by microMRI and histochemistry. J Magn Reson Imaging 2008;28:151-157.

100. Nieminen MT, Menezes NM, Williams A, Burstein D. T2 of articular cartilage in the presence of gd-DTPA2-. Magn Reson Med 2004;51:1147-1152.

101. Nissi MJ, Rieppo J, Toyras J, Laasanen MS, Kiviranta I, Nieminen MT, et al. Estimation of mechanical properties of articular cartilage with MRI - dGEMRIC, T2 and T1 imaging in different species with variable stages of maturation. Osteoarthritis Cartilage 2007;15:1141-1148.

102. Dunn TC, Lu Y, Jin H, Ries MD, Majumdar S. T2 relaxation time of cartilage at MR imaging: Comparison with severity of knee osteoarthritis. Radiology 2004;232:592-598.

103. Domayer SE, Welsch GH, Dorotka R, Mamisch TC, Marlovits S, Szomolanyi P, et al. MRI monitoring of cartilage repair in the knee: A review. Semin Musculoskelet Radiol 2008;12:302-317.

104. Laouar L, Fishbein K, McGann LE, Horton WE, Spencer RG, Jomha NM. Cryopreservation of porcine articular cartilage: MRI and biochemical results after different freezing protocols. Cryobiology 2007;54:36-43.

105. Watrin-Pinzano A, Ruaud JP, Olivier P, Grossin L, Gonord P, Blum A, et al. Effect of proteoglycan depletion on T2 mapping in rat patellar cartilage. Radiology 2005;234:162-170.

106. Fishbein KW, Canuto HC, Bajaj P, Camacho NP, Spencer RG. Optimal methods for the preservation of cartilage samples in MRI and correlative biochemical studies. Magn Reson Med 2007;57:866-873.

107. Damion RA, Pawaskar SS, Ries ME, Ingham E, Williams S, Jin Z, et al. Spin-lattice relaxation rates and water content of freeze-dried articular cartilage. Osteoarthritis Cartilage 2012;20:184-190.

108. Berberat JE, Nissi MJ, Jurvelin JS, Nieminen MT. Assessment of interstitial water content of articular cartilage with T1 relaxation. Magn Reson Imaging 2009;27:727-732.

109. Guermazi A, Burstein D, Conaghan P, et al. Imaging in osteoarthritis. Rheum Dis Clin North Am 2008;34:645–687.

110. Gold GE, Burstein D, Dardzinski B, Lang P, Boada F, Mosher T. MRI of articular cartilage in OA: novel pulse sequences and compositional/functional markers. Osteoarthritis Cartilage 2006;14 Suppl A:A76– A86.

111. Crema MD, Roemer FW, Marra MD, Burstein D, Gold GE, Eckstein F, et al. Articular cartilage in the knee: Current MR imaging techniques and applications in clinical practice and research. Radiographics 2011;31:37-61.

112. Potter HG, Black BR, Chong le R. New techniques in articular cartilage imaging. Clin Sports Med 2009;28:77-94.

113. Roemer FW, Eckstein F, Guermazi A. Magnetic resonance imaging-based semiquantitative and quantitative assessment in osteoarthritis. Rheum Dis Clin North Am 2009;35:521-555.

114. Trattnig S, Domayer S, Welsch GW, Mosher T, Eckstein F. MR imaging of cartilage and its repair in the knee--a review. Eur Radiol 2009;19:1582-1594.

115. Tsushima H, Okazaki K, Takayama Y, Hatakenaka M, Honda H, Izawa T, et al. Evaluation of cartilage degradation in arthritis using T1 rho magnetic resonance imaging mapping. Rheumatol Int 2012;32:2867-2875.

116. Domayer SE, Trattnig S, Stelzeneder D, Hirschfeld C, Quirbach S, Dorotka R, et al. Delayed gadolinium-enhanced MRI of cartilage in the ankle at 3 T: Feasibility and preliminary results after matrix-associated autologous chondrocyte implantation. J Magn Reson Imaging 2010;31:732-739.

117. Domayer SE, Welsch GH, Nehrer S, Chiari C, Dorotka R, Szomolanyi P, et al. T2 mapping and dGEMRIC after autologous chondrocyte implantation with a fibrin-based scaffold in the knee: Preliminary results. Eur J Radiol 2010;73:636-642.

118. Jazrawi LM, Alaia MJ, Chang G, FitzGerald EF, Recht MP. Advances in magnetic resonance imaging of articular cartilage. J Am Acad Orthop Surg 2011;19:420-429.

119. Jobke B, Bolbos R, Saadat E, Cheng J, Li X, Majumdar S. Mechanism of disease in early osteoarthritis: Application of modern MR imaging techniques - a technical report. Magn Reson Imaging 2013;31:156-161.

120. Tiderius CJ, Jessel R, Kim YJ, Burstein D. Hip dGEMRIC in asymptomatic volunteers and patients with early osteoarthritis: The influence of timing after contrast injection. Magn Reson Med 2007;57:803-805.

121. Menendez MI, Clark DJ, Carlton M, Flanigan DC, Jia G, Sammet S, et al. Direct delayed human adenoviral BMP-2 or BMP-6 gene therapy for bone and

cartilage regeneration in a pony osteochondral model. Osteoarthritis Cartilage 2011;19:1066-1075.

122. Bolen GE, Haye D, Dondelinger RF, Massart L, Busoni V. Impact of successive freezing-thawing cycles on 3-T magnetic resonance images of the digits of isolated equine limbs. Am J Vet Res 2011;72:780-790.

123. Widmer WR, Buckwalter KA, Hill MA, Fessler JF, Ivancevich S. A technique for magnetic resonance imaging of equine cadaver specimens. Vet Radiol Ultrasound 1999;40:10-4.

124. Wiener E, Hodler J, Pfirrmann CW. Delayed gadolinium-enhanced MRI of cartilage (dGEMRIC) of cadaveric shoulders: Comparison of contrast dynamics in hyaline and fibrous cartilage after intraarticular gadolinium injection. Acta Radiol 2009;50:86-92.

125. Bittersohl B, Hosalkar HS, Werlen S, Trattnig S, Siebenrock KA, Mamisch TC. Intravenous versus intra-articular delayed gadolinium-enhanced magnetic resonance imaging in the hip joint: A comparative analysis. Invest Radiol 2010;45:538-542.

126. Boesen M, Jensen KE, Qvistgaard E, Danneskiold-Samsoe B, Thomsen C, Ostergaard M, et al. Delayed gadolinium-enhanced magnetic resonance imaging (dGEMRIC) of hip joint cartilage: Better cartilage delineation after intra-articular than intravenous gadolinium injection. Acta Radiol 2006;47:391-396.

127. Kwack KS, Cho JH, Kim MMS, Yoon CS, Yoon YS, Choi JW, et al. Comparison study of intraarticular and intravenous gadolinium-enhanced magnetic resonance imaging of cartilage in a canine model. Acta Radiol 2008;49:65-74.

128. Burstein D, Velyvis J, Scott KT, Stock KW, Kim YJ, Jaramillo D, et al. Protocol issues for delayed gd(DTPA)(2-)-enhanced MRI (dGEMRIC) for clinical evaluation of articular cartilage. Magn Reson Med 2001;45:36-41.

129. Tiderius CJ, Svensson J, Leander P, Ola T, Dahlberg L. dGEMRIC (delayed gadolinium-enhanced MRI of cartilage) indicates adaptive capacity of human knee cartilage. Magn Reson Med 2004;51:286-290.

130. Tiderius CJ, Olsson LE, Leander P, Ekberg O, Dahlberg L. Delayed gadolinium-enhanced MRI of cartilage (dGEMRIC) in early knee osteoarthritis. Magn Reson Med 2003;49:488-492.

131. Lammentausta E, Hakulinen MA, Jurvelin JS, Nieminen MT. Prediction of mechanical properties of trabecular bone using quantitative MRI. Phys Med Biol 2006;51:6187-6198.

CHAPTER 3

HYPOTHESES

The aims of the study were to formulate a technique to perform quantitative MRI of the cartilage of the distal metacarpus3/metatarsus3 in the normal Thoroughbred horse, utilizing dGEMRIC and T2 mapping. The information will serve as a guide to perform the techniques, to provide initial reference values, and to determine the effects of cryopreservation of the limbs on these reference values. The specific research hypotheses of the study were the following:

1. dGEMRIC mapping measurement parameters result in the same distal metacarpus3/metatarsus3 cartilage thickness as histomorphometric (gold standard) parameters.
2. T2 mapping measurement parameters result in the same distal metacarpus3/metatarsus3 cartilage thickness as histomorphometric (gold standard) parameters.
3. dGEMRIC mapping of five regions of interest (ROIs) of the distal metacarpus3/metatarsus3 cartilage can be performed.
4. dGEMRIC mapping of the entire distal metacarpus3/metatarsus3 cartilage can be performed.
5. The optimal time of scanning the distal metacarpus3/metatarsus3 cartilage for dGEMRIC mapping after intra-articular injection of Gd-$DTPA^{2-}$ is 30 minutes
6. T2 mapping of five ROIs of the distal metacarpus3/metatarsus3 cartilage can be performed.
7. T2 mapping of the entire distal metacarpus3/metatarsus3 cartilage can be performed.
8. Chilling/freezing does not affect T2 mapping at five different ROIs of the distal metacarpus3/metatarsus3 cartilage.
9. Chilling/freezing does not affect T2 mapping of the distal metacarpus3/metatarsus3 entire cartilage.

10. Chilling/freezing does not affect dGEMRIC mapping at five different ROIs of the distal metacarpus3/metatarsus3.
11. Chilling/freezing does not affect dGEMRIC mapping of the distal metacarpus3/metatarsus3 entire cartilage.

The first two hypotheses are addressed in chapter 4, hypotheses 3 and 5 in chapter 5, hypotheses 6, 7, 8 and 9 in chapter 6, and hypotheses 4, 10 and 11 in chapter 7.

CHAPTER 4

Validation of delayed gadolinium-enhanced magnetic resonance imaging of cartilage and T2 mapping for quantifying distal metacarpus/metatarsus cartilage thickness in Thoroughbred racehorses

Ann Carstens, Robert M. Kirberger, Leif E. Dahlberg, Leon Prozesky, Lizelle Fletcher, Eveliina Lammentausta

Key words: cartilage, dGEMRIC, horse, MRI, T2 mapping, validation.

From the Section of Diagnostic Imaging, Department of Compan- ion Animal Clinical Studies (Carstens, Kirberger), and the Department of Pathology (Prozesky), Faculty of Veterinary Science, and the Department of Statistics (Fletcher), University of Pretoria, South Africa; the Joint and Soft Tissue Unit, Department of Clinical Sciences, Lund University, and Department of Orthopaedics, Malmö University Hospital, Malmö, Sweden (Dahlberg, Lammentausta); and Department of Diagnostic Radiology, the Oulu University Hospital, Oulu, Finland (Lammentausta).

As published in Veterinary Radiology and Ultrasound 2013;54:139-148.

4.1 ABSTRACT

The purpose of this study was to determine whether delayed gadolinium-enhanced magnetic resonance imaging of cartilage (dGEMRIC) and T2 mapping are accurate techniques for measuring cartilage thickness in the metacarpus3/metatarsus3 (Mc3/Mt3) of Thoroughbred racehorses. Twenty-four Mc3/Mt3 cadaver specimens were acquired from six healthy racehorses. Cartilage thickness was measured from post intra-articular Gd-DTPA^{2-} images acquired using short tau inversion recovery (STIR), and proton density weighted (PDw) sequences, and compared with cartilage thickness measured from corresponding histologic images. Two observers performed each histologic measurement twice at three different sites, with measurement times spaced at least 5 days apart. Histologic cartilage thickness was measured at each of the three sites from the articular surface to the bone-cartilage interface, and from the articular surface to the mineralized cartilage interface (tidemark). Intra-observer repeatability was good to moderate for dGEMRIC where Mc3/Mt3 cartilage was not in contact with the proximal phalanx. Where the Mc3/Mt3 cartilage was in contact with the proximal phalanx cartilage, dGEMRIC STIR and T2 mapping PDw cartilage thicknesses of Mc3/Mt3 could not be measured reliably. When measured from the articular surface to the bone–cartilage interface, histologic cartilage thickness did not differ from STIR or PDw cartilage thickness at the site where the Mc3/Mt3 cartilage surface was separated from the proximal phalanx cartilage ($P>0.05$). Findings indicated that dGEMRIC STIR and T2 mapping PDw are accurate techniques for measuring Mc3/Mt3 cartilage thickness at locations where the cartilage is not in direct contact with the proximal phalanx cartilage.

4.2 INTRODUCTION

Lameness is the primary cause of poor performance and wastage in horses.[1–6] This decrease in athletic ability has been estimated to cost the performance horse industry in North America an estimated $1 billion annually, with an incidence of 8.5% to 13.7%.[7] In studies performed at racetracks throughout the world, the most common source of lameness is the distal limb.[5,8–13] Twenty five percent of racing Thoroughbreds experience metacarpophalangeal and metatarsophalangeal joint pain,[5] with this joint being the most commonly affected by traumatic and degenerative lesions of the appendicular skeleton resulting in osteoarthritis.[6,10,14–16] Osteoarthritis is characterized by matrix fibrillation, the appearance of fissures, and ulceration and full-thickness loss of the cartilage.[17–20]

Magnetic resonance imaging, including the use of gadolinium (Gd-DTPA^{2-}) has been used in human studies to visualize osteoarthritis early in the disease process.[21–25] Parametric mapping of cartilage entails post-processing of images to give relaxation time-associated colour-maps that provide a visual interpretation of the specific area's relaxation times. This has been described in T2, T2*, and delayed gadolinium enhancement of MR in cartilage (dGEMRIC) techniques.[26] T2 mapping is a noninvasive technique that can characterize hyaline articular cartilage and repair tissue.[27] In dGEMRIC, the negatively charged Gd-DTPA^{2-}, injected either intra-articularly or intravenously, penetrates hyaline cartilage in an inverse relationship to the proteoglycan concentration of the cartilage. When proteoglycan concentration is decreased due to cartilage degradation, as seen in osteoarthritis, the penetration of Gd-DTPA^{2-} is increased due to a relative decrease in negative charge of the proteoglycan-depleted cartilage. Delayed gadolinium enhanced MR in cartilage has been shown to be an excellent indicator of early degenerative cartilaginous changes in humans.[24] The MRI parameter maps for T2 and dGEMRIC can be made by freehand drawing of cartilage regions of interest (ROIs). Signal intensity can be then fitted pixel by pixel into mono-exponential relaxation equations using image analysis software (MATLAB Mathworks Inc., Natick, MA, USA). Results of these calculations yield a

relaxation time value for each pixel. A mean of the relaxation time values for pixels within a ROI can be then used to characterize the cartilage within each ROI.

To ensure that the bone–cartilage interface and the cartilage surface of the dGEMRIC and T2 mapping sites are consistent with true anatomical areas, previous validation studies have compared MRI measurements to histological measurements as the gold standard. A study validating MRI imaging measurements of equine carpal cartilage thickness found a significant correlation between gradient echo and spoiled gradient echo, and spoiled gradient echo and histologic measurements.[28] The same study found that, when calcified cartilage was excluded from the histologic measurement, MRI measurements were significantly greater than histologic measurements.[28]

Another previous human study reported good repeatability for cartilage thickness measurements using a 7T scanner, with a coefficient of variation of 1.13%.[29] Good repeatability of MRI cartilage thickness measurements was also found in a study of asymptomatic human hip joints.[30] Inter-rater and intra-rater reliability of human cadaver femoral head cartilage thickness measurements from 3D-spoiled gradient echo pulse sequences have been found to be very high (<0.98)[31] and high-resolution MRI cartilage thickness evaluation was also found to have good correlation with direct imaging analysis of surgically removed cartilage.[32] For accurate determination of highly curved and thin articular cartilage volume and thickness three dimensionally, a 3D gradient echo sequence with selective water excitation acquisition can be used together with semi-automatic segmentation using a spline Snake algorithm.[33]

Previous studies have also validated MRI cartilage measurement techniques for assessing progression of osteoarthritis. In one previous study, MRI detected a 1–2% decrease in cartilage thickness annually in human patients with some identifiable risk factors.[24] Another study reported that MRI cartilage thickness and volume measurements decrease in patients with symptomatic knee osteoarthritis.[34] In an experimental study using a guinea pig meniscectomy model, MRI cartilage thickness measurement precision (repeatability) was good, with positive agreement and a significant partial

correlation between measurements.[35] Cartilage thickness changes were also seen in serial MRI examinations of guinea pig stifle joints after meniscectomy.[36] Computer-aided methods for quantifying cartilage thickness and volume changes using MRI have also been validated.[37] In a computer-aided technique where measurements were tested and re-tested (paired imaging analysis), improved precision of cartilage segmentation for articular surfaces of the femur, tibia, and patella was found.[38] Using MRI-based 3D cartilage models, the thickness of cartilage was overestimated in regions where cartilage thickness was less than 2.5 mm and correctly predicted in regions where the cartilage was greater than 2.5 mm.[39]

In a study comparing a standard MRI knee protocol and T2 mapping, T2 mapping was found to be feasible in a clinical setting and also revealed cartilage lesions not visible with standard clinical MRI protocols.[40] Day-to-day repeatability of the dGEMRIC measurements has also been reported at different knee joint surfaces of healthy humans, and has been found to be good for small, deep, or superficial segments, for full thickness ROIs and for bulk ROIs.[41]

The purpose of the current study was to validate T2 mapping and dGEMRIC techniques for measuring cartilage thickness in Thoroughbred racehorses, using three selected sites of the distal Mc3/Mt3 condyle of normal Thoroughbred cadaver specimens. The first objective of the study was to determine intra- and inter-observer agreement for histomorphometrical measurements of cartilage thickness for the three sites, measured from the articular surface to the most superficial bone Haversian canals (bone–cartilage interface) and to the most superficial aspect of mineralized cartilage (tidemark (mineralized cartilage interface)). The second objective was to determine intra-observer agreement for measurements of cartilage thickness for the three sites and for two MRI techniques, the TI = 200 ms (hereafter referred to as the STIR) images during dGEMRIC mapping and the TE = 16.7 ms (hereafter referred to as PDw (proton density weighted)) images during T2 mapping. The third objective was to compare histologic measurements of bone–cartilage interface and mineralized cartilage interface to cartilage surface with measurements of cartilage thickness from the STIR images in dGEMRIC mapping and the PDw images in T2 mapping. The last objective

was to compare cartilage thickness measurements from the STIR images in dGEMRIC mapping to measurements from the PDw images in T2 mapping.

4.3 MATERIALS AND METHODS

This was a prospective cross-sectional study using 24 cadaver limbs of six clinically sound Thoroughbred horses. The project (V067/10) was approved by the Animal Use and Care Committee of the Faculty of Veterinary Science University of Pretoria and all horses were treated according to South African Veterinary Council ethical standards. Inclusion criteria were that the horses were to be Thoroughbreds aged between 3 and 6 years, of any gender, with no pain on flexion of the metacarpophalangeal or metatarsophalangeal joints and no signs of lameness at a walk or trot. There had to be no clinically apparent signs of marked appendicular skeletal abnormalities and no history of corticosteroid or glycosaminoglycan treatments in the past week. The horses were obtained from a welfare horse care organization where racing Thoroughbreds are sent for adoption or euthanasia.

The horses were shot intracranially and the limbs removed at the middiaphyses of the third metacarpal or metatarsal bones. The limbs were wrapped in cling plastic, identified, placed in a cool bag, and transported to an MRI facility (Pretoria MR Trust, Faerie Glen Branch, Pretoria, South Africa) with a Siemens Avanto 1.5 T MRI machine with A B17 Software upgrade (Siemens Healthcare, Erlangen, Germany). The scanning took place with the limbs at room temperature (20°C) approximately 6 h posteuthanasia. A vitamin E oil capsule was taped to the lateral aspect of every Mc3/Mt3 specimen. The limbs were placed on the scanner table with the dorsal surface facing down and with the toe facing into the gantry. A head and neck 12-channel receiver coil combination was used. The forelimbs were randomly selected and scanned, followed by those of the randomly selected hind limbs. A leapfrog time schedule was used to ensure optimal time use, with the four metacarpo/metatarsophalangeal joints' scans finishing approximately 8 h after commencement of the scans. The T1-weighted images were acquired using turbo spinecho sequences in the sagittal plane with TR: 557 ms; TE: 23 ms;

FOV: 100 × 100; matrix: 256 × 256; and receiver bandwidth: 130 Hz/pix. The T2 mapping images were acquired using multi-slice multi-echo spin-echo sequences with TR: 2170 ms; six TEs at between 16.7 and 116.9 ms; FOV: 140 × 140; matrix: 256 × 256; slice thickness: 3 mm; and kHz receiver bandwidth: 130 Hz/pix. A 17-line software template was used on a transverse localizer of the distal Mc3/Mt3 to identify the midlateral Mt3 condyle and the midmedial Mc3 condyle (Fig. 4.1 A).

A B

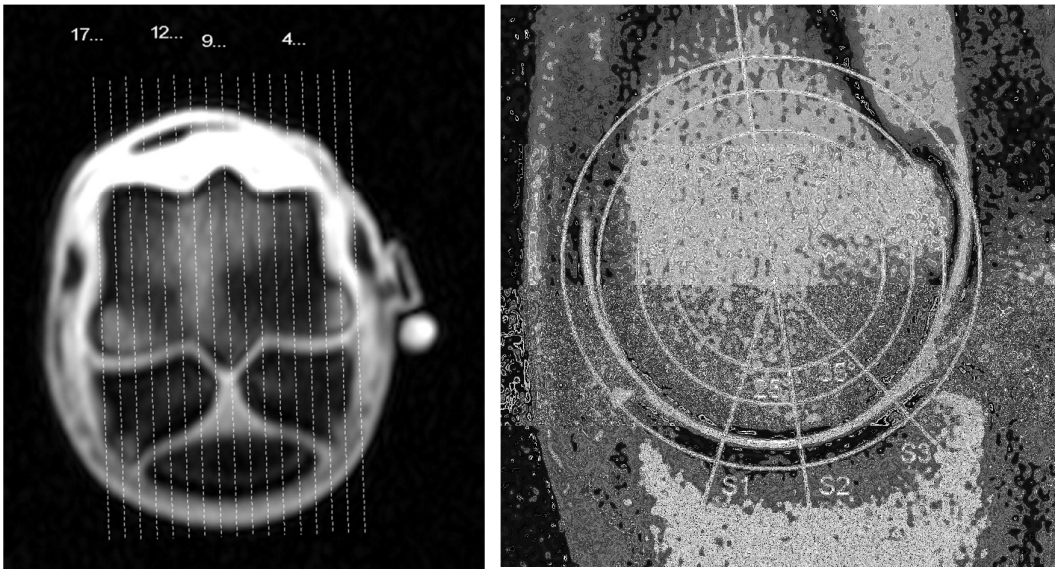

Figure 4.1 (A) Transverse pilot MRI image of the distal third metatarsal bone of a normal Thoroughbred horse, demonstrating how MRI slices were marked for histologic comparisons. A 17-line template has been placed on the slice and centered over the distal sagittal ridge. Slice 1 is positioned on the lateral epicondyle cortex and slice 17 is positioned slightly axial to the medial epicondyle cortex. A hyperintense vitamin E oil capsule has been used as a marker for the lateral metatarso-phalangeal joint surface. (B) Lateral midcondylar parasagittal PDw (of T2 mapping) MRI image with a representation of the translucent template illustrating concentric circles placed using a “best-of-fit” method over the third metacarpal condyle and with a line transecting the midline of the Mc3 distal metaphysis. Sites 1–3 are also identified (S = site).

To acquire the parasagittal images for dGEMRIC T1 relaxation time calculation, six precontrast inversion recovery sequences were performed on the mid lateral condyle for the hind limb and the mid medial condyle for the forelimb, respectively. As much synovial fluid as possible was aspirated from the palmar/plantar recess of the metacarpo/metatarsophalangeal joints to minimize dilution of the Gd-DTPA^{2-} and minimize fluid-related sources of

variability. Gadolinium-DTPA^{2-} (Magnevist®, gadopentetate dimeglumine, Bayer Health Care Pharmaceuticals, Isando, Gauteng, South Africa) was injected at 0.05 ml in 5 ml saline (0.025 mmol/joint). The joints were manually flexed at approximately one flexion per second for 5 min to ensure adequate contrast distribution in all parts of the joint. The same six inversion recovery T1 sequences as those used for precontrast images were repeated at 30, 60, 120, and 180 min postinjection and at the same midcondylar areas. The joint fluid was examined cytologically the following day and the balance aliquoted and frozen at –80° for later further analysis. Three distal articulation sites of Mc3/Mt3 were identified for histological and MRI measurements. Site 1 was defined based on a 25° dorsal angle and from a point in the centre of the rotation of the joint. Site 2 was defined as the distal aspect of a line drawn down the axis of the diaphysis of Mc3/Mt3 and corresponding to the transverse ridge. Site 3 was defined based on a 35° palmar/ plantar angle from a point in the centre of the rotation of the joint and using the sagittal template of slices 5 and 13 (Fig. 4.1 B). The palmar site location was chosen based on the site where cartilage injury has been previously reported, most often in conjunction with subchondral sclerosis and signs of fatigue condylar fractures.[42,43] The locations of sites 1–3 were chosen to be the same as sites previously evaluated by researchers studying stages of condylar fatigue fractures.[42]

The metacarpo-/metatarsophalangeal joints were radiographed and scanned with computed tomography and limbs discarded from this study if there were overt signs of pathology, such as osteochondritis dissecans or osteoarthritis changes with osteophytes larger than 2 × 2 mm. Metacarpus3 and Mt3 were dissected loose from the rest of the limb and the midmedial and midlateral condyles of Mc3 and Mt3, respectively, were identified using the transverse MRI template and sectioned into 3–5 mm thick slices using a band saw. The dorsal and medial aspects of each bone section were marked and the sample was placed into an 8% nitric acid made up in 10% buffered formalin solution for fixation and decalcification. The solution was replaced every week to optimize demineralization until the bone floated in the solution. Sites 1, 2, and 3 were identified using the sagittal template of the midmedial and midlateral distal condyles of Mc3 and Mt3, respectively, the cut blocks

processed, embedded into paraffin wax, sectioned on a rotary microtome and stained using standard Hematoxylin and Eosin. Sections were then mounted with Entellan (Merck Chemicals, Darmstadt, Germany). For cartilage thickness measurement analysis, the stained sections were viewed with a Nikon (Centurion, South Africa) light microscope equipped with an Axio Cam camera (Axiovision VS40V4.8.1.0 Carl Zeiss Imaging Solutions GmbH). Two observers measured cartilage thickness from the articular surface to the first Haversian canal (bone–cartilage interface) and from the articular surface to the mineralized cartilage interface (tidemark) if visible (Fig. 4.2).

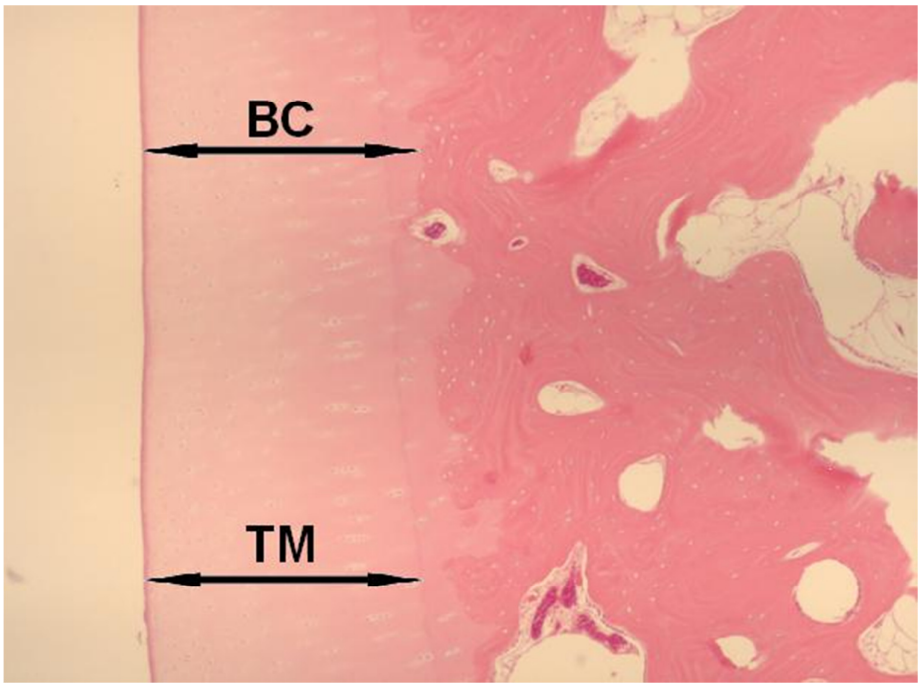

Figure 4.2. Hematoxylin and eosin histology slide indicating how measurements were made for the distance between the articular surface and the beginning of the Haversion canal system (BC, bone–cartilage interface), and the distance between the articular surface and the beginning of the mineralized cartilage interface (TM, calcified cartilage tide mark).

Three measurements were made at each site and the mean determined. Each set of metacarpo-/metatarsophalangeal measurements was acquired at least 5 days apart. To determine whether ROIs to be mapped on the T2 and dGEMRIC mapped images were representative of true cartilage dimensions,

the histomorphometric thicknesses of cartilage at sites 1–3 were compared to measurements from MRI images.[28] Cartilage thickness was measured using a Siemens SYNGO workstation (Siemens Healthcare, Erlangen, Germany). The optimal inversion recovery sequence for visualizing the surface of the cartilage was determined subjectively by the first author and based on an evaluation of all 600 inversion recovery series of the dGEMRIC mapping images (four limbs × five times (pre-Gd, 30, 90, 120, 180 min) × five sites (the extra two were not used in this study) × six different TIs = 600) of a randomly picked horse's distal Mc3/Mt3 (Horse 6). Each image was zoomed and panned into an optimal position where a translucent template (Fig. 4.1B) could determine the midline of the relevant condyle of Mc3/Mt3 and the centre of rotation of distal Mc3/Mt3. The optimal window was found using the windowing tool in the software package and the sites determined where the cartilage surface and bone–cartilage interface could best be identified. The mineralized cartilage interface could not be visualized so no attempt was made to measure this. Based on results of these assessments, the TI = 200 ms IR (STIR) in the 180-min post Gd-DTPA^{2-} time series was chosen as the best for measuring all horses' Mc3/Mt3 using the Syngo electronic callipers (Fig. 4.3 A). A similar procedure was used for the T2mapping TEs (using all 24 limbs × five sites × six TE = 720 sites) and the TE of 16.7 ms (PDw) was subjectively deemed the best image for visualizing the cartilage surface (Fig. 4.3 B). The thickness of the articular cartilage was then measured for sites 1–3 for all the PDw and STIR images of all 24 limbs, respectively, three times and the mean determined for each site and MRI measurement. This measurement procedure was repeated at least 2 months later by the same observer.

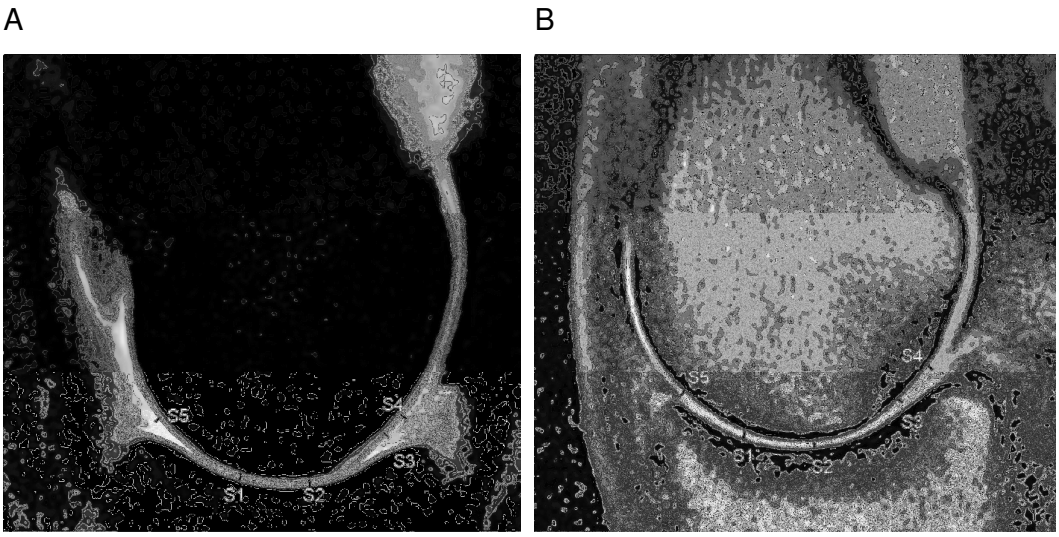

Figure 4.3. (A) STIR image at 180 min post Gd-DTPA^{2-} demonstrating a parasagittal slice of the distal mid-Mt3 condyle for Horse 5 and locations where the hyperintense articular cartilage depth was measured at sites 1–3. Window width 1734; window level 964. (B) Proton density weighted image of the distal mid Mc3 condyle for Horse 4, demonstrating where the hyperintense articular cartilage depth was measured at sites 1–3. Window width 1445; window level 706. Note that there is minimal synovial fluid within the joint and that this T2 image is prior to Gd injection. There is minimal fluid signal within the joint itself (S = site).

Histologic cartilage thicknesses were evaluated at Sites 1–3 by the same observer at least 3 months after the MRI measurements. Statistical analyses were performed using SPSS software (version 19, SPSS Inc., Chicago, IL, USA). The selection and conduction of all statistical tests were made in collaboration with statisticians. The level of significance for all tests was set at $P < 0.05$. Repeatability for cartilage thickness measurements was determined using the intraclass correlation coefficient (ICC), which represents the error free proportion of the intersubject score variation with a 95% confidence interval (CI). The ICC values above 0.75 were classified as good, values between 0.74 and 0.40 as moderate and values below 0.40 were deemed to have poor reliability[44] with a negative ICC also indicating low true intraclass correlation.[45] Differences between cartilage thickness measurements were tested using Wilcoxon signed rank tests, performed *post*

hoc. Forelimb and hindlimb cartilage thickness values (mm) recorded from histologic bone–cartilage interface, histologic mineralized cartilage interface, STIR and PDw were compared for sites 1, 2, and 3 separately as well as sites 1–3 combined using Wilcoxon signed rank tests.

4.4 RESULTS

Twenty limbs met the inclusion criteria and four limbs were excluded, two for osteoarthritis, one for synovitis, and the other for an osseous cyst-like lesion. T2 mapping data was lost in Horse 1 right and left hindlimbs, and Horse 2's right hindlimb due to technical errors; therefore, 17 limbs were available for T2 mapping ROI tracing. Means, standard deviations and intra and interobserver ICCs of cartilage thickness at sites 1–3 for bone– cartilage interface and mineralized cartilage interface, and combined sites 1–3, respectively, are summarized in Table 4.1.

TABLE 4.1 Mean and Standard Deviation Values for Histological Cartilage Thickness of Distal Metacarpal 3 /Metatarsal 3 at Sites 1–3, Measured at Least 5 Days Apart by Observers A and B.

	BC mm (SD)								
Site	Observer A				Observer B				
	1	2	ICC 1*vs*2	Mean 1&2	1	2	ICC 1 *vs* 2	Mean 1&2	ICC BC means of A1&2 *vs* B1&2
1	0.87 (0.11)	0.88 (0.10)	0.97	0.87 (0.10)	0.88 (0.10)	0.86 (0.07)	0.67	0.87 (0.07)	0.89
2	0.98 (0.08)	1.00 (0.67)	0.80	0.99 (0.07)	0.99 (0.06)	1.02 (0.15)	0.61	1.00 (0.1)	0.66
3	0.79 (0.14)	0.77 (0.10)	0.87	0.79 (0.11)	0.77 (0.08)	0.74 (0.12)	0.85	0.76 (0.09)	0.95
1-3	0.88 (0.08)	0.89 (0.06)	0.89	0.88 (0.07)	0.88 (0.05)	0.87 (0.07)	0.61	0.88 (0.05)	0.92
	TM (SD)								
Site	Observer A				Observer B				
	1	2	ICC 1 *vs* 2	Mean 1&2	1	2	ICC 1 *vs* 2	Mean 1&2	ICC means of A(1&2) *vs* B(1&2)
1	0.64 (0.1)	0.63 (0.09)	0.91	0.64 (0.09)	0.62 (0.10)	0.60 (0.08)	0.54	0.61 (0.07)	0.73
2	0.77 (0.09)	0.75 (0.09)	0.66	0.76 (0.07)	0.73 (0.08)	0.73 (0.24)	0.55	0.73 (0.14)	0.66
3	0.62 (0.12)	0.59 (0.06)	0.82	0.61 (0.09)	0.59 (0.05)	0.54 (0.11)	0.10	0.57 (0.06)	0.5
1-3	0.67 (0.07)	0.66 (0.05)	0.76	0.67 (0.05)	0.64 (0.05)	0.63 (0.08)	-0.21	0.63 (0.04)	0.37

BC: measurement from the articular surface to the beginning of the Haversian canals; TM: measurement from the articular surface to the beginning of the mineralized cartilage (tide mark); ICC = intraclass correlation coefficient; SD = standard deviation, mm = millimeters, Mc3 = metacarpal 3, Mt3 = metatarsal 3.

For histomorphometric cartilage thickness using the bone–cartilage interface, intraobserver repeatability for Observer A was good, with the least repeatable results at site 2 (ICC 0.80) and the most repeatable results at site 1 (0.97). Intraobserver repeatability for Observer B was good to moderate, with the most repeatable results at site 3 (0.85) and less repeatable results for site 2 (0.61). Repeatability based on means of Observer A1 and Observer A2 measurements and means of Observer B1 and Observer B2 measurements was good (≥ 0.89) for sites 1 and 3 and sites 1–3, and moderate (0.66) for site 2.

For histomorphometric cartilage thickness using the mineralized cartilage interface, intraobserver repeatability for Observer A was good at sites 1 and 3, with least repeatability for site 2 (0.66) and most repeatability for site 1 (0.91). Observer B measurements were moderately repeatable for sites 1 and 2, but poorly repeatable for site 3 (0.10). The repeatability between means of Observer A1 and Observer A2 measurements, versus means of Observer B1 and Observer B2 measurements, was moderate for sites 1, 2, and 3, respectively, and poor for sites 1–3.

Means, standard deviations and intraobserver ICCs of cartilages thicknesses at sites 1–3, separately, and 1–3 combined, for the STIR images at 180-min post Gd-DTPA^{2-} and the PDw images are summarized in Table 4.2.

For the STIR cartilage thickness measurements, Observer A showed good repeatability for site 3 (0.79), moderate repeatability for site 2 (0.58), and poor repeatability for Site 1 (0.11). For the PDw cartilage thickness measurements, Observer A showed good repeatability for site 1 (0.77), moderate repeatability for site 3 (0.69), and poor repeatability for site 2 (0.31).

TABLE 4.2. Mean and Standard Deviation Values for Cartilage Thickness of Distal Metacarpal 3 / Metatarsal 3, at Sites 1–3, Measured using a STIR Sequence at 180 min post Gd-DTPA^{2-} and a Proton Density weighted T2 Mapping Sequence, Repeated at Least 5 days Apart by Observer A.

Site	STIR (SD) mm				PDw (SD) mm			
	1	2	ICC 1 *vs*	mean 1&2	1	2	ICC 1 *vs* 2	mean 1&2
1	0.56 (0.06)	0.53 (0.02)	0.11	0.54 (0.04)	0.54 (0.08)	0.56 (0.07)	0.77	0.55 (0.07)
2	0.51 (0.07)	0.54 (0.07)	0.58	0.52 (0.06)	0.44 (0.05)	0.51 (0.06)	0.31	0.47 (0.05)
3	0.87 (0.13)	0.80 (0.15)	0.79	0.84 (0.13)	0.77 (0.1)	0.86 (0.13)	0.69	0.81 (0.11)
4	1.02 (0.06)	1.03 (0.08)	0.73	1.03 (0.06)	0.95 (0.1)	0.93 (0.06)	-0.15	0.94 (0.05)
5	0.94 (0.06)	0.91 (0.05)	0.74	0.92 (0.05)	0.83 (0.06)	0.85 (0.08)	0.91	0.84 (0.07)
1-3	0.65 (0.07)	0.62 (0.07)	0.48	0.63 (0.06)	0.71 (0.05)	0.74 (0.05)	0.47	0.72 (0.04)
1-5	0.78 (0.07)	0.76 (0.05)	0. 70	0.77 (0.05)	0.58 (0.05)	0.64 (0.05)	0.53	0.61 (0.04)

STIR = short tau inversion recovery; PDw = proton density weighted; ICC = intraclass correlation coefficient; SD = standard deviation, mm =millimeters, Mc3 = metacarpal 3, Mt3 = metatarsal 3.

Table 4.3 summarizes the Wilcoxon signed rank test results for cartilage thickness differences among histologic bone–cartilage interface, histologic mineralized cartilage interface, STIR, and PDw at sites 1–3 (separately and combined); and between STIR and PDw images at sites 1–3 (separately and combined). Histologic cartilage thickness measured using the bone–cartilage interface differed significantly from STIR and PDw measurements at sites 1 and 2 and at sites 1–3 combined, but not at site 3 ($P < 0.05$). Histologic cartilage thickness measured using the mineralized cartilage interface differed significantly from STIR and PDw measurements at site 2 and differed from PDw at site 3 and sites 1–3 combined ($P < 0.05$). Histologic cartilage thickness measured using the mineralized cartilage interface differed moderately from STIR cartilage thickness at sites 1 and 3 ($P = 0.063$).[46] Cartilage thickness from PDw did not significantly differ from STIR cartilage thickness at any sites. No differences were found between forelimb and hind limb cartilage thickness values for all measurement methods; sites 1, 2, and 3 separately; and sites 1–3 combined using Wilcoxon signed rank tests and $P < 0.05$.

TABLE 4.3. Mean, Standard Deviation Values and Wilcoxon Signed Rank Evaluation of Mean Measurements of Cartilage Thickness of Distal Metacarpal 3/ Metatarsal 3 Measured by Observer A, at Sites 1–3 using MRI and Histologic Techniques.

Site	Histomorphometric (SD)		STIR (SD)	PDw (SD)	Wilcoxon signed rank test	
	BC mm	TM mm	mm	mm	Technique comparison	p
1	0.87 (0.10)	0.64 (0.09)	0.54 (0.04)	0.55 (0.07)	BC vs STIR	0.031*
					BC vs PDw	0.031*
					TM vs STIR	0.063
					TM vs PDw	0.063
					PDw vs STIR	0.563
2	0.99 (0.07)	0.76 (0.07)	0.52 (0.06)	0.47 (0.05)	BC vs STIR	0.031*
					BC vs PDw	0.031*
					TM vs STIR	0.031*
					TM vs PDw	0.031*
					PDw vs STIR	0.688
3	0.79 (0.11)	0.61 (0.09)	0.84 (0.13)	0.81 (0.11)	BC vs STIR	0.69
					BC vs PDw	0.563
					TM vs STIR	0.063
					TM vs PDw	0.031*
					PDw vs STIR	0.688
4	-	-	1.03 0.06)	0.94 (0.05)	STIR vs PDw	0.156
5	-	-	0.92 (0.05)	0.84 (0.07)	STIR vs PDw	0.031*
1-3	0.88 (0.07)	0.67 (0.05)	0.63 (0.06)	0.61 (0.04)	BC vs STIR	0.031*
					BC vs PDw	0.031*
					TM vs STIR	0.688
					TM vs PDw	0.031*
					PDw vs STIR	0.563
1-5	-	-	0.77 (0.05)	0.72 (0.04)	PDw vs STIR	0.156

STIR (short tau inversion recovery) = IR measured on TI = 200 ms at 180 min post Gd-DTPA^{2-} sequence; PDw (proton density weighted) = a T2 mapping sequence at TE = 16.7 ms; Wilcoxon signed rank test (two-tailed). Significant differences at $P < 0.05$ are marked with*. BC = articular surface to bone–cartilage interface; TM = articular surface to beginning of mineralized cartilage; SD = standard deviation, mm = millimeters, Mc3 = metacarpal 3, Mt3 = metatarsal 3.

4.5 DISCUSSION

The most important finding in this study was that the histological bone interface cartilage thickness and the STIR and PDw cartilage thicknesses of Mc3/Mt3 did not differ significantly when the distal Mc3/Mt3 was not in contact with the proximal phalanx, validating the STIR and PDw measurements for later studies using these sequences and particularly dGEMRIC and T2 mapping of articular cartilage of the distal Mc3/Mt3. It has previously been reported that cartilage thickness for dorsal and palmar sites of distal Mc3 in racehorses is approximately 0.79 ± 0.16 mm when measured histologically, and 0.90 ± 0.17 mm when measured using fat-suppressed spoiled gradient-recalled images.[47] The current study's mean histological cartilage thickness measurement was slightly higher, which could be a result of individual observer technique, e.g. Observer A and B's measurements did differ significantly at some sites. Overestimation of cartilage thickness when the actual thickness is less than 1 mm thick has been observed with MRI based 3D cartilage models.[48] This is similar to findings in the current study where the STIR and PDw bone–cartilage interface measurements were larger than the histomorphometric dimensions at site 3 where the cartilage surface could be seen and less at sites 1 and 2 where the cartilage made contact with phalanx 1. For sites 1 and 2, when windowing the STIR and PDw images to attempt to identify the articular cartilage surface, partial volume averaging of the thin intra-articular space (often on the 1-pixel threshold) tended to determine the boundary between the articular surfaces of distal Mc3/Mt3 and proximal phalanx to be half way between them, resulting in a halving of the measured distance. In a previous human knee cartilage report, the weight bearing and central areas on each femoral and tibial condyle yielded more accurate measurements than boundary and non-weight bearing regions based on sagittal plane MR imaging.[8] However, the normal human knee cartilage is 1.3 to 2.5 mm thick vs. the approximately 1 mm thickness of the distal Mc3/Mt3 horse cartilage. Human knee cartilage also has a meniscus that is not present in the equine metacarpo/metatarsophalangeal joint, therefore similar comparisons with the equine Mc3/Mt3 joint cannot be made.[49] The use of traction to separate the two cartilage surfaces and better evaluate them has

been described in human knees[50] and should therefore be considered in the future when evaluating the metacarpo/metatarsophalangeal cartilages using dGEMRIC and T2 mapping in the horse and in the clinical setting.

Histomorphometrically, the bone–cartilage interface measurements of cartilage thickness were consistently higher than the mineralized cartilage interface measurements. This finding was expected, since the tideline of calcified cartilage is found in the articular cartilage between the Haversian canals and the cartilage surface. The amount of mineralized cartilage interface measurements that could be made with confidence were less than the bone–cartilage interface measurements, because the border of the mineralized cartilage could not be clearly ascertained in several of the slides.

Mineralized cartilage interface cartilage thicknesses were consistently found to be higher than STIR and PDw measurements at sites 1 and 2, but lower at site 3, likely for the same reason as for the bone–cartilage interface measurements. These findings support previously reported findings where MRI measurements of equine carpal cartilage were significantly greater than the histologic measurements.[28]

The subjective choice of STIR and PDw sequences as being the best for visualizing cartilage in the current study was supported by the fact that TI = 200 ms is quite close to STIR imaging at 1.5T (where TI = 150 ms), which means that the fat signal of the image is close to zero, and cartilage with relatively high water content can be well differentiated from its surroundings. For T2, the image with the shortest TE has the best signal-to-noise ratio and least T2 weighting, therefore closer to a proton density weighting, which yields a good contrast between cartilage and surrounding tissues. One possible limitation of the study was that only one horse's limb was used to determine the selection of these sequences. However, a very rigorous review process was followed for all the limbs to ensure the cartilage examined was as normal as possible. Also, the MRI properties of fat and water were expected to be constant and behave similarly when using a constant set of imaging parameters at a constant field strength.

It was encouraging that findings from the current study indicated that intraobserver repeatability of MRI measurements was good to moderate where cartilage was not in contact with other cartilage. This finding was

similar to previously published findings.[29–31] One limitation of the current study was that no interobserver comparisons were made. However, previous studies have found good interobserver repeatability for MRI measurements.

Another limitation of the current study was that histomorphometric measurements were not measured at more sites away from adjacent cartilage. Histomorphometric cartilage thickness measurements of the dorsal and palmar aspects of distal Mc3 have not been found to differ in previous studies.[47] Therefore, it is reasonable to assume that measurements from these sites would be relatively similar to site 3's measurements.

If a higher field strength magnet had been used, higher resolution images could have resulted in superior cartilage thickness measurements as has been reported in a human study comparing 3T with 1.5T images. However, even in that study, correlation coefficients for values obtained at 3T and 1.5T were high.[51] Using thinner slices for MRI scans was considered for the current study, but this would have resulted in a lower signal-to-noise ratio and would have been more time consuming. The effect of slice thickness on assessment of human knee cartilage volume has been previously reported and findings indicated that there was little difference in human tibial cartilage volume as slice thickness increased from 1.5 to 7.5 mm.[52] Conclusions from the previous study were that increasing slice thicknesses could be used and that this would result in decreased acquisition and post processing times. However, since human knee cartilage thickness is much greater than that of the equine fetlock, this extrapolation may not be valid in equine fetlock joints. Cartilage curvature is another important factor to consider. If cartilage is very thin but not curved in the region being evaluated, thicker slices will also give reliable results. The small sites evaluated in the distal Mc3/Mt3 had very little curvature. Another limitation to this study was the relatively low number of horses and limbs used, decreasing the power of the findings.

In spite of these limitations, bone–cartilage interface histomorphometric cartilage thickness measurements did not differ from MRI measurements using a selected inversion recovery sequence for dGEMRIC mapping, and a selected time to echo image for T2 mapping in the palmaro/plantarodistal aspect of the distal Mc3/Mt3. This finding validates the use of dGEMRIC and T2 mapping for measuring cartilage thickness in locations where cartilage is

not in close approximation to opposing adjacent cartilage in Mc3/Mt3 of Thoroughbred horses. Future studies are needed to evaluate these dGEMRIC and T2 mapping techniques in live horses with and without joint disease.

ACKNOWLEDGEMENTS

The authors thank the Pretoria MR Trust for the use of the MRI machine and their radiographers who helped so ably; also the radiographers of the Onderstepoort Veterinary Academic Hospital, the entire staff of the Highveld Horsecare Unit, Meyerton, South Africa and Mrs Joyce Jordaan, data analyst from the Department of Statistics, University of Pretoria, South Africa.

REFERENCES

1. Dyson PK, Jackson BF, Pfeiffer DU, Price JS. Days lost from training by two- and three-year-old Thoroughbred horses: a survey of seven UK training yards. Equine Vet J 2008;40:650–657.

2. Perkins NR, Reid SW, Morris RS. Profiling the New Zealand Thoroughbred racing industry. 2. conditions interfering with training and racing. N Z Vet J 2005;53:69–76.

3. Parente EJ, Russau AL, Birks EK. Effects of mild forelimb lameness on exercise performance. Equine Vet J Suppl 2002;34:252–256.

4. Hernandez J, Hawkins DL. Training failure among yearling horses. Am J Vet Res 2001;62:1418–1422.

5. Bailey CJ, Reid SW, Hodgson DR, Bourke JM, Rose RJ. Flat, hurdle and steeple racing: risk factors for musculoskeletal injury. Equine Vet J 1998;30:498–503.

6. Olivier A, Nurton JP, Guthrie AJ. An epizoological study of wastage in Thoroughbred racehorses in Gauteng, South Africa. J S Afr Vet Assoc 1997;68:125–129.

7. Anonymous. A comparison of the economic costs of equine lameness, colic, and equine protozoal myeloencephalitis (EPM) in the United States. Animal and Plant Health Inspection service. 2001. Available at http://www.aphis.usda.gov/animal_health/nahms/equine/downloads/equine98/Equine98_is_Colic.pdf. (accessed May 2011).

8. Broster CE, Burn CC, Barr AR, Whay HR. The range and prevalence of pathological abnormalities associated with lameness in working horses from developing countries. Equine Vet J 2009;41:474–481.

9. de Grauw JC, van de Lest CH, van Weeren R, Brommer H, Brama PA. Arthrogenic lameness of the fetlock: synovial fluid markers of inflammation and cartilage turnover in relation to clinical joint pain. Equine Vet J 2006;38:305–311.

10. Wilsher S, Allen WR, Wood JL. Factors associated with failure of thoroughbred horses to train and race. Equine Vet J 2006;38:113–118.

11. Dabareiner RM, Cohen ND, Carter GK, Nunn S, Moyer W. Musculoskeletal problems associated with lameness and poor performance among horses used for barrel racing: 118 cases (2000–2003). J Am Vet Med Assoc 2005;227:1646–1650.

12. Rossdale PD, Hopes R, Digby NJ, Offord K. Epidemiological study of wastage among racehorses 1982 and 1983. Vet Rec 1985;116:66–69.

13. Bailey CJ, Reid SW, Hodgson DR, Rose RJ. Impact of injuries and disease on a cohort of two- and three-year-old Thoroughbreds in training. Vet Rec 1999;145:487–493.

14. Brommer H, van Weeren PR, Brama PA, Barneveld A. Quantification and age-related distribution of articular cartilage degeneration in the equine fetlock joint. Equine Vet J 2003;35:697–201.

15. Pool RR. Pathologic manifestations of joint disease in the athletic horse. In: McIlwraith CW, Trotter GW (eds): Joint disease in the horse. Philadelphia: W. B. Saunders Co., 1996;87–104.

16. McIlwraith CW. General pathology of the joint and response to injury. In: McIlwraith CW, Trotter GW (eds): Joint disease in the horse. Philadelphia: W. B. Saunders Co., 2006;40–70.

17. Martel-Pelletier J. Pathophysiology of osteoarthritis. Osteoarthr Cartilage 2004;12(Suppl A):S31–S33.

18. Pearle AD, Warren RF, Rodeo SA. Basic science of articular cartilage and osteoarthritis. Clin Sports Med 2005;24:1–12.

19. Rannou F, Sellam J, Berenbaum F. Pathophysiology of osteoarthritis: updated concepts. Presse Med 2010;39:1159–1163.

20. Goldring MB, Goldring SR. Osteoarthritis. J Cell Physiol 2007;213:626–634.

21. Gold GE, Burstein D, Dardzinski B, Lang P, Boada F, Mosher T. MRI of articular cartilage in OA: novel pulse sequences and compositional/functional markers. Osteoarthr Cartilage 2006;14 Suppl A:A76– A86.

22. Guermazi A, Burstein D, Conaghan P, et al. Imaging in osteoarthritis. Rheum Dis Clin North Am 2008;34:645–687.

23. Trattnig S, Domayer S, Welsch GW, Mosher T, Eckstein F. MR imaging of cartilage and its repair in the knee -a review. Eur Radiol 2009;19:1582–1594.

24. Roemer FW, Eckstein F, Guermazi A. Magnetic resonance imaging-based semiquantitative and quantitative assessment in osteoarthritis. Rheum Dis Clin North Am 2009;35:521–555.

25. Potter HG, Black BR, Chong le R. New techniques in articular cartilage imaging. Clin Sports Med 2009;28:77–94.

26. Domayer SE, Welsch GH, Dorotka R, et al. MRI monitoring of cartilage repair in the knee: a review. Semin Musculoskelet Radiol 2008;12:302–317.

27. Goodwin DW. Visualization of the macroscopic structure of hyaline cartilage with MR imaging. Semin Musculoskelet Radiol 2001;5:305–312.

28. Murray RC, Branch MV, Tranquille C, Woods S. Validation of magnetic resonance imaging for measurement of equine articular cartilage and subchondral bone thickness. Am J Vet Res 2005;66:1999–2005.

29. Zuo J, Bolbos R, Hammond K, Li X, Majumdar S. Reproducibility of the quantitative assessment of cartilage morphology and trabecular bone structure with magnetic resonance imaging at 7T. Magn Reson Imaging 2008;26:560–566.

30. Naish JH, Xanthopoulos E, Hutchinson CE, Waterton JC, Taylor CJ. MR measurement of articular cartilage thickness distribution in the hip. Osteoarthr Cartilage 2006;14:967–973.

31. McGibbon CA. Inter-rater and intra-rater reliability of subchondral bone and cartilage thickness measurement from MRI. Magn Reson Imaging 2003;21:707–714.

32. Graichen H, von Eisenhart-Rothe R, Vogl T, Englmeier KH, Eckstein F. Quantitative assessment of cartilage status in osteoarthritis by quantitative magnetic resonance imaging: technical validation for use in analysis of cartilage volume and further morphologic parameters. Arthritis Rheum 2004;50:811–816.

33. Graichen H, Jakob J, von Eisenhart-Rothe R, Englmeier KH, Reiser M, Eckstein F. Validation of cartilage volume and thickness measurements in the human shoulder with quantitative magnetic resonance imaging. Osteoarthr Cartilage 2003;11:475–482.

34. Raynauld JP, Martel-Pelletier J, Abram F, et al. Analysis of the precision and sensitivity to change of different approaches to assess cartilage loss by quantitative MRI in a longitudinal multicenter clinical trial in patients with knee osteoarthritis. Arthritis Res Ther 2008;10:R129, doi:10.1186/ar2543.

35. Bolbos R, Benoit-Cattin H, Langlois JB, et al. Measurement of knee cartilage thickness using MRI: a reproducibility study in a meniscectomized guinea pig model of osteoarthritis. NMR Biomed 2008;21:366– 375.

36. Bolbos R, Benoit-Cattin H, Langlois JB, et al. Knee cartilage thickness measurements using MRI: a 4(1/2)-month longitudinal study in the meniscectomized guinea pig model of OA. Osteoarthr Cartilage 2007;15: 656–665.

37. Kauffmann C, Gravel P, Godbout B, et al. Computer-aided method for quantification of cartilage thickness and volume changes using MRI: validation study using a synthetic model. IEEE Trans Biomed Eng 2003;50:978– 988.

38. Brem MH, Lang PK, Neumann G, et al. Magnetic resonance image segmentation using semi-automated software for quantification of knee artticular cartilage-initial evaluation of a technique for paired scans. Skeletal Radiol 2009;38:505–511.

39. Koo S, Giori NJ, Gold GE, Dyrby CO, Andriacchi TP. Accuracy of 3D cartilage models generated from MR images is dependent on cartilage thickness: laser scanner based validation of *in vivo* cartilage. J Biomech Eng 2009;131:121004, doi:10.1115/1.4000087.

40. Hannila I, Nieminen MT, Rauvala E, Tervonen O, Ojala R. Patellar cartilage lesions: comparison of magnetic resonance imaging and T2 relaxation-time mapping. Acta Radiol 2007;48:444–448.

41. Multanen J, Rauvala E, Lammentausta E, et al. Reproducibility of imaging human knee cartilage by delayed gadolinium-enhanced MRI of cartilage (dGEMRIC) at 1.5 Tesla. Osteoarthr Cartilage 2009;17: 559–564.

42. Firth EC, Doube M, Boyde A. Changes in mineralised tissue at the site of origin of condylar fracture are present before athletic training in Thoroughbred horses. NZ Vet J 2009;57:278–283.

43. O'Brien T, Baker TA, Brounts SH, et al. Detection of articular pathology of the distal aspect of the third metacarpal bone in Thoroughbred racehorses: comparison of radiography, computed tomography and magnetic resonance imaging. Vet Surg 2011;40:942–951.

44. Bland JM, Altman DG. Measurement error and correlation coefficients. BMJ 1996;313:41–42.

45. Taylor PJ. An introduction to intraclass correlation that resolves some common confusions. 2011 Available at http://faculty.umb.edu/pjt/9b.pdf (accessed July 21, 2011).

46. Albright SC, Winston WL, Zappe CJ. Statistical inference. In: Albright SC, Winston WL, Zappe CJ (eds): Data analysis and decision making, 4th ed. Australia: South-Western Cengage Learning, 2010; 503.

47. Olive J, D'Anjou MA, Girard C, Laverty S, Theoret C. Fat-suppressed spoiled gradient-recalled imaging of equine metacarpophalangeal articular cartilage. Vet Radiol Ultrasound 2010;51:107– 115.

48. Koo S, Gold GE, Andriacchi TP. Considerations in measuring cartilage thickness using MRI: factors influencing reproducibility and accuracy. Osteoarthr Cartilage 2005;13:782–789.

49. Eckstein F, Reiser M, Englmeier KH, Putz R. *In vivo* morphometry and functional analysis of human articular cartilage with quantitative magnetic resonance imaging-from image to data, from data to theory. Anat Embryol 2001;203:147–173.

50. Nakanishi K, Tanaka H, Nishii T, Masuhara K, Narumi Y, NakamuraH. MR evaluation of the articular cartilage of the femoral head during traction. Correlation with resected femoral head. ActaRadiol 1999;40:60–63.

51. Eckstein F, Charles HC, Buck RJ, et al. Accuracy and precision of quantitative assessment of cartilage morphology by magnetic resonance imaging at 3.0T. Arthritis Rheum 2005;52:3132–3136.

52. Cicuttini F, Morris KF, GlissonM,Wluka AE. Slice thickness in the assessment of medial and lateral tibial cartilage volume and accuracy for the measurement of change in a longitudinal study. J Rheumatol 2004;31:2444–2448.

CHAPTER 5

Feasibility for mapping cartilage T1 relaxation times in the distal metacarpus3/metatarsus3 of Thoroughbred racehorses using delayed gadolinium enhanced magnetic resonance imaging of cartilage (dGEMRIC): normal cadaver study

Ann Carstens, Robert M. Kirberger, Mark Velleman, Leif E. Dahlberg, Lizelle Fletcher, Eveliina Lammentausta

Keywords: Cartilage, gGEMRIC, horse, metacarpus, metatarsus, MRI, T1 mapping

From the Section Diagnostic Imaging, Department of Companion Animal Clinical Studies, Faculty of Veterinary Science, University of Pretoria, Private Bag X04 Onderstepoort 0110 (Carstens, Kirberger), Pretoria South Africa; Little Company of Mary Hospital, George Storrar Ave. (Velleman), Pretoria South Africa; Joint and Soft Tissue Unit, Department of Clinical Sciences, Malmö, Lund University, Department of Orthopaedics, Malmö University Hospital, SE-205 02 (Dahlberg, Lammentausta), Malmö, Sweden; Department of Statistics, University of Pretoria (Fletcher), Pretoria South Africa; Department of Diagnostic Radiology, Oulu University Hospital, POB 50, FI-90029 OYS (Lammentaust), Oulu, Finland.

As published in Veterinary Radiology and Ultrasound (early view),2013;DOI:10.1111/vru.12030

5.1 ABSTRACT

Osteoarthritis of the metacarpo/metatarsophalangeal joints is one of the major causes of poor performance in horses. Delayed gadolinium-enhanced magnetic resonance imaging of cartilage (dGEMRIC) may be a useful technique for non-invasively quantifying articular cartilage damage in horses. The purpose of this study was to describe dGEMRIC characteristics of the distal metacarpus3/metatarsus3 (Mc3/Mt3) articular cartilage in twenty cadaver specimens collected from normal Thoroughbred horses. For each specimen, T1 relaxation time was measured from scans acquired pre-contrast and at 30, 60, 120 and 180 minutes post intra-articular injection of Gd-DTPA^{2-} (dGEMRIC series). For each scan, T1 relaxation times were calculated using five regions of interest (sites 1-5) in the cartilage. For all sites, a significant decrease in T1 relaxation times occurred between pre-contrast scans and 30, 60, 120 and 180 min scans of the dGEMRIC series (P<0.0001). A significant increase in T1 relaxation times occurred between 60 and 180 min and between 120 and 180 min post Gd-injection for all sites. For sites 1-4, a significant increase in T1 relaxation time occurred between 30 and 180 min post-injection (P<0.05). Sites 1-5 differed significantly among one another for all times (P<0.0001). Findings from this cadaver study indicated that dGEMRIC using intra-articular Gd-DTPA^{2-} is a feasible technique for measuring and mapping changes in T1 relaxation times in equine metacarpo/metatarsophalangeal joint cartilage. Optimal times for post-contrast scans were 60-120 minutes. Future studies are needed to determine whether these findings are reproducible in live horses.

5.2 INTRODUCTION

Lameness in horses is the primary cause of poor performance and wastage. [1-3] Costs to the horse industry in North America were an estimated $1 billion in 1998. [4] The fetlock (metacarpo/metatarsophalangeal) joint is commonly affected by trauma, degeneration, [5] and osteoarthritis. [6] Lesions often involve both lateral and medial condyles of distal metacarpus3/metatarsus3 (Mc3/Mt3). [7, 8] Osteoarthritis is defined as degeneration of articular cartilage and is characterized by matrix fibrillation, fissures, ulceration and full-thickness loss of cartilage. [9] Diagnosis of osteoarthritis in the metacarpo/ metatarsophalangeal joints of horses is based on clinical evaluation, perineural or intra-articular nerve blocks, and combinations of radiography, ultrasonography, computed tomography, scintigraphy and magnetic resonance imaging (MRI). Many of these modalities detect disease only after the degenerative process has become advanced. [10,11]

Magnetic resonance imaging has been previously established as a method for visualizing early articular cartilage pathology in human studies.[12,13] In delayed gadolinium-enhanced MRI of cartilage (dGEMRIC), negatively charged Gd-DTPA^{2-} is injected either intra-articularly or intravenously. The contrast agent penetrates hyaline cartilage and distributes in an inverse relationship to the proteoglycan content of the cartilage. When the proteoglycan concentration is decreased as result of cartilage degradation, as seen in osteoarthritis, the gadolinium uptake is increased as result of the relative decrease in negative charge of the proteoglycan-depleted cartilage. This dGEMRIC technique has been described as an excellent indicator of degenerative cartilaginous changes and has been found to correlate with mechanical properties of cartilage such as cartilage stiffness.[14, 11] Parametric mapping of cartilage can be accomplished by post-processing dGEMRIC images and creating relaxation time colour maps. These maps provide a visual representation of relaxation times within specific cartilage locations.

The use of dGEMRIC has been reported once in a group of ponies, where it was used to test effects of administered bone morphogenic protein in experimentally-created femoral condyle lesions.[16] The adjacent non-injured

cartilage had significantly lower dGEMRIC T1 relaxation times than lesion repair tissue at 12 weeks post lesion creation. At 52 weeks, dGEMRIC T1 relaxation times were lower in both the lesion and the adjacent cartilage. Authors proposed that these findings could have been due to early osteoarthritis or because the bone morphogenic protein caused cartilage degeneration. Other proposed theories were that changes were caused by immobilization and un-loading of the cartilage because of pain. Other experimental animal studies and dGEMRIC studies have found that un-loaded cartilage has a lower dGEMRIC T1 relaxation time after compression.[17]

The purposes of the current study were to determine the feasibility of dGEMRIC mapping in the metacarpo/metatarsophalangeal joint of horses and optimal imaging times post intra-articular administration of Gd-DTPA^{2-} into the same joint. Our hypothesis was that T1 relaxation times for 5 sites within the articular cartilage of distal Mc3/Mt3 would decrease after intra-articular injection of Gd-DTPA^{2-}.

5.3 METHODS

This project was approved by the Animal Use and Care Committee of the Faculty of Veterinary Science University of Pretoria and all horses were treated according to South African Veterinary Council ethical standards. Six Thoroughbred horses were prospectively recruited from the Highveld Horsecare Unit, Meyerton, South Africa. Study inclusion criteria were as follows: age 3-6 years, any gender, no signs of lameness and no history of recent corticosteroid or proteoglycan treatments. Horses meeting inclusion criteria underwent a clinical examination to confirm absence of lameness. Immediately following the examination, horses were shot intra-cranially and all four limbs were removed at the mid Mc3/Mt3 diaphyses. Limbs were kept cool and transported to a magnetic resonance imaging (MRI) facility. A vitamin E oil capsule was taped to the lateral aspect of each metacarpo/metatarsophalangeal joint and each limb was positioned with the dorsum facing downward and the toe facing into the gantry. A head and neck 12-channel radiofrequency coil was used. The forelimbs were first scanned in

random order using a 1.5 T MRI scanner (Avanto, Siemens Healthcare. Erlangen, Germany). The hind limbs were then scanned in random order using the same scanner. All limbs were scanned at room temperature (20℃). For each joint, T1 weighted images were acquired in the sagittal plane (TR 557 ms, TE 23 ms, field of view (FOV) 100x100 mm, matrix 256x256, slice thickness 3 mm, receiver band-width 130 Hz/pix). Seventeen slices were acquired with the central slice positioned in the middle of the distal Mc3/Mt3 sagittal ridge. (Fig. 5.1 A).

A B

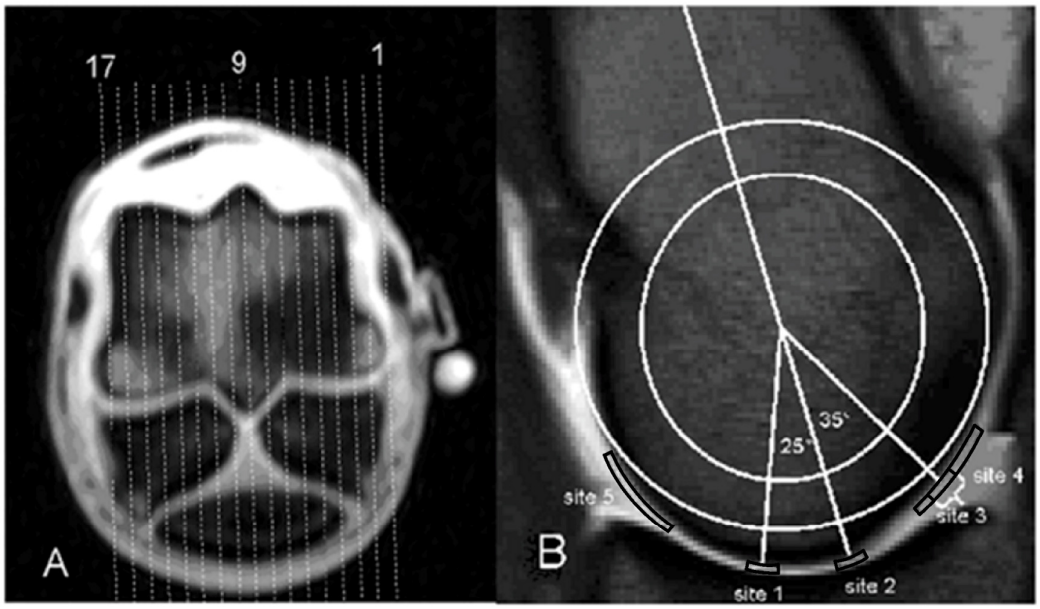

Figure 5.1. (A) Transverse MRI image of a distal Mt3 with a 17 line template with the central slice 9 placed sagitally over the distal sagittal ridge, slice 1 positioned on the lateral, and slice 17 positioned slightly beyond the medial epicondyle cortices. Note the hyperintense vitamin E oil capsule on the lateral epicondylar surface. (B) Parasagittal mid-condylar MRI image of distal Mc3/Mt3 with representation of the translucent template illustrating concentric circles placed “best-of-fit” over the condyle with a line transecting the midline of Mc3/Mt3 diaphysis/distal metaphysis. Region of interest sites are outlined. Sites 1-3 are identified. Site 4 is where cartilage is clearly defined at the edges of palmar/plantar articulations and site 5 is where cartilage is clearly defined at the edges of dorsal articulations.

For each lateral and medial midcondylar slice, pre-contrast T1 relaxation time was measured using single slice inversion recovery spin echo

sequences (TR 3000 ms, TE 13 ms, six TIs between 100 and 2800 ms, FOV 140x140 mm, matrix 256x256 mm, slice thickness 3 mm, receiver band-width 130 Hz/pix). Subsequently, joint fluid was aspirated from each joint and Gd-DTPA^{2-} (Magnevist®, gadopentetate dimeglumine, Bayer Health Care Pharmaceuticals. Bayer (Pty.)Ltd. 27 Wrench Road, Isando, 1600, South Africa) was injected using a dose of 0.05 ml in 5 ml saline (0.025 mmol/joint). Joints were manually flexed at one flexion per second for 5 minutes. Using the same mid-condylar slice locations as those used for the pre-contrast scans, T1 relaxation time measurements were repeated at 30, 60, 120, and 180 minutes post-injection. Following MRI examinations, joints were evaluated using radiography and computed tomography. Joints with gross abnormalities were excluded from further analyses.

Five sites were analysed for each mid-condylar slice and each scan. Site 1 was defined using a 25° dorsal angle from a point in the center of the rotation of the joint. Site 2 was defined as the distal aspect of a line drawn down the axis of the diaphysis of Mc3/Mt3 and corresponding to the transverse ridge. Site 3 was defined using a 35° palmar/plantar angle from a point in the center of the rotation of the joint. Sites 4 and 5 were defined as the most palmar/planter and dorsal locations where Mc3 and Mt3 cartilage could be clearly distinguished from adjacent first phalanx cartilage (Fig. 5.1 B). Often site 3 was partially or totally included within site 4.Immediately following imaging, each Mc3 and Mt3 bone was dissected away from the rest of the limb and the distal condylar cartilage surface was evaluated macroscopically before and after 3-5 minute staining with India ink (Parker Quink Ink, Post Net Suite #283, Private Bag X1005, Claremont, 7735, South Africa). All cartilage and synovial tissues were examined, and gross abnormalities recorded. The cartilage was also graded using the Neundorf grading system.[18] Only joints with Grade 1 cartilage were used for further analyses. Grade1 was defined using the following criteria: no gross abnormalities, minimal loss of reflectance, minimal cartilage hypertrophy at the joint margins, minimal partial thickness wear lines, minimal thinning of cartilage, minimal thickening of cartilage, and no enlarged synovial fossae. Mid-portions of the medial and lateral condyles of Mc3 and Mt3 were sectioned into 3-5 mm thick slices in a sagittal plane. The samples were fixed

and decalcified in an 8% nitric acid made up in 10% buffered formalin solution. Sites 1, 2 and 3 were identified using a sagittal template of the corresponding lateral and medial condyles (Fig. 5.1 B). Each cut block was processed and stained using standard hematoxylin and eosin. The cartilage at sites 1-3 for each mid-condylar slice was evaluated for pathology using a modification of an Osteoarthritis Research Society International (OARSI) microscopic cartilage grading system.[19] Only cartilage with a grade less than 2 was used for further analyses.

5.3.1 dGEMRIC Data Analysis

Full-thickness regions of interest (ROIs) were placed on sites 1-3 by one of the authors (AC) Each ROI extended 3°on either side of the template lines. Each ROI was manually positioned between the cartilage bone interface and the articular surface at site 3. The ROIs for sites 1 and 2 were positioned adjacent to the bone-cartilage interface of phalanx 1 since the cartilage surface could not be positively identified in most of the limbs at these sites. Larger regions of interest were segmented at sites 4 and 5 from the bone-cartilage interface to the articular surface of Mc3/Mt3 which was clearly visible at these sites (Fig. 5.1 B). T1 maps were created by fitting the respective data into mono-exponential relaxation equations using an in-house MATLAB application (MATLAB, MathWorks Inc., Natick, MA, USA). Mean values for each ROI were calculated.

5.3.2 Statistical Analysis

All statistical tests were selected and performed by a statistician. Non-parametric Friedman tests (SAS. Version 9.2, 2011, SAS Institute, Cary, NC, USA) were used to compare T1 relaxation times for pooled limbs across the five time periods. For comparisons with significant differences from these tests, Wilcoxon signed rank tests were performed *post hoc*. The level of significance for all tests was defined as $P< 0.05$. An effect size (r) was calculated for significant results. A small effect was defined as $0.1<r<0.3$; medium effect $0.3<r<0.5$; and large effect $r \geq 0.5$.

5.4 RESULTS

Of the 24 limbs collected, 20 met all inclusion criteria and four were excluded. Two were excluded for osteoarthritis, one for an osseous cyst-like lesion and one for synovitis. It took 12 minutes per limb to acquire the 6 inversion recovery images required for T1 mapping analyses.

Table 5.1 summarizes T1 relaxation times measured at each time interval for all 5 cartilage sites and results of the Friedman tests. Figure 5.2 demonstrates a representative set of colour maps at sites 1-5 prior to injection of Gd-DTPA^{2-} and at 30, 60, 120 and 180 minutes post injection. A higher relaxation time range was set for the pre-contrast series (0-2000 ms) than the post-contrast series (0-1300 ms).

The T1 relaxation times measured at the 5 sites are graphically displayed in Figure 5.3. A significant decrease in T1 relaxation time occurred at Sites 1-5 between pre-contrast and 30, 60, 120 and 180 min dGEMRIC series ($P \leq 0.0001$; Friedman ANOVA). All sites had a significant increase in T1 relaxation time between 60 and 180 min, and between 120 and 180 min post–contrast.

TABLE 5.1. Mean (and standard deviation) Delayed Gadolinium Enhanced Magnetic Resonance Imaging of Cartilage (dGEMRIC) T1 Relaxation Times (in ms) of the Distal Metacarpus3/Metatarsus3 Cartilage (sites 3-5) and Metacarpus3/Metatarsus3-Proximal Phalanx Combined Cartilage (sites 1-2) per Site and Time period.

Min	Site 1		Site 2		Site 3		Site 4		Site 5		Among sites
	Mean	SD	Mean	SD	Mean	SD	Mean	SD	Mean	SD	
Pre	1012.1	233.9	855.0	154.6	1370.7	264.8	1474.1	111.7	990.5	265.9	*P*<0.0001
30	701.3	143.7	667.9	191.7	682.7	44.0	662.1	72.6	685.9	179.8	*P*<0.0001
60	674.3	156.8	668.7	209.1	673.6	115.2	667.4	140.3	642.3	191.8	*P*=0.006
120	670.6	201.4	668.0	205.2	652.3	144.5	661.3	147.8	646.3	209.6	*P*<0.0001
180	700.7	199.9	725.8	229.9	685.6	213.9	683.0	209.0	630.7	213.3	*P*<0.0001
	P<0.0001*		*P*=0.0001*		*P*=0.0001*		*P*=0.0001*		*P*=0.0001*		

Significant differences at the 5% level. (*P* values - Friedman's ANOVA).
min, minutes; Pre, pre-Gd-DTPA^{2-} injection; SD, standard deviation.

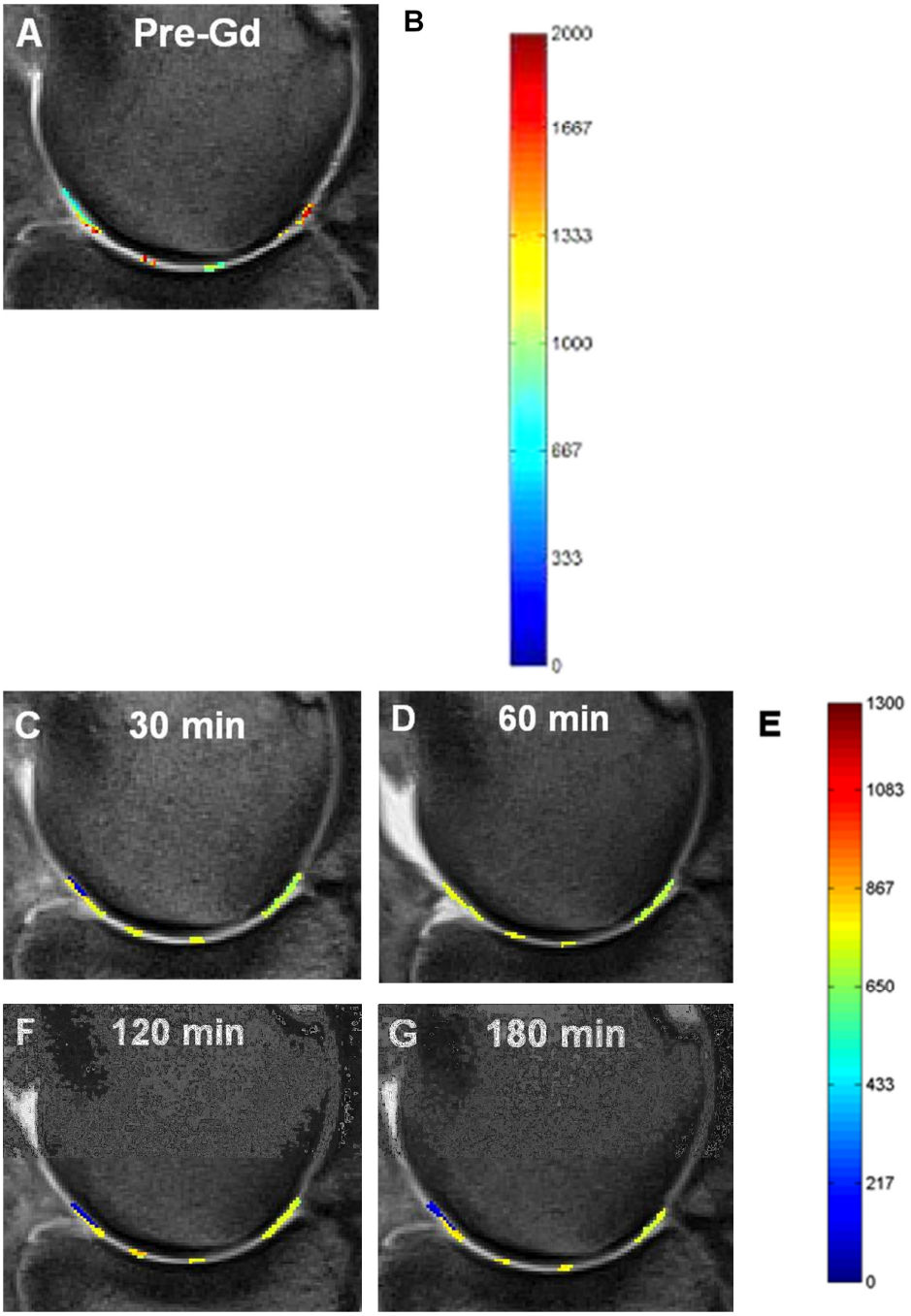

Figure 5.2. Delayed gadolinium-enhanced magnetic resonance imaging of cartilage (dGEMRIC) maps of the mid medial condyle of the right forelimb of Horse 2, illustrating the colour-coded relaxation times (in ms) for each of the regions of interest measured over times pre- and post-Gd-DTPA^{2-} intra-articular administration. Sites 3 and 4 overlap in this figure. (B) and (E) are the colour keys for pre-Gd (A) and post-Gd (C, D, F, G), respectively.

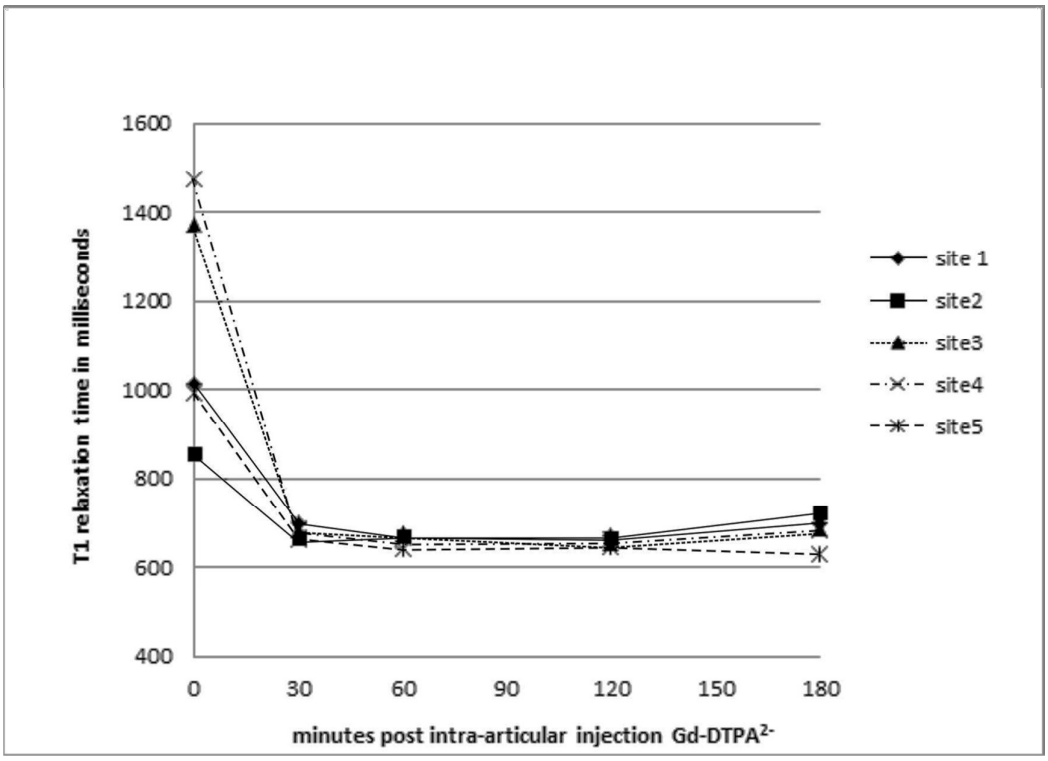

Figure 5.3. Mean of T1 relaxation times of sites 1-5 of the cartilage of distal Mc3/Mt3 of twenty limbs of six horses. For standard deviations see Table 5.1.

For sites 1-4, a significant increase in T1 relaxation time occurred between 30 and 180 min post-injection (Table 5.2).

TABLE 5.2. Wilcoxon Signed Rank Test Indicating Differences among T1 Delayed Gadolinium Enhanced Magnetic Resonance Imaging of Cartilage (dGEMRIC) Relaxation Times at Different Times Measured Pre- and Post Gd-DTPA^{2-} Administration.

	Site 1	Site 2	Site 3	Site 4	Site 5
Pre vs 30 (19)	*P*<0.0001*	*P*<0.0001*	*P*<0.0001*	*P*<0.0001*	*P*<0.0001*
Pre vs 60 (20)	*P*<0.0001*	*P*=0.003*	*P*<0.0001*	*P*<0.0001*	*P*<0.0001*
Pre vs 120 (18)	*P*<0.0001*	*P*=0.002*	*P*<0.0001*	*P*<0.0001*	*P*<0.0001*
Pre vs 180 (19)	*P*<0.0001*	*P*=0.024*	*P*<0.0001*	*P*<0.0001*	*P*<0.0001*
30 vs 60 (19)	*P*=0.798	*P*=0.352	*P*=0.104	*P*=0.040*	*P*=0.096
30 vs 120 (17)	*P*=0.306	*P*=0.243	*P*=0.207	*P*=0.040*	*P*=0.263
30 vs 180 (18)	*P*=0.043*	*P*=0.004*	*P*=0.018*	*P*=0.026*	*P*=0.182
60 vs 120 (18)	*P*=0.284	*P*=0.702	*P*=0.899	*P*=0.865	*P*=0.609
60 vs 180 (19)	*P*=0.006*	*P*=0.036*	*P*=0.021*	*P*=0.019*	*P*=0.898
120 vs 180 (17)	*P*=0.001*	*P*=0.014*	*P*=0.027*	*P*=0.021*	*P*=0.265

* Significant differences at the 5% level.

For all sites, the effect size was large between pre-contrast and all dGEMRIC series (between r=0.5 and r=0.88). For sites 1, 3, and 4, the effect size was large between 60 and 180 min, and between 120 and 180 min (r=0.52 and r=0.73). For site 2, the effect size was medium between 60 and 180 min (r=0.47). Results of Wilcoxon signed rank test comparisons among sites and time periods are summarized in Table 5.3.

TABLE 5.3. Wilcoxon Signed Rank Test Indicating Differences between Delayed Gadolinium Enhanced Magnetic Resonance Imaging of Cartilage (dGEMRIC) T1 Relaxation Times at Different Sites 1-5.

	Pre-Gd	30 min	60 min	120 min	180 min
S1 vs S2	P=0.003*	P=0.738	P=0.216	P=1.000	P=0.932
S1 vs S3	P<0.0001*	P=0.011*	P=0.154	P=0.021*	P=0.007*
S1 vs S4	P<0.0001*	P=0.008*	P=0.097	P=0.130	P=0.002*
S1 vs S5	P=0.729	P=0.441	P=0.729	P=0.702	P=0.005*
S2 vs S3	P<0.0001*	P=0.018*	P=0.123	P=0.048*	P=0.001*
S2 vs S4	P<0.0001*	P=0.018*	P=0.053	P=0.142	P=0.001*
S2 vs S5	P=0.036*	P=0.275	P=0.133	P=0.212	P=0.005*
S3 vs S4	P=0.261	P=0.016*	P=0.388	P=1.000	P=0.596
S3 vs S5	P=0.001*	P=0.020*	P=0.674	P=0.246	P=0.349
S4 vs S5	P<0.0001*	P=0.032*	P=0.475	P=0.284	P=0.388

* Significant differences at the 5% level.
Pre, pre-Gd-DTPA^{2-} injection; S, site; min, minutes.

Table 5.4 summarizes means and standard deviations of T1 relaxation times for the combined sites 1-5 for the different limbs as well as for the combined sites for all four limbs. The T1 relaxation times differed between the time periods for the left forelimb, right hind limb, and left hind limb (P-values<0.05; Friedman test). Differences were not significant in the right forelimb (P=0.06).[20]

TABLE 5.4 Mean (and standard deviation) Delayed Gadolinium Enhanced Magnetic Resonance Imaging of Cartilage (dGEMRIC) T1 Relaxation times (in ms) of the Distal Metacarpus3/Metatarsus3 Cartilage (sites 3-5) and Metacarpus3/Metatarsus3–Proximal Phalanx Combined Cartilage (sites 1-2) per Limb and Time Period (min), also of all Limbs Tested Combined.

Min	RF		LF		RH		LH		All limbs	
	Mean	SD	Mean	SD	Mean	SD	Mean	SD	Mean	SD
pre	1162.4	139.5	1162.8	98.9	1107.3	156.5	1118.3	161.6	1150.9	117.9
30	655.5	79.4	720.7	25.9	710.2	47.3	626.6	174.1	673.4	53.8
60	665.4	116.8	658.4	90.5	716.2	39.0	632.7	252.6	655. 4	76.8
120	626.0	204.5	727.8	18.7	712.0	40.1	564.4	275.9	647. 4	110.5
180	601.2	267.7	718.6	24.9	741.7	12.0	701.4	347.5	659.0	147. 8
	P=0.060		*P*=0.004*		*P*=0.014*		*P*=0.035*		*P*=0.006*	

* Significant differences at the 5% level.
RF, right fore; LF, left fore; RH, right hind; LF, left hind; Pre, pre-Gd-DTPA^{2-} injection; min, minutes.

5.5 DISCUSSION

We chose 3- to 6-year-old Thoroughbred horses for our study because horses in this age group are used for active flat-racing and are most likely to have some degree of mild osteoarthritis in their metacarpo/meta-tarsophalangeal joints. The modified Neundorf and OARSI scoring systems used a set of parameters that was easy to evaluate and should be repeatable within and among observers for future studies.[18,19] We excluded limbs from our study if gross abnormalities were present, or if there was minimal macroscopic (Grade 1) or microscopic (<Grade 2) cartilage damage at sites 1-3 of the condyles.

Regions of interest for T1 relaxation time measurements were constrained by the resolution of the 1.5 T MRI scanner used in our study. The dGEMRIC measuring technique on distal horse Mc3/Mt3 cartilage has previously been validated by comparing histologic cartilage thickness measurements at site 3 with a single STIR sequence used in the dGEMRIC mapping technique,[21] as was done between MRI and histological measurements of horse carpal articular cartilage using a 1.5T machine.[22] Distal Mc3 and Mt3 cartilage in normal horses is approximately 1 mm thick (0.90±0.17 mm).[23] Since the cartilage of distal Mc3/Mt3 at sites 1 and 2 could not be differentiated from the cartilage of the adjacent P1, the ROIs drawn

were a combination of the two adjacent cartilages and the thin layer of synovial fluid between them. Combined analysis of articulating surfaces has been previously described as an acceptable method for dGEMRIC analysis of joints with thin cartilage, such as the human hip.[24] In future clinical dGEMRIC studies of horse joints with thin cartilage, this combined articular dGEMRIC ROI technique may also be helpful for scans acquired using relatively low field MRI machines. [24]

Both the lateral and medial condyles of Mc3/Mt3 are prone to palmar/plantar osteochondral disease. [8] As the joint is extended, the dorsal and palmar/plantar surfaces of the condyle become increasingly compressed.[25] With further acceleration, stress to the palmar/plantar surface of the metacarpal/metatarsal condyle can be more than twice that applied to the dorsal surface. These findings support the theory that biomechanics may play an important role in osteoarthritis pathogenesis.[26]

The 12 minutes needed to acquire the 6 inversion recovery images for T1 mapping was a relatively long period of time. In the clinical situation, a horse would be anesthetized and would have to be repositioned to ensure all limbs were placed within the iso-centre of the gantry. However, repositioning times could be reduced by simultaneously imaging both forelimbs or both hind limbs, even though they would not then be within the iso-centre of the gantry. Three-dimensional techniques are available that will shorten acquisition time even further, although these will unlikely be available for dedicated equine scanners in the near future.

The pattern of decreasing T1 relaxation times we observed over 120 minutes in our horse cadaver specimens was similar to that previously reported in human studies, where dGEMRIC series were acquired between 30 and 100 min.[27] Human cadaver results have been found to be similar to live patient results for dGEMRIC.[28] We assume that the same would apply in horses. A previous study in normal dog elbows found a mean T1 dGEMRIC value of 400 ± 47 ms at 30 minutes post intravenous injection of gadopentate dimeglumine, as opposed to the current study's post intra-articular injection mean value at site 3 of 682.7 ± 44 for the same time period. [29] This discrepancy could be due to the method of administering the contrast,

cartilage thickness differences or other inherent cartilage differences between the two species and joints.

Significant differences in T1 relaxation times between most of the pre-contrast sites were likely because of inherent differences in cartilage substrate, as has been previously seen in the human knee.[30] Differences in cartilage substrate could occur as an adaptation to the varying forces applied. There are more viable chondrocytes in palmar condyle cartilage than dorsal condyle cartilage in the equine fetlock and this finding has been correlated with proteoglycan content.[31,32] The number of sites with significant differences between them decreased to a minimum at 60 and 120 minutes post-Gd-DTPA^{2-}[13, 14] injection and then increased again at 180 minutes post injection. This finding could have occurred because the gadolinium that was incorporated into the cartilage resulted in a more homogenous T1 relaxation time. Our study showed an increase in T1 relaxation time from 120-180 minutes in 4 of the 5 sites, indicating a wash-out from the cartilage. This finding was likely due to diffusion of the Gd-DTPA^{2-} from areas with high intra-articular and intra-cartilaginous concentration to areas with lower concentration.[33] This washout would likely occur even earlier *in vivo*, due to perfusion washout. Good correlation has been previously found between dGEMRIC *in vivo* and *in vitro* human studies after total knee replacement surgery.[28] It is likely that findings in this equine cadaver study will be similar to those in an equine *in vivo* study, but this would need to be confirmed. Previous studies have shown that dGEMRIC values are sensitive to mechanical cartilage stress.[34] Therefore, in the recumbent, non-weight-bearing joint, dGEMRIC values could differ from those of the weight-bearing cartilage, although the degree thereof is unknown. The dGEMRIC technique has been previously reported to have good day-to-day reproducibility in humans and is likely to be the same in the horse.[35]

The lack of a significant difference between T1 relaxation times of the right fore limb as opposed to significant differences among T1 relaxation times of the other limbs could be due to different loading and ambulating patterns of the right fore limb relative to the other limbs. This different loading could have an effect on the proteoglycan concentration of the cartilage. All these horses had recently come off the racetrack, where the inside limb would have been

subjected to different forces compared to the outside limb.[36,37,38] This could have translated into different cartilage loading of distal Mc3/Mt3 in the right forelimb. However, this theory is only speculative and would require further investigation in a larger number of horses to confirm.

Limitations of this study included the relatively poor spatial resolution of the thin distal Mc3/Mt3 cartilage, which could be improved in future studies with the use of a dedicated surface coil and decreased FOV. A higher field strength magnet would also improve resolution but since the highest field strength in general use currently is 1.5T, it is unlikely this adaptation will be in use soon. The setup used in the current study was chosen because it was realistic for *in vivo* studies and would allow a reasonable imaging time. The use of traction to separate the two cartilage surfaces could also be considered to improve visibility of articular margins.[39] The low number of limbs used in our study was also a limitation, although the non-parametric techniques used were able to detect significant differences. Another limitation was the lack of repeatability studies for intra- and inter observer evaluations. In spite of these limitations, results supported our hypothesis that T1 relaxation time in Mc3/Mt3 cartilage decreases significantly after Gd-DTPA^{2-} administration.

Future studies of the dGEMRIC technique in equine clinical patients will need to address the above limitations. Standing MRI currently utilizes only low magnetic field strengths, e.g. 0.27T, and the resolution may not be adequate for accurate dGEMRIC measurements of the thin cartilage in equine metacarpo/metatarsal joints. Before determining whether dGEMRIC could be applied in the clinical scenario, it should be also established that dGEMRIC can identify early cartilage degeneration in horses with varying degrees of osteoarthritis. Future research should address whether differences in T1 relaxation time post- Gd-DTPA^{2-} would be affected by the following factors: (1) chilling or freezing of cadaver limbs; (2) the administration route of Gd-DTPA^{2-}; (3) exercise or non-exercise post- Gd-DTPA^{2-} administration; or (4) the presence of osteoarthritis.

In conclusion, findings from this study indicated that dGEMRIC is a feasible technique for mapping cartilage T1 relaxation times in the equine distal Mc3/Mt3. Locations with thin cartilage in the fetlock joint may be measured using ROIs that combine analysis of adjacent articulating

cartilages. For future studies, authors recommend that dGEMRIC scans in horse metacarpo/metatarsophalangeal joints be conducted 60-120 minutes post intra-articular Gd-DTPA^{2-} injection.

ACKNOWLEDGEMENTS

The authors thank the Faerie Glen Hospital MR Trust for use of their MRI machine; A Bester, A Helberg, I Martin, and S Tarantino for MRI technical support; all the OVAH radiographers, and the staff of the Highveld Horse Care unit for radiographic technical support and case recruitment, respectively; and Mrs J C Jordaan for statistical analysis.

REFERENCES

1. Dyson PK, Jackson BF, Pfeiffer DU, Price JS. Days lost from training by two- and three-year-old Thoroughbred horses: A survey of seven UK training yards. Equine Vet J 2008;40:650-657.

2. Perkins NR, Reid SW, Morris RS. Profiling the New Zealand Thoroughbred racing industry. 2. Conditions interfering with training and racing. NZ Vet J 2005;53:69-76.

3. Bailey CJ, Reid SW, Hodgson DR, Bourke JM, Rose RJ. Flat, hurdle and steeple racing: Risk factors for musculoskeletal injury. Equine Vet J 1998;30:498-503.

4. Anonymous. A comparison of the economic costs of equine lameness, colic, and equine protozoal myeloencephalitis (EPM) in the United States. Animal and Plant Health Inspection service. 2001. Available at http://www.aphis.usda.gov/animal_health/nahms/equine/downloads/equine98/Equine98_is_Colic.pdf. (accessed May 2011).

5. Wilsher S, Allen WR, Wood JL. Factors associated with failure of Thoroughbred horses to train and race. Equine Vet J 2006;38:113-118.

6. McIlwraith CW. General pathology of the joint and response to injury. In: McIlwraith CW, Trotter GW, eds. Joint disease in the horse. Philadelphia: WB Saunders Co, 1996;40-70.

7. Smith KJ, Bertone AL, Weisbrode SE, Radmacher M. Gross, histologic, and gene expression characteristics of osteoarthritic articular cartilage of the metacarpal condyle of horses. Am J Vet Res 2006;67:1299-306 .

8. Barr ED, Pinchbeck GL, Clegg PD, Boyde A, Riggs CM. Post mortem evaluation of palmar osteochondral disease (traumatic osteochondrosis) of the metacarpo /metatarsophalangeal joint in Thoroughbred racehorses. Equine Vet J 2009;41: 366-371.

9. Goldring MB, Goldring SR. Osteoarthritis. J Cell Physiol 2007;213:626-634.

10. Javaid MK, Lynch JA, Tolstykh I, Guermazi A, Roemer F, Aliabadi P, et al. Pre-radiographic MRI findings are associated with onset of knee symptoms: The most study. Osteoarthritis Cartilage 2010;18:323-328.

11. Butler JA, Colles CM, Dyson SJ, Kold S, Poulos P. General principles. In: Butler JA, Colles CM, Dyson SJ, et al, eds. Clinical radiology of the horse. Chichester, United Kingdom: Wiley-Blackwell, 2009;1-36.

12. Crema MD, Roemer FW, Marra MD, Burstein D, Gold GE, Eckstein F, et al. Articular cartilage in the knee: current MR imaging techniques and applications in clinical practice and research. Radiographics 2011;31:37-61.

13. Roemer FW, Eckstein F, Guermazi A. Magnetic resonance imaging-based semiquantitative and quantitative assessment in osteoarthritis. Rheum Dis Clin North Am 2009;35:521-555.

14. Gray ML, Burstein D, Kim YJ, Maroudas A. 2007 Elizabeth Winston Lanier Award Winner. Magnetic resonance imaging of cartilage glycosaminoglycan: basic principles, imaging technique, and clinical applications. J Orthop Res 2008;26:281-291.

15. Baldassarri M, Goodwin JS, Farley ML, Bierbaum BE, Goldring SR, Goldring MB, et al. Relationship between cartilage stiffness and dGEMRIC index: Correlation and prediction. J Orthop Res 2007;25:904-912.

16. Menendez MI, Clark DJ, Carlton M, Flanigan DC, Jia G, Sammet S, et al. Direct delayed human adenoviral BMP-2 or BMP-6 gene therapy for bone and cartilage regeneration in a pony osteochondral model. Osteoarthritis Cartilage 2011;19:1066-1075.

17. Mayerhoefer ME, Welsch GH, Mamisch TC, Kainberger F, Weber M, Nemec S, et al. The *in vivo* effects of unloading and compression on T1-gd (dGEMRIC) relaxation times in healthy articular knee cartilage at 3.0 Tesla. Eur Radiol 2010;20:443-449.

18. Neundorf RH, Lowerison MB, Cruz AM, Thomason JJ, McEwen BJ, Hurtig MB. Determination of the prevalence and severity of metacarpophalangeal joint osteoarthritis in Thoroughbred racehorses via quantitative macroscopic evaluation. Am J Vet Res 2010;71:1284-1293.

19. McIlwraith CW, Frisbie DD, Kawcak CE, Fuller CJ, Hurtig M, Cruz A.The OARSI histopathology initiative - recommendations for histological assessments of osteoarthritis in the horse. Osteoarthritis Cartilage 2010;18 Suppl 3:S93-105.

20. Albright SC, Winston WL, Zappe CJ. Data analysis and decision making. Australia: South-Western Cengage Learning. 2010;503.

21. Carstens A, Kirberger RM, Dahlberg LE, Prozesky L, Fletcher L, Lammentausta E. Validation of delayed gadolinium-enhanced magnetic resonance imaging of cartilage and T2 mapping for quantifying distal metacarpus/metatarsus cartilage thickness in Thoroughbred racehorses. Vet Radiol Ultrasound 2013;54:139–148.

22. Murray RC, Branch MV, Tranquille C, Woods S. Validation of magnetic resonance imaging for measurement of equine articular cartilage and subchondral bone thickness. Am J Vet Res 2005;66:1999-2005 .

23. Olive J, D'Anjou MA, Girard C, Laverty S, Theoret C. Fat-suppressed spoiled gradient-recalled imaging of equine metacarpophalangeal articular cartilage. Vet Radiol Ultrasound 2010;51:107-115.

24. Lattanzi R, Petchprapa C, Glaser C, Dunham K, Mikheev AV, Krigel A et al. A new method to analyze dGEMRIC measurements in femoroacetabular impingement: preliminary validation against arthroscopic findings. Osteoarthritis and Cartilage 2012;20:1127-1133.

25. Pool RR. Pathologic manifestations of joint disease in the athletic horse. In: McIlwraith CW, Trotter GW editors. Joint disease in the horse. Philadelphia: WB Saunders Co. 1996;87-104.

26. Riggs CM, Whitehouse GH, Boyde A. Structural variation of the distal condyles of the third metacarpal and third metatarsal bones in the horse. Equine Vet J 1999;31:130-139.

27. Tiderius CJ, Jessel R, Kim YJ, Burstein D. Hip dGEMRIC in asymptomatic volunteers and patients with early osteoarthritis: The influence of timing after contrast injection. Magn Reson Med 2007;57:803-805.

28. Bashir A, Gray ML, Hartke J, Burstein D. Nondestructive imaging of human cartilage glycosaminoglycan concentration by MRI. Magn Reson Med 1999;41:857-65.

29. Wucherer KL, Ober CP, Conzemius MG. The use of delayed gadolinium enhanced magnetic resonance imaging of cartilage and T2 mapping to evaluate articular cartilage in the normal canine elbow. Vet Radiol Ultrasound 2012;53:57-63.

30. Krishnan N, Shetty SK, Williams A, Mikulis B, McKenzie C, Burstein D. Delayed gadolinium-enhanced magnetic resonance imaging of the meniscus: An index of meniscal tissue degeneration? Arthritis Rheum 2007; 56:1507-1511.

31. Dykgraaf S, Firth EC, Rogers CW, Kawcak CE. Effects of exercise on chondrocyte viability and subchondral bone sclerosis in the distal third metacarpal and metatarsal bones of young horses. Equine Vet J 2008;178:53-61.

32. Rosenberg L. Chemical basis for the histological use of Safranin O in the study of articular cartilage. J Bone Joint Surg Am 1971;53:69-82.

33. Salo E-N, Nissi MJ, Kulmala KAM, Tiitu V, Töyräs J,Nieminen MT. Diffusion of Gd-DTPA^{2-} into articular cartilage. Osteoarthritis Cartilage 2012;20:117-26.

34. Tiderius CJ, Olsson LE, Leander P, Ekberg O, Dahlberg L. Delayed gadolinium-enhanced MRI of cartilage (dGEMRIC) in early knee osteoarthritis. Magn Reson Med 2003;49:488-492.

35. Multanen J, Rauvala E, Lammentausta E, Ojala R, Kiviranta I, Häkkinen A, et al. Reproducibility of imaging human knee cartilage by delayed gadolinium-enhanced MRI of cartilage (dGEMRIC) at 1.5 Tesla. Osteoarthritis Cartilage 2009;17:559-564

36. Beccati F, Pepe M, Di Meo A, Davanzo S, Moriconi F. Radiographic evaluation of changes in the proximal phalanx of Thoroughbreds in race training. Am J Vet Res 2011;72:1482-1488.

37. Firth EC, Rogers CW, Doube M, Jopson NB. Musculoskeletal responses of 2-year-old Thoroughbred horses to early training. 6. Bone parameters in the third metacarpal and third metatarsal bones. NZ Vet J 2005;53:101-112.

38. Davies HM, Merritt JS. Surface strains around the midshaft of the third metacarpal bone during turning. Eq Vet J 2004;36:689-692.

39. Nakanishi K, Tanaka H, Nishii T, Masuhara K, Narumi Y, Nakamura H. MR evaluation of the articular cartilage of the femoral head during traction: correlation with resected femoral head. Acta Radiol 1999;40:60-63.

CHAPTER 6

The effect of chilling and freezing on T2 mapping in the normal Thoroughbred horse cadaver distal metacarpus3/metatarsus3 cartilage

Ann Carstens, Robert M. Kirberger, Leif E. Dahlberg, Lizelle Fletcher, Eveliina Lammentausta

Keywords: articular cartilage; T2 mapping; horse; metacarpus/metatarsus, chill, frozen

From the Department of Companion Animal Clinical Studies, Faculty of Veterinary Science, University of Pretoria, Private Bag X04 Onderstepoort 0110 (Carstens, Kirberger), Pretoria South Africa; Joint and Soft Tissue Unit, Department of Clinical Sciences, Malmö, Lund University, Department of Orthopaedics, Malmö University Hospital, SE-205 02 (Dahlberg, Lammentausta), Malmö, Sweden; Department of Statistics, University of Pretoria (Fletcher), Pretoria South Africa; Department of Diagnostic Radiology, Oulu University Hospital, POB 50, FI-90029 OYS (Lammentausta), Oulu, Finland.

Submitted

6.1 ABSTRACT

Metacarpo/metatarsophalangeal joint osteoarthritis is a major cause of poor performance in horses. T2 mapping is a quantitative MRI technique developed for non-invasive characterization of hyaline articular cartilage, repair tissue and hydration, thereby detecting early degradative changes. Cadaver limbs for research often require chilling or freezing prior to scanning, necessitating testing to determine whether these techniques affect T2 mapping. Seventeen distal metacarpus3/metatarsus3 (Mc3/Mt3) of 6 normal control Thoroughbred racehorse cadavers (GrA), were scanned using a 1.5T MRI machine. Combined distal Mc3/Mt3 and adjacent proximal phalanx cartilage T2 relaxation times were calculated at sites 1 and 2. Distal Mc3/Mt3 cartilage T2 relaxation times were calculated at sites 3-5 as was the entire distal Mc3/Mt3 cartilage. In another six normal Thoroughbred racehorses eight randomly selected forelimbs and hind limbs were chilled for 48 hours (GrBchill) and five contralateral limbs frozen (GrBfrozen) for 60-90 days. The limbs were thawed, allowed to return to room temperature and scanned similarly to GrA. The mean T2 relaxation times of the full cartilage of GrA, GrBchill, GrBfrozen were 85±14, 80±6, 87±11 ms, respectively. No statistical differences were found among the three groups full cartilage measurements. There was moderate evidence of some differences at site 2 (P=0.054). Freezing appears to affect cartilage T2 relaxation time more than chilling, although not significantly so. Magic angle effect was seen at the palmar/plantar condylar cartilage. T2 mapping in the horse cadaver distal Mc3/Mt3 can thus be conducted after limb chilling and freezing with minimal effect on T2 relaxation time.

6.2 INTRODUCTION

Lameness in horses is the primary cause of poor performance and wastage [1-3] and costs the horse industry in North America an estimated $1 billion in 1998. [4] The metacarpo/metatarsophalangeal joints are the most commonly affected by trauma and degeneration, [5] most of which results in osteoarthritis,[6] affecting both the lateral and medial condyles of metacarpus3/metatarsus3 (Mc3/Mt3). [7, 8]

Osteoarthritis is defined as degeneration of articular cartilage and is characterized by matrix fibrillation, the appearance of fissures and ulceration and full-thickness loss of the cartilage. [9] Confirmation of osteoarthritis in the metacarpo/metatarsophalangeal joints in the horse, is by means of clinical evaluation, perineural or intra-articular nerve blocks and relevant combinations of radiography, ultrasonography, computed tomography, scintigraphy and magnetic resonance imaging (MRI), if available. [10] Many of these modalities are, however, only useful after the degenerative process has progressed somewhat. [10, 11]

Magnetic resonance imaging has been utilized in human studies to visualize pathological articular cartilage early in the disease process. [12, 13] MRI mapping of cartilage entails acquiring the image in certain MRI sequences and the manual drawing (segmenting) of regions of interest (ROI) of the articular cartilage. This has been described in humans in T2, T2*, T1rho and delayed Gd enhanced MRI of cartilage (dGEMRIC) or (T1(Gd)) sequences. [14-17] and in horses. [18,19] T2 mapping can characterize hyaline articular cartilage and repair tissue and T2-weighted sequences are sensitive to tissue hydration, [19] and can therefore detect early degradative changes in the extracellular matrix when overall water content is increased. T2 relaxation time has been shown to be inversely correlated with collagen concentration, the integrity of the collagen network and mechanical properties of articular cartilage [20, 21] T2 relaxation time has also been reported to increase in osteochondrotic cartilage in man. [22] In horses T2 mapping has been

described in the equine femoropatellar joint, aiding differentiation between hyaline cartilage and reparative fibrocartilage. [23]

MRI research of the distal limb of the average size horse can often only be performed in the dismembered cadaver limb, since relatively few institutions have MRI facilities to accommodate an average size live horse, and costs, logistics and possible general anaesthetic risks for a live horse are factors that often preclude examinations of this kind. Since scan time is often limited, limbs may require chilling or freezing to be examined more conveniently at a later date. It is therefore important to establish whether T2 mapping results are significantly affected by these cryopreservation techniques. There is much research being conducted on the effect of chilling and/or freezing in cartilage; particularly in in bovine nasal cartilage [24, 25] and bovine or porcine articular cartilage, [26, 27] much of which has utilized micro MRI. Chilling and freezing has also been investigated in horse articular cartilage [28-30] particularly of the distal limb with different MRI sequences. These reports in horses were mostly subjective evaluation of images pre- and post-chilling or freezing. One report evaluated distal limbs that were scanned within 12 hours after death and then at 1, 2, 7 and 14 days post 4ºC refrigeration. [29] The image quality was evaluated subjectively with only bone marrow appearing slightly hyperintense in short tau inversion recovery (STIR) sequences and slightly hypointense in turbo spin echo (TSE) T2 sequences compared with day zero. Signal to noise ratio was utilized as a quantitative evaluation technique with a significant decrease seen again in the bone marrow in the TSE T2 and double-echo steady state sequences. In another study by the same authors equine distal limbs underwent repeated freeze-thaw cycles and other limbs that were only frozen once but allowed to return to scanning temperature in different ambient temperature areas. [30] Their subjective findings were that overall image quality was unchanged except for the hoof capsule, but that there were significant differences in some of the sequences (T1-weighted, turbo spin-echo proton density-weighted) and tissues when evaluated quantitatively. Neither of these reports described the effect of chilling or freezing on the articular cartilage.

To the authors' knowledge, no T2 mapping work in horse metacarpo/metatarsophalangeal joints have as yet been published, nor has

the effect of chilling and freezing on T2 mapping of cartilage in horses been reported. The purpose of the study was to demonstrate the feasibility of T2 mapping in the metacarpo/metatarsophalangeal joints of the horse and secondly to establish whether 48 hour chilling or freezing and thawing of the limbs have a significant effect on T2 mapping of the distal Mc3/Mt3 articular cartilage. The hypothesis tested was that there is no significant difference in T2 relaxation values of the distal Mc3/Mt3 cartilage between control, chilled and frozen limbs.

6.3 MATERIALS AND METHODS

This project (V067/10) was approved by the Animal Use and Care Committee of the Faculty of Veterinary Science, University of Pretoria and all horses were treated according to South African Veterinary Council ethical standards. Six Thoroughbred horses (GrA), aged 3-6 years, of any gender, with no signs of lameness or history of recent corticosteroid or glycosaminoglycan treatments were obtained from a welfare horse care organization where racing Thoroughbreds are sent for adoption or euthanasia.

The horses were clinically examined and then shot intra-cranially and the limbs removed at the mid Mc3/Mt3 diaphyses, wrapped in clear plastic and transported to an MRI facility within 6 hours post euthanasia. Another six horses (GrB) were treated identically, except that a randomly selected forelimb and hind limb of each horse was kept for 48 hours at a household fridge temperature of 5ºC (GrBchill) and the other two limbs frozen (GrBfrozen) from 60 to 90 days at a household freezer temperature of -20ºC. After these two time periods, the limbs of GrBfrozen were thawed and both GrBfrozen and GrBchill limbs were left to return to room temperature (20°C) and scanned immediately thereafter.

On scanning of both groups A and B, a vitamin E oil capsule was taped to the lateral aspect of every metacarpo/tarsophalangeal joint and the limbs placed with the dorsum downwards with the toe facing into the gantry. A head and neck 12 channel coil and a Siemens Avanto 1.5 T MRI machine (Siemens Healthcare. Erlangen, Germany) was used. The forelimbs of GrA were randomly selected and scanned followed by the randomly selected hind limbs.

Sagittal plane T2 mapping images were acquired using multi-slice multi-echo spin echo sequences with TR: 2170 ms; six TEs at between 16.7 and 116.9 ms; FOV: 140x140; matrix: 256x256; slice thickness: 3 mm; and kHz receiver bandwidth: 130 Hz/pix. Seventeen slices were acquired with the central slice placed over the distal Mc3/Mt3 sagittal ridge. (Fig.6.1 A).

Five sites were analysed: site 1: 25° dorsal angle from a point in the center of the rotation of the joint; site 2: distal aspect of a line down the axis of the diaphysis of Mc3/Mt3 corresponding to the transverse ridge; site 3: 35° palmar/plantar angle from a point in the center of the rotation of the joint; the ROIs for sites 1-3 were drawn 3 degrees dorsal to and 3 degrees palmar/plantar to sites 1-3. Sites 4 and 5 were where the cartilage was clearly seen at the palmar/dorsal aspect of Mc3/Mt3, respectively where no adjacent phalanx one bone cartilage was present (Fig.6.1 B). Site 3 was occasionally completely incorporated within site 4.

After the MRI the Mc3 and Mt3 were dissected loose from the rest of the limb and the distal condylar cartilage surface evaluated macroscopically before and after 3-5 minute staining with India ink (Parker Quink Ink, Post Net Suite #283, Private Bag X1005, Claremont, 7735, South Africa). All cartilage and synovia were examined, gross abnormalities noted and the cartilage graded using the Neundorf grading system, accepting only Grade 1 into the study. [31] Grade 1 included no abnormalities as well as minimal changes of loss of reflectance, minimal cartilage hypertrophy at the joint margins, minimal partial thickness wear lines, minimal thinning of cartilage, minimal thickening of cartilage, and no enlarged synovial fossae. Grades 2 and 3 had progressively worse lesions. Mid-medial and lateral condyles of Mc3 and Mt3, respectively, were sectioned into 3-5 mm thick slices in a sagittal plane, and the samples fixed and decalcified in a 8% nitric acid made up in 10% buffered formalin solution. Sites 1, 2 and 3 were identified using the sagittal template of the respective lateral and medial condyles (Fig.6.1 B), and the cut blocks processed and stained using standard Hematoxylin and Eosin. The cartilage at sites 1-3 of the respective mid-condylar Mt3 and Mc3, was evaluated for pathology using a modification of an Osteoarthritis Research Society International (OARSI) microscopic cartilage grading system, accepting only a grade 1 out of 3 into the study. [32]

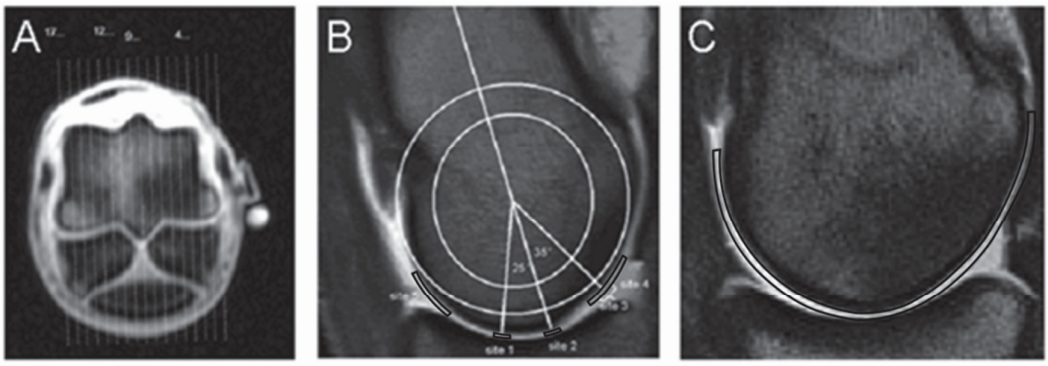

Figure 6.1. (A) Transverse pilot MRI image of the distal third metatarsal bone of a normal Thoroughbred horse, demonstrating how MRI slices were marked for histologic comparisons. A 17-line template was placed on the slice and centred over the distal sagittal ridge. Slice 1 was positioned on the lateral epicondyle cortex with slice 17 extending slightly beyond the medial epicondyle cortex. A hyperintense vitamin E oil capsule was used as a marker for the lateral epicondylar surface.
(B) Lateral mid-condylar parasagittal T2 MRI image with a representation of the translucent template illustrating concentric circles placed using a "best-of-fit" method over the third metacarpal condyle and with a line transecting the midline of the Mc3 distal metaphysis. Sites 1-5 are also identified, outlined in black
(C) Medial mid-condylar parasagittal T2 MRI image illustrating the segmentation of the entire distal Mc3 cartilage including the proximal phalanx 1 cartilage where the 2 surfaces could not be distinguished, outlined in black.

6.3.1 MRI Data Analysis

Full-thickness region of interest (ROI) of sites 1-5, 3° to either side of the template lines, were manually segmented from the cartilage bone interface to the articular surface of site 3, and to the bone-cartilage interface of phalanx 1 of sites 1-2 since the cartilage surface could not be positively identified in most of the limbs at these sites. Larger regions of interest were segmented at sites 4 and 5 from the bone-cartilage interface to the articular surface of Mc3/Mt3 which was clearly visible at these sites (Fig.6.1 B). Finally, for each limb the entire visible distal Mc3 cartilage (or combination of Mc3 and proximal phalanx cartilage where Mc3 cartilage surface was not visible) was segmented (Fig.6.1 C). T2 maps were created by fitting the respective data into mono-exponential relaxation equations using an in-house MATLAB

application (MATLAB, MathWorks Inc., Natick, MA, USA). Mean values for each ROI were calculated.

6.3.2 **Statistical Analysis**

Since the sample sizes are small, non-parametric tests (which are more robust) were conducted. Unfortunately, small sample sizes result in low power for statistical tests, hence we reported exact *P*-values where possible. The Kruskal-Wallis test, which is analogous to an ANOVA, was used to determine whether there were statistically significant differences among the T2 relaxation times of the three different groups. In the case of significant results, Mann-Whitney U tests were performed *post hoc* to determine specifically which groups' relaxation times differed from each other. The tests were performed for each of the five sites as well as for the full cartilage measurements. Within each group, Friedman tests were performed to determine whether the five sites differed significantly and if there were differences, Wilcoxon signed rank tests were run to determine which sites differed from one another. The level of significance, α, was specified at 0.05. The evaluator was not blinded to the group.

6.4 RESULTS

For GrA (control), twenty limbs met the inclusion criteria and four limbs were excluded, two for OA, one for synovitis, and one for an osseous cyst-like lesion. T2 data was lost in three limbs due to technical errors; therefore 17 limbs from GrA were available for ROI tracing (segmentation). For GrB, only thirteen limbs met the inclusion criteria, as eleven were excluded for excessive cartilage wearlines, osteochondritis dissecans lesions, and palmar/plantar arthroses, resulting in GrBchill with 8 limbs and GrBfrozen with 5 limbs. The presence of arthrosis could only be detected after the macroscopic and microscopic grading, hence the disparate numbers in the two B groups. Typical T2-map images for groups A, Bchill and Bfrozen are shown in figure 6.2, with segmented colour maps of the relaxation times visible at each of the 5 site ROIs as well as for the entire cartilage.

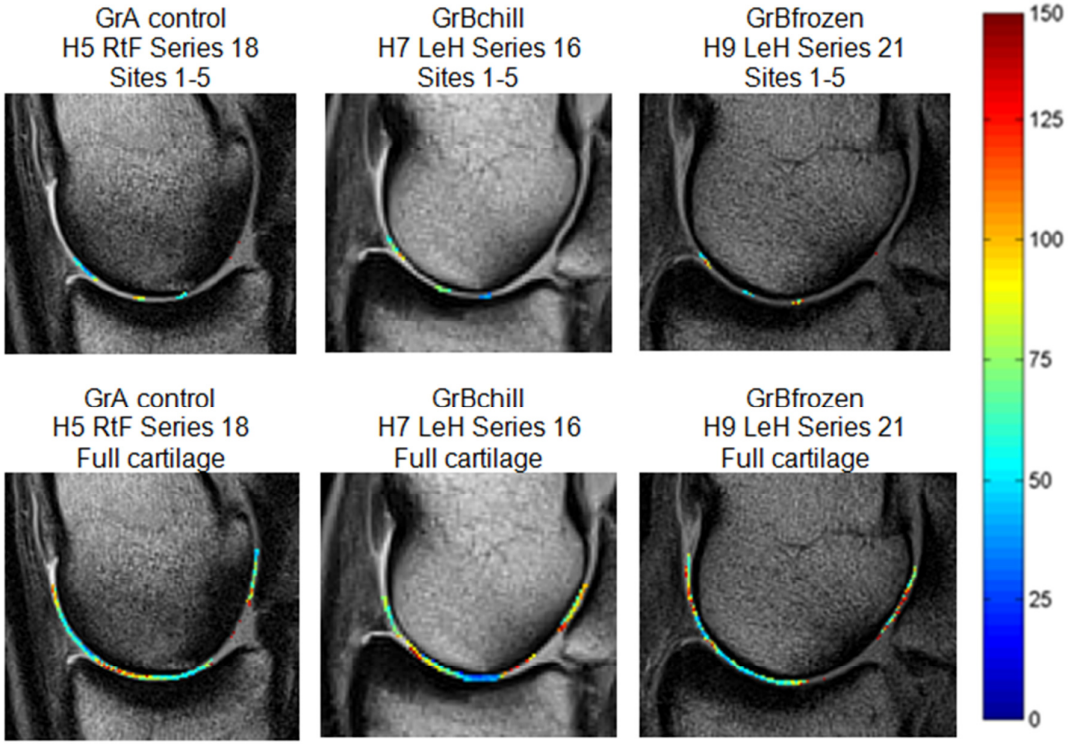

Figure 6.2. Comparative representative T2 maps of the mid condyles (either forelimb or hind limb), illustrating the colour-coded relaxation times (in ms) for each of the regions of interest for sites 1-5 and full cartilage segmentation for GrA (control), GrBchill and GrBfrozen.

The time to acquire all the images required for the T2 mapping procedure is approximately 5 minutes per joint. Table 6.1 displays the means (and standard deviations) of the T2 relaxation times of the distal Mc3/Mt3 cartilage for the separate and combined sites 1-5 for all the limbs, as well as the full cartilage measurements. The last four columns in table 6.1 display the *P*-values of the statistical tests comparing the three groups. There was no evidence of differences among the three groups when the full cartilage T2 relaxation times were compared although there was moderate evidence of differences among the groups at site 2 (Kruskal-Wallis test P=0.054). The post hoc Mann-Whitney U-tests showed that groups A and Bchill differ significantly from GrBfrozen at site 2 (P=0.039 and P=0.018, respectively). The box plots in figure 6.3 confirm that the measurements for the frozen limbs

at site 2 are substantially higher than for the chilled and the control limbs, which in turn do not differ from each other. There was also moderate evidence (P=0.074) of differences among the three groups when the sites were combined. From the *post hoc* tests, it was determined that the chilled and frozen limbs differ from each other (P=0.027). This result is illustrated in the last box plot in figure 6.3; once again the frozen limbs had higher measurements.

With regards to the assessment of the measurements within each group it was found that in GrA the T2 relaxation time means differed significantly among the sites (Friedman test P<0.01). From the Wilcoxon signed rank post hoc tests it was determined that S1 differed significantly from S3, S4 and S5 (P=0.01, <0.01 and 0.04 respectively), S2 differed significantly from S4 (P<0.01), while S3 and S4 both differed significantly from S5 (P=<0.01.) It was not possible to test whether there were differences among sites in either of the group B sections due to the sparse data.

TABLE 6.1 Mean and Standard Deviation of T2 Relaxation Time of GrA, GrBchill and GrBfrozen of Distal Mc3/Mt3 (in ms) at sites 3-5, Combined with the Proximal Phalanx at sites 1-2, and Full Cartilage.

Site	GrA (ms) [n]	GrBchill (ms) [n]	GrBfrozen (ms) [n]	Kruskal Wallis GrA vs GrBchill vs GrBfrozen	Mann Whitney GrA vs GrBchill	Mann Whitney GrA vs GrBfrozen	**Mann Whitney GrBchill vs GrBfrozen**
1	92±29 [17]	77±30 [6]	101±31 [4]	0.378	-	-	-
2	78±28 [17]	71±33 [8]	117±34 [4]	0.054	0.483	0.039*	0.018*
3	114±21 [10]	97 [1]	102 [1]	0.682	-	-	-
4	123±20 [16]	115±22 [5]	114±33 [3]	0.643	-	-	-
5	77±19 [17]	79±16 [8]	90±17 [5]	0.337	-	-	-
full cart	85±14 [17]	80±6 [8]	87±11 [5]	0.7	-	-	-

Mc3, metacarpus3; Mt3, metatarsus3; full cart, full cartilage ; *, Significant difference (P<0.05) ; [n], number of limbs measured. Blank areas indicate no reliable result because of too low numbers.

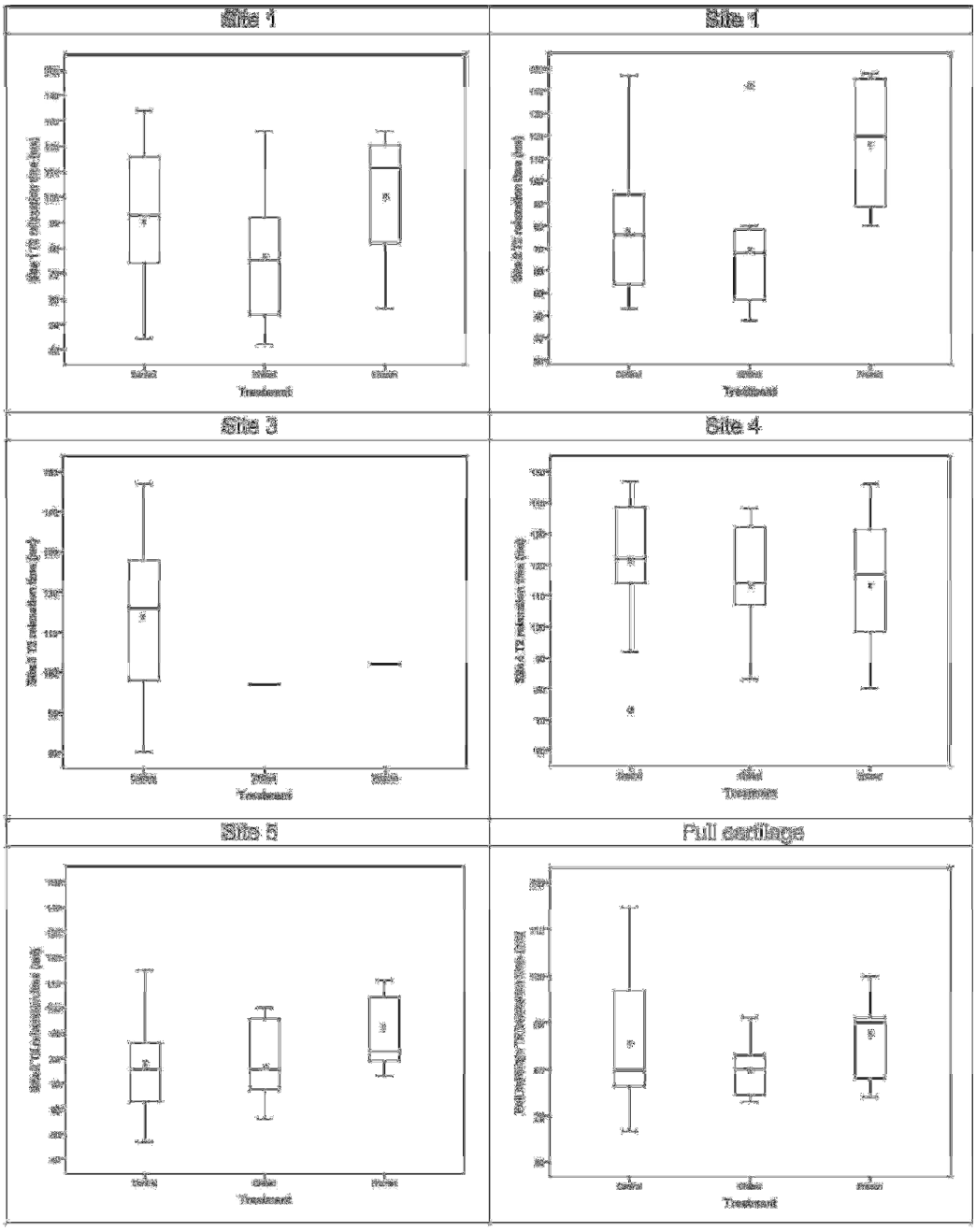

Figure 6.3. Boxplot representations of mean T2 relaxation times GrA (control), GrBchill and GrBfrozen cartilage at sites 1-5 and for the full cartilage.

6.5 DISCUSSION

The two most important findings from this study are that T2 mapping of the distal Mc3/Mt3 of horses is feasible and that the T2 relaxation times did not differ significantly among the 3 groups, except at site 2. This indicates that the storage techniques used, namely 48 hour chilling and 60-90 day freezing probably do not severely impact on the T2 relaxation times of the areas evaluated. There is some evidence that the frozen cartilage results in increased T2 relaxation times. The magic angle affects T2 relaxation at particularly the sloping dorsal and palmar aspects of distal Mc3/Mt3.

The technique of T2 mapping of the distal Mc3/Mt3 has been previously validated, as has the inability to differentiate the cartilage of distal Mc3/Mt3 at sites 1 and 2 from that of the adjacent phalanx 1 using a 1.5T machine. [33] The ROIs drawn at sites 1 and 2 were a combination of the two adjacent cartilages and the thin layer of fluid between them. The distal Mc3 and Mt3 cartilage is approximately 1 mm thick (0.90±0.17 mm), [34] resulting in the resolution of the MR images being on the limit of the measurement setup used in this study. The T2 relaxation times give a baseline of values which can be compared to horses with cartilage damage of the distal Mc3/Mt3 and at sites 1 and 2 of combined distal Mc3/Mt3 and proximal phalanx 1.

The typical mean T2 values for different ROIs of human cartilage is between 15 and 60 ms, varying slightly with the magnetic field strength used, [35] and can vary up to between 10 and 80 ms. The horse control (GrA) T2 values of the distal Mc3/Mt3 in the current study ranged from 43.1-147.17 ms, although the average values ranged from 50 to 143 ms. This generally higher T2 relaxation time may be as result of higher water content, lower collagen concentration, and differing mechanical properties of the horse cartilage in comparison to that of normal human cartilage. Likely of even more significance, where the angle of the segmented cartilage and that of the static magnetic field (B_0) approximates the magic angle of 54.7º (or 125,3º) at sites 3, 4 and 5 (the sloping dorsal and palmar surfaces of distal Mc3/Mt3), higher T2 values were found, indicating that the values found are site dependent.

The protons in water within structures with highly ordered collagen- and water rich tissues (tendons, ligaments, cartilage), are subject to dipolar

interactions of which the strength depends on the orientation of the fibres to B_0. These interactions result in quick dephasing of the MR signal after excitation, resulting in a hypointense signal. The dipolar interactions are minimised when $3\cos^2\theta-1=0$ (θ= the angle of the structure relative to B_0, in this case when θ is approximately 55º or 125º), resulting in an increase in T2 and therefore increased intensity of the structure. [36] This magic angle effect has been reported in ligaments, tendons and cartilage in humans, and in ligaments and tendons in the distal horse limb. [37-39] It has not as yet been reported in equine cartilage. It is therefore important to note the initial positioning of Mc3/Mt3 and that this should be kept as constant as possible. [40, 41]The horse distal femoral medial condyle hyaline cartilage mean T2 values were found to be respectively 40.7, 53.6, and 61.6 ms, at deep, middle, and superficial sites, [23] generally higher than human cartilage but lower than the current study's distal Mc3/Mt3 T2 relaxation values, likely because the distal condylar cartilage is more perpendicular to the B_0, although in the study it appeared that some of the cartilage segmentations had been done at angles approximating the magic angle, although this was not discussed. Additionally, since synovial fluid is inevitably segmented within the ROIs, this may also result in higher T2 relaxation values.

Initially the control limbs (GrA; n=17) were compared to the treatment limbs (GrB; n=13, i.e. 8 chilled and 5 frozen). No statistically significant differences were found, the smallest *P*-value being 0.335. However, inspection of the means and medians of the three groups revealed that there may be differences. Therefore the chilled and frozen groups were also compared separately with one another and the control group.

In the current study site 1 likely differed from sites 3, 4, and 5 because of the magic angle effect, site 1 being more perpendicular to B_0 and having a lower T2 relaxation time. The fact that site 1 included the proximal aspect of phalanx 1 cartilage may also have contributed to the difference. Sites 3 and 4 had relatively similar relaxation times, likely because they often overlapped. Sites 1 and 2 did not differ significantly, likely because the combined distal Mc3/Mt3 and proximal phalanx were relatively close to one another in the dorsal condyle/transverse ridge area. Site 4 differed significantly from sites 1 and 2, likely again because of the magic angle effect, but again may also

have the contributing factor of not including proximal phalanx one cartilage. Site 4 likely differed from site 5 because of being on the palmar/plantar surface; it has been reported that there are more viable chondrocytes palmarly than dorsally in the equine fetlock indicating an inherent difference in water content and /or collagen matrix, between the dorsal and palmar/plantar condylar cartilage, warranting further research. [42] The magic angle effect is unlikely to contribute to the difference since sites 4 and 5 are both angled similarly to B_0 albeit as mirror images to one another.

The limbs in this study were placed on the dorsum with the metacarpo/metatarsophalangeal joint in extension so that the distal Mc3/Mt3 and digit were in a relatively straight line and positioned as such parallel to B_0. This, however, was not measured or quantified in any way and some minor angulation of distal Mc3/Mt3 may have occurred relative to B_0.

The fact that resolution limitations prevented discrimination of the distal Mc3/Mt3 and proximal phalanx at sites one and two is similar to that found in the human hip with relatively thin opposing cartilage, where dGEMRIC combined analysis of the articulating surfaces has been reported to not affect the analysis of dGEMRIC findings. [43] Further work evaluating this in T2 mapping in the metacarpo/metatarsophalangeal joint of the horse particularly those with osteoarthritis is required.

Articular cartilage consists of four functionally and structurally divided zones, namely the zone of calcified cartilage, the deep zone, the middle or transitional (radial) zone and the superficial (articular or tangential) zone. [44] This stratification is well visualized on T2 mapping images of normal human cartilage and correlates well with histological zones, where the shorter T2 relaxation values are in the radial zone, due to the highly organized radially orientated fibrils resulting in increased internuclear dipolar relaxations and relative restriction of water motion. The longer T2 relaxation values in the transitional zone are as result of the more haphazard organization of collagen. [45, 46] Clinically this has also been utilized in humans. [47]This typical visible layered pattern with increasing T2 values from the subchondral bone to the articular surface, has been seen in the distal femur of the horse, [23] which could not be appreciated in this study, because of the relatively poor resolution of the very thin cartilage of distal Mc3/Mt3, but likely still affects the

results by modulating T2 as a function of the angle between the cartilage surface and B_0.

The T2 measurement technique has been reported to show good intra- and inter repeatability in human articular cartilage [48-50] and is likely to be the same in the horse. It has been shown that T2 values are sensitive to mechanical cartilage stress in humans. [51] A 0.65 mm decrease in cartilage thickness has been seen in weight-bearing cartilage, [52] and signal intensity of superficial cartilage layers is decreased with increasing levels of compression. [53] Another report specifically ascribes the increase in signal intensity in T2 mapped cartilage of humeral femoral condyles to cartilage compression. [54]It is debatable whether the cartilage of the current study's specimens had cartilage that was under compression. GrA's limbs had not been weight-bearing for up to 7 hours, and GrB's limbs not weight-bearing for 48 hours to up to 90 days. In the recumbent, non-weight-bearing joint, T2 values are likely to differ from that of the weight-bearing cartilage.

Repositioning of equine limbs to utilize the magic angle effect to determine the T1 relaxation time of the tendinous structures palmar to Mc3 has been reported to be feasible, [55] and should be considered for future studies to determine its effect on equine distal Mc3/Mt3 cartilage.

Cryopreservation of cartilage in humans, either by refrigeration or freezing, is done for research and allograft purposes [56] to preserve the specimen for the former until an optimal time for the MRI scan, and until transplantation for the latter. The two important factors to consider in cryopreservation for particularly osteochondral transplants but also for minimizing damage for research purposes is cell viability and matrix integrity. [26]

Freezing of cartilage has quite a marked effect on its tissue structure and composition, [57] likely caused by catabolic enzyme degradation after freezing and thawing, [58] e.g. metalloproteinases destroying collagen, [59] stromlysin degradation of the core and link proteins in aggrecan, [60] and the polysaccharide components of aggrecan by hyaluronidase, chondroitinase and other glycosidases LD. [61] Freezing can also physically damage chondrocytes and the matrix as result of ice crystal formation [26, 57] and is often

also associated with loss of water from the matrix. The mechanical destruction that occurs by the expansion of water turning to ice is likely also involved.

When cartilage is damaged or degraded, T2 relaxation time increases. [26, 62, 63] This is mostly due to disintegration of the collagen network, [35, 62] but also due to an increase in free extracellular fluid, [27, 57] and to a lesser extent due to a loss of proteoglycans [63] and has also been postulated to be as result of a combination of changes in cartilage molecular conformation. [57] The study reporting this, using magnetic resonance microimaging of bovine nasal cartilage also found that T2 relaxation time increased with increased time being frozen or stored at 4ºC. [57] Less matrix structural changes have been described to occur when cartilage is cooled or frozen quickly as compared to slow freezing techniques. [26]

There was some indication of increased T2 values in the frozen limbs vs the other limbs in this study (Figure 6.3) and this would have to be confirmed with a larger study or a meta-analysis. The tendency for a mildly increased T2 relaxation time seen in the frozen group could be as result of the damage to the cartilage after the freeze/thaw cycle. Even though this was not visualized histologically, we cannot exclude that the chilled or frozen cartilage could have been affected by the cryopreservation techniques at a molecular level, but did not significantly affect T2 relaxation times.

When cartilage is freeze-dried thereby decreasing its water content T1 relaxation times have been shown to be linearly dependent on the solid-to-water ratio and inversely to the water content, however also dependent on the amount of free and loosely-bound water and percentage of proteoglycan content. [27] Usually T2 relaxation time is more sensitive to water content than T1 relaxation, but T2 relaxation is strongly dependent on, and can be affected by collagen fiber integrity and its orientation in relation to B_0. [64, 65]

A large amount of the MRI cartilage research done in the non-veterinary field evaluating the effect of cryopreservation is done with microimaging MRI where the resolution can be in the range of 13.7µm, [46] tissue sample sizes are small and temperature changes can be instigated quickly as opposed to the relatively slow freezing of entire horse cadaver digits. Therefore some care must be taken in directly comparing macro and micro MRI imaging with relevance to T2 relaxation times.

There were no differences between the T2 relaxation times between controls and chilled and frozen specimens except at site 2, where there is evidence of differences between the frozen limbs' measurements on the one hand, and the fresh and frozen limbs' on the other. At site 2 the ROIs were of the combined Mc3/Mt3 and proximal phalanx cartilages. This combined cartilage T2 relaxation time may explain the difference at site 2. It is possible that the combined cartilage measurements at site 2 when measured could have inadvertently have included more of the subchondral bone during the ROI segmentation resulting in the lower T2 relaxation values, since here at the distal transverse ridge of Mc3/Mt3, the measured combined cartilage using proton density weighted images have been reported to be narrower than at sites 1 and 3. [33] Excluding the site 2 differences, it is encouraging that minimal differences in T2 relaxation times are present in the remaining sites and most importantly for the full cartilage, leading us to conclude that if limbs are to be stored using chilling or freezing prior to MRI T2 mapping, the resultant T2 maps and relaxation times are credible.

Limitations of this study include the low number of limbs used, particularly since only half the number of limbs were used respectively in the 2 parts of GrB. Another limitation is the relatively poor spatial resolution of the thin distal Mc3/Mt3 cartilage, which could be improved with the use of a dedicated volume coil, higher magnetic field strength and a decreased FOV. The use of traction to separate the two cartilage surface can also be considered to improve visibility of articular surfaces. [66] The fact that the temperature of the limbs was not measured prior to scanning may have affected the results since they were not allowed to acclimatize to room temperature for at least 24 hours prior to scanning for logistical reasons, and it is well recognised that temperature of the sample affects T2 relaxation time; [67] however since samples were treated relatively similarly in this study it is unlikely to have had a significant effect on the results. In spite of these limitations, the results illustrate that T2 mapping is feasible in the distal Mc3/Mt3 and combined distal Mc3/Mt3-proximal phalanx. The results strongly suggest that T2 relaxation time changes minimally after chilling and freezing/thawing in the distal horse metacarpus3/metatarsus 3 where the cartilage is not adjacent to the proximal phalanx.

Additional studies further evaluating the effect of the magic angle phenomenon on T2 values of the sites should be conducted. Future research should also address whether T2 mapping changes can be seen in horses with osteoarthritis of the metacarpo/metatarsophalangeal joints.

T2 mapping of the horse distal Mc3/Mt3 is feasible and can be conducted after chilling and freezing of the limbs with minimal effect on T2 relaxation time and mapping, except at the transverse ridge where the cartilage of Mc3/Mt3 overlaps with that of the proximal phalanx. Chilling appears to affect cartilage T2 relaxation time less than freezing. Magic angle has an effect on the dorsal and palmar/plantar condyles.

ACKNOWLEDGMENTS

No author has any conflict of interest related to this work. The study was jointly financed by the University of Pretoria Veterinary Faculty Research Fund, the Department of Companion Animal Clinical Studies and a grant to Prof RM Kirberger from the National Research Foundation of South Africa. Thanks go to Faerie Glen Hospital Pretoria MR Trust for the use of the MRI machine and to the radiographers of the Pretoria MR Trust and the OVAH. Thank you to the staff of the Highveld Horse Care unit, and Mrs J C Jordaan for the data analysis.

REFERENCES

1. Dyson PK, Jackson BF, Pfeiffer DU, Price JS. Days lost from training by two- and three-year-old Thoroughbred horses: A survey of seven UK training yards. Equine Vet J 2008;40:650-657.

2. Perkins NR, Reid SW, Morris RS. Profiling the New Zealand Thoroughbred racing industry. 2. conditions interfering with training and racing. N Z Vet J 2005;53:69-76.

3. Parente EJ, Russau AL, Birks EK. Effects of mild forelimb lameness on exercise performance. Equine Vet J Suppl 2002;Supplement:252-256.

4. Anonymous. A comparison of the economic costs of equine lameness, colic, and equine protozoal myeloencephalitis (EPM) in the United States. Animal and Plant Health Inspection service. 2001. Available at http://www.aphis.usda.gov/animal_health/nahms/equine/downloads/equine98/Equine98_is_Colic.pdf. (accessed May 2011).

5. Bailey CJ, Reid SW, Hodgson DR, Rose RJ. Impact of injuries and disease on a cohort of two- and three-year-old Thoroughbreds in training. Vet Rec 1999;145:487-493.

6. McIlwraith CW. General pathology of the joint and response to injury. In: McIlwraith CW, Trotter GW, editors. Joint disease in the horse. Philadelphia: WB Saunders; 2006. p. 40-70.

7. Barr ED, Pinchbeck GL, Clegg PD, Boyde A, Riggs CM. Post mortem evaluation of palmar osteochondral disease (traumatic osteochondrosis) of the metacarpo/metatarsophalangeal joint in Thoroughbred racehorses. Equine Vet J 2009;41:366-371.

8. Smith KJ, Bertone AL, Weisbrode SE, Radmacher M. Gross, histologic, and gene expression characteristics of osteoarthritic articular cartilage of the metacarpal condyle of horses. Am J Vet Res 2006;67:1299-306.

9. Goldring MB, Goldring SR. Osteoarthritis. J Cell Physiol 2007;213:626-634.

10. Butler JA, Colles CM, Dyson SJ, Kold SE, Poulos PW. General principles. In: Clinical radiology of the horse. 3rd ed. Chichester, United Kingdom: Wiley-Blackwell; 2009. p. 1-36.

11. Javaid MK, Lynch JA, Tolstykh I, Guermazi A, Roemer F, Aliabadi P, et al. Pre-radiographic MRI findings are associated with onset of knee symptoms: The most study. Osteoarthritis Cartilage 2010;18:323-328.

12. Trattnig S, Domayer S, Welsch GW, Mosher T, Eckstein F. MR imaging of cartilage and its repair in the knee - a review. Eur Radiol 2009;19:1582-1594.

13. Roemer FW, Eckstein F, Guermazi A. Magnetic resonance imaging-based semiquantitative and quantitative assessment in osteoarthritis. Rheum Dis Clin North Am 2009;35:521-555.

14. Domayer SE, Welsch GH, Dorotka R, Mamisch TC, Marlovits S, Szomolanyi P, et al. MRI monitoring of cartilage repair in the knee: A review. Semin Musculoskelet Radiol 2008;12:302-317.

15. Watanabe A, Wada Y. [Progress of research in osteoarthritis. quantitative magnetic resonance imaging of cartilage in knee osteoarthritis. Clin Calcium 2009;19:1638-1643.

16. Qian Y, Williams AA, Chu CR, Boada FE. Multicomponent T2* mapping of knee cartilage: Technical feasibility ex vivo. Magn Reson Med 2010;64:1426-1431.

17. Menezes NM, Gray ML, Hartke JR, Burstein D. T2 and T1rho MRI in articular cartilage systems. Magn Reson Med 2004;51:503-509.

18. Menendez MI, Clark DJ, Carlton M, Flanigan DC, Jia G, Sammet S, et al. Direct delayed human adenoviral BMP-2 or BMP-6 gene therapy for bone and cartilage regeneration in a pony osteochondral model. Osteoarthritis Cartilage 2011;19:1066-1075.

19. Carstens A, Kirberger RM, Velleman M, Dahlberg LE, Fletcher L, Lammentausta E. Feasibility for mapping cartilage T1 relaxation times in the

distal metacarpus3/metatarsus3 of Thoroughbred racehorses using delayed gadolinium-enhanced magnetic resonance imaging of cartilage (dGEMRIC): Normal cadaver study. Vet Radiol US 2013. DOI:10-111/vru.12030.

20. Goodwin DW. Visualization of the macroscopic structure of hyaline cartilage with MR imaging. Semin Musculoskelet Radiol 2001;5:305-312.

21. Nieminen MT, Menezes NM, Williams A, Burstein D. T2 of articular cartilage in the presence of gd-DTPA2-. Magn Reson Med 2004;51:1147-1152.

22. Lammentausta E, Kiviranta P, Toyras J, Hyttinen MM, Kiviranta I, Nieminen MT, et al. Quantitative MRI of parallel changes of articular cartilage and underlying trabecular bone in degeneration. Osteoarthritis Cartilage 2007;15:1149-1157.

23. Marik W, Apprich S, Welsch GH, Mamisch TC, Trattnig S. Biochemical evaluation of articular cartilage in patients with osteochondrosis dissecans by means of quantitative T2- and T2-mapping at 3T MRI: A feasibility study. Eur J Radiol 2012;81:923-927.

24. White LM, Sussman MS, Hurtig M, Probyn L, Tomlinson G, Kandel R. Cartilage T2 assessment: Differentiation of normal hyaline cartilage and reparative tissue after arthroscopic cartilage repair in equine subjects. Radiology 2006;241:407-14.

25. Reiter DA, Lin PC, Fishbein KW, Spencer RG. Multicomponent T2 relaxation analysis in cartilage. Magn Reson Med 2009;61:803-809.

26. Lin PC, Reiter DA, Spencer RG. Classification of degraded cartilage through multiparametric MRI analysis. J Magn Reson 2009;201:61-71.

27. Laouar L, Fishbein K, McGann LE, Horton WE, Spencer RG, Jomha NM. Cryopreservation of porcine articular cartilage: MRI and biochemical results after different freezing protocols. Cryobiology 2007;54:36-43.

28. Damion RA, Pawaskar SS, Ries ME, Ingham E, Williams S, Jin Z, et al. Spin-lattice relaxation rates and water content of freeze-dried articular cartilage. Osteoarthritis Cartilage 2012;20:184-190.

29. Widmer WR, Buckwalter KA, Hill MA, Fessler JF, Ivancevich S. A technique for magnetic resonance imaging of equine cadaver specimens. Vet Radiol Ultrasound 1999;40:10-4.

30. Bolen G, Haye D, Dondelinger R, Busoni V. Magnetic resonance signal changes during time in equine limbs refrigerated at 4 degrees C. Vet Radiol Ultrasound 2010;51:19-24.

31. Bolen GE, Haye D, Dondelinger RF, Massart L, Busoni V. Impact of successive freezing-thawing cycles on 3-T magnetic resonance images of the digits of isolated equine limbs. Am J Vet Res 2011;72:780-790.

32. Neundorf RH, Lowerison MB, Cruz AM, Thomason JJ, McEwen BJ, Hurtig MB. Determination of the prevalence and severity of metacarpophalangeal joint osteoarthritis in Thoroughbred racehorses via quantitative macroscopic evaluation. Am J Vet Res 2010;71:1284-1293.

33. McIlwraith CW, Frisbie DD, Kawcak CE, Fuller CJ, Hurtig M, Cruz A. The OARSI histopathology initiative - recommendations for histological assessments of osteoarthritis in the horse. Osteoarthritis Cartilage 2010;18 Suppl 3:S93-105.

34. Carstens A, Kirberger RM, Dahlberg LE, Prozesky L, Fletcher L, Lammentausta E. Validation of delayed gadolinium-enhanced magnetic resonance imaging of cartilage and T2 mapping for quantifying distal metacarpus/metatarsus cartilage thickness in Thoroughbred racehorses. Vet Radiol Ultrasound 2013;54:139-148.

35. Olive J, D'Anjou MA, Girard C, Laverty S, Theoret C. Fat-suppressed spoiled gradient-recalled imaging of equine metacarpophalangeal articular cartilage. Vet Radiol Ultrasound 2010;51:107-115.

36. Mosher TJ, Dardzinski BJ. Cartilage MRI T2 relaxation time mapping: Overview and applications. Semin Musculoskelet Radiol 2004;8:355-368.

37. Bydder M, Rahal A, Fullerton GD, Bydder GM. The magic angle effect: A source of artifact, determinant of image contrast, and technique for imaging. J Magn Reson Imaging 2007;25:290-300.

38. Smith MA, Dyson SJ, Murray RC. Is a magic angle effect observed in the collateral ligaments of the distal interphalangeal joint or the oblique sesamoidean ligaments during standing magnetic resonance imaging? Vet Radiol Ultrasound 2008;49:509-515.

39. Spriet M, McKnight A. Characterization of the magic angle effect in the equine deep digital flexor tendon using a low-field magnetic resonance system. Vet Radiol Ultrasound 2009;50:32-36.

40. Werpy NM, Ho CP, Kawcak CE. Magic angle effect in normal collateral ligaments of the distal interphalangeal joint in horses imaged with a high-field magnetic resonance imaging system. Vet Radiol Ultrasound 2010;51:2-10.

41. Shiomi T, Nishii T, Myoui A, Yoshikawa H, Sugano N. Influence of knee positions on T(2), T*(2), and dGEMRIC mapping in porcine knee cartilage. Magn Reson Med 2010;64:707-714.

42. Elhawary H, Zivanovic A, Tse ZT, Rea M, Davies BL, Young I, et al. A magnetic-resonance-compatible limb-positioning device to facilitate magic angle experiments *in vivo*. Proc Inst Mech Eng H 2008;222:751-760.

43. Dykgraaf S, Firth EC, Rogers CW, Kawcak CE. Effects of exercise on chondrocyte viability and subchondral bone sclerosis in the distal third metacarpal and metatarsal bones of young horses. Vet J 2008;178:53-61.

44. Lattanzi R, Petchprapa C, Glaser C, Dunham K, Mikheev AV, Krigel A, et al. A new method to analyze dGEMRIC measurements in femoroacetabular impingement: Preliminary validation against arthroscopic findings. Osteoarthritis Cartilage 2012;20:1127-1133.

45. Pearle AD, Warren RF, Rodeo SA. Basic science of articular cartilage and osteoarthritis. Clin Sports Med 2005;24:1-12.

46. Nieminen MT, Rieppo J, Toyras J, Hakumaki JM, Silvennoinen J, Hyttinen MM, et al. T2 relaxation reveals spatial collagen architecture in articular cartilage: A comparative quantitative MRI and polarized light microscopic study. Magn Reson Med 2001;46:487-493.

47. Xia Y, Moody JB, Burton-Wurster N, Lust G. Quantitative in situ correlation between microscopic MRI and polarized light microscopy studies of articular cartilage. Osteoarthritis Cartilage 2001;9:393-406.

48. Maier CF, Tan SG, Hariharan H, Potter HG. T2 quantitation of articular cartilage at 1.5 T. J Magn Reson Imaging 2003;17:358-364.

49. Koff MF, Parratte S, Amrami KK, Kaufman KR. Examiner repeatability of patellar cartilage T2 values. Magn Reson Imaging 2009;27:131-136.

50. Glaser C, Horng A, Mendlik T, Weckbach S, Hoffmann RT, Wagner S, et al. T2 relaxation time in patellar cartilage--global and regional reproducibility at 1.5 Tesla and 3 Tesla. Rofo 2007;179:146-152.

51. Glaser C, Mendlik T, Dinges J, Weber J, Stahl R, Trumm C, et al. Global and regional reproducibility of T2 relaxation time measurements in human patellar cartilage. Magn Reson Med 2006;56:527-534.

52. Nishii T, Kuroda K, Matsuoka Y, Sahara T, Yoshikawa H. Change in knee cartilage T2 in response to mechanical loading. J Magn Reson Imaging 2008;28:175-180.

53. Waterton JC, Solloway S, Foster JE, Keen MC, Gandy S, Middleton BJ, et al. Diurnal variation in the femoral articular cartilage of the knee in young adult humans. Magn Reson Med 2000;43:126-132.

54. Rubenstein JD, Kim JK, Henkelman RM. Effects of compression and recovery on bovine articular cartilage: Appearance on MR images. Radiology 1996;201:843-850.

55. Mosher TJ, Smith H, Dardzinski BJ, Schmithorst VJ, Smith MB. MR imaging and T2 mapping of femoral cartilage: *In vivo* determination of the magic angle effect. Am J Roentgenol 2001;177:665-669.

56. Spriet M, Wisner ER, Anthenill LA, Buonocore MH. Determination of T1 relaxation time of normal equine tendons using magic angle magnetic resonance imaging. Vet Radiol Ultrasound 2011;52:149-153.

57. Williams RJ,3rd, Ranawat AS, Potter HG, Carter T, Warren RF. Fresh stored allografts for the treatment of osteochondral defects of the knee. J Bone Joint Surg Am 2007;89:718-726.

58. Fishbein KW, Canuto HC, Bajaj P, Camacho NP, Spencer RG. Optimal methods for the preservation of cartilage samples in MRI and correlative biochemical studies. Magn Reson Med 2007;57:866-873.

59. Ellis AJ, Curry VA, Powell EK, Cawston TE. The prevention of collagen breakdown in bovine nasal cartilage by TIMP, TIMP-2 and a low molecular weight synthetic inhibitor. Biochem Biophys Res Commun 1994;201:94-101.

60. Kozaci LD, Buttle DJ, Hollander AP. Degradation of type II collagen, but not proteoglycan, correlates with matrix metalloproteinase activity in cartilage explant cultures. Arthritis Rheum 1997;40:164-174.

61. Bottomley KM, Borkakoti N, Bradshaw D, Brown PA, Broadhurst MJ, Budd JM, et al. Inhibition of bovine nasal cartilage degradation by selective matrix metalloproteinase inhibitors. Biochem J 1997;323 (Pt 2):483-488.

62. Shikhman AR, Brinson DC, Lotz M. Profile of glycosaminoglycan-degrading glycosidases and glycoside sulfatases secreted by human articular chondrocytes in homeostasis and inflammation. Arthritis Rheum 2000;43:1307-1314.

63. Dunn TC, Lu Y, Jin H, Ries MD, Majumdar S. T2 relaxation time of cartilage at MR imaging: Comparison with severity of knee osteoarthritis. Radiology 2004;232:592-598.

64. Watrin-Pinzano A, Ruaud JP, Olivier P, Grossin L, Gonord P, Blum A, et al. Effect of proteoglycan depletion on T2 mapping in rat patellar cartilage. Radiology 2005;234:162-170.

65. Grunder W, Kanowski M, Wagner M, Werner A. Visualization of pressure distribution within loaded joint cartilage by application of angle-sensitive NMR microscopy. Magn Reson Med 2000;43:884-891.

66. Momot KI, Pope JM, Wellard RM. Anisotropy of spin relaxation of water protons in cartilage and tendon. NMR Biomed 2010;23:313-324.

67. Nakanishi K, Tanaka H, Nishii T, Masuhara K, Narumi Y, Nakamura H. MR evaluation of the articular cartilage of the femoral head during traction. correlation with resected femoral head. Acta Radiol 1999;40:60-63.

68. Reiter DA, Peacock A, Spencer RG. Effects of frozen storage and sample temperature on water compartmentation and multiexponential transverse relaxation in cartilage. Magn Reson Imaging 2011;29:561-567.

CHAPTER 7

The effect of chilling and freezing on dGEMRIC mapping in the normal Thoroughbred horse cadaver distal metacarpus3/metatarsus3 cartilage

Ann Carstens, Robert M Kirberger, Mark Velleman, Leif E Dahlberg, Lizelle Fletcher, Eveliina Lammentausta

Keywords: articular cartilage; dGEMRIC mapping; horse; metacarpus/metatarsus, chill, frozen

From the Department of Companion Animal Clinical Studies, Faculty of Veterinary Science, University of Pretoria, Private Bag X04 Onderstepoort 0110 (Carstens, Kirberger), Pretoria South Africa; Little Company of Mary Hospital, George Storrar Ave. (Velleman), Pretoria South Africa; Joint and Soft Tissue Unit, Department of Clinical Sciences, Malmö, Lund University, Department of Orthopaedics, Malmö University Hospital, SE-205 02 (Dahlberg, Lammentausta), Malmö, Sweden; Department of Statistics, University of Pretoria (Fletcher), Pretoria South Africa; Department of Diagnostic Radiology, Oulu University Hospital, POB 50, FI-90029 OYS (Lammentausta), Oulu, Finland.

Submitted

7.1 ABSTRACT

Osteoarthritis of the metacarpo-/metatarsophalangeal joints is a major cause of lameness in horses. In delayed gadolinium enhanced MRI of cartilage (dGEMRIC), a useful technique developed for non-invasive assessment of early cartilage degradation, Gd-DTPA^{2-} distributes inversely proportional to the proteoglycan content thereof. Research studies often necessitate chilling or freezing of limbs, requiring evaluation of whether these techniques affect the mapping images. The cadaver distal metacarpus3/metatarsus3 of 6 normal Thoroughbred racehorses (GrA), were scanned using a 1.5T MRI machine. In a similar sized group (GrB), one randomly selected forelimb and hind limb were chilled for 48 hours and the contralateral limbs frozen for at least 60 days. After returning to room temperature the limbs underwent MRI imaging. T1 relaxation time was measured from scans acquired pre-contrast and at 30, 60, 120 and 180 minutes post intra-articular injection of Gd-DTPA^{2-}. T1 relaxation times were calculated for the full cartilage and at five regions of interest (sites 1-5) in the cartilage. T1 relaxation time did not differ between the groups at any of the scanning times for the full cartilage, and only differed between the groups at site 2 pre-gadolinium and at site 3 at 30 minutes. All groups showed significant decrease in T1 relaxation time between pre-gadolinium injection and the later scan times. Results suggest that dGEMRIC mapping in the horse cadaver metacarpo-/metatarsophalangeal joints can be conducted after chilling and freezing of the limbs with minimal effect on the T1 relaxation times and mapping.

7.2 INTRODUCTION

Lameness in horses is the primary cause of poor performance and wastage[1-3] and costs the horse industry in North America an estimated $1 billion in 1998.[4] The fetlock (metacarpo/metatarsophalangeal) joint is the most commonly affected by trauma and degeneration,[5] most of which results in osteoarthritis,[6] affecting both the lateral and medial condyles of metacarpus3/metatarsus3 (Mc3/Mt3).[7, 8]

Osteoarthritis is defined as degeneration of articular cartilage and is characterized by matrix fibrillation, the appearance of fissures and ulceration and full-thickness loss of the cartilage.[9] Confirmation of osteoarthritis in the metacarpo/metatarsophalangeal joints in the horse, is by means of clinical evaluation, perineural or intra-articular nerve blocks and relevant combinations of radiography, ultrasonography, computed tomography, scintigraphy and magnetic resonance imaging (MRI), if available. Many of these modalities are, however, only useful after the degenerative process has become advanced.[10]

Magnetic resonance imaging has been previously established as a method for visualizing early articular cartilage pathology in human studies.[11,12] In delayed gadolinium-enhanced MRI of cartilage (dGEMRIC), negatively charged Gd-DTPA^{2-} is injected either intra-articularly or intravenously. The contrast agent penetrates hyaline cartilage and distributes in an inverse relationship to the proteoglycan content of the cartilage. When the proteoglycan concentration is decreased as result of cartilage degradation, as seen in osteoarthritis, the gadolinium uptake is increased as result of the relative decrease in negative charge of the proteoglycan-depleted cartilage. This dGEMRIC technique has been described as an excellent indicator of early degenerative cartilaginous changes and has been found to correlate with mechanical properties of cartilage such as cartilage stiffness.[13,14] Parametric mapping of cartilage can be accomplished by post-processing dGEMRIC images and creating relaxation time colour maps. These maps provide a visual representation of relaxation times within specific cartilage locations.

The use of dGEMRIC has been reported once in a group of ponies, where it was used to test effects of administered bone morphogenic protein in experimentally-created femoral condyle lesions.[15] The feasibility of using dGEMRIC in the metacarpo/metatarsophalangeal joint in normal Thoroughbred horses has been reported, with significant decrease in T1 relaxation time occurring 60-120 minutes post intra-articular administration of Gd-DTPA.[2- 16] The technique has also been validated by determining that the cartilage thickness of the distal Mc3/Mt3 measured by means of dGEMRIC images and histopathological slides did not differ.[17]

Delayed gadolinium enhanced MRI of cartilage is not feasible in the current low field standing MRI units for horses due to their limited imaging resolution. However, for higher field magnets general anaesthesia is required for horses to be scanned in recumbency.

Magnetic resonance imaging research of the distal limb of the average size horse can often only be performed using dismembered cadaver limbs, since relatively few institutions have MRI facilities to accommodate an average size live horse, and costs, logistics and possible general anaesthetic risks for a live horse are factors that often preclude examinations of this kind. Since scan time is often limited, limbs may require chilling or freezing to be examined more conveniently at a later date. It is therefore important to establish whether dGEMRIC results are significantly affected by these cryopreservation techniques.

There is much research being conducted on the effect of chilling and/or freezing in cartilage; particularly in bovine nasal cartilage,[18] and bovine or porcine articular cartilage,[19,20] much of which has utilized micro MRI. Chilling and freezing has also been investigated in horses[21-23] particularly of the distal limb with different MRI sequences. These reports were mostly subjective evaluation of images pre- and post-chilling or freezing. One report evaluated distal limbs that were scanned within 12 hours after death and then at 1, 2, 7 and 14 days post 4ºC refrigeration using turbo spin echo (TSE) T1, TSE T2, short tau inversion recovery (STIR) and double echo steady state sequences.[22] Signal to noise ratio was utilized as a quantitative evaluation technique with a significant decrease seen in the bone marrow in the TSE T2 and double-echo steady state sequences. In another study by the same

authors, equine distal limbs underwent repeated freeze-thaw cycles and other limbs that were only frozen once but allowed to return to scanning temperature in different ambient temperature areas.[23] Their subjective findings were that overall image quality was unchanged except for the hoof capsule, but that there were significant differences in some of the sequences (T1-weighted, turbo spin-echo proton density-weighted) and tissues when evaluated quantitatively. Neither of these reports described the effect of chilling or freezing on the articular cartilage.

To the authors' knowledge, the effect of chilling and freezing on dGEMRIC in the horse metacarpo/metatarsophalangeal joints has not been reported. The purpose of the study was to establish whether 48 hour chilling or freezing and thawing of the limbs has a significant effect on T1 relaxation time in dGEMRIC of the distal Mc3/Mt3 articular cartilage. The hypothesis tested was that there is no significant difference in T1 relaxation values of the distal Mc3/Mt3 cartilage between control, chilled and frozen limbs.

7.3 MATERIALS AND METHODS

This project was approved by the institutional Animal Use and Care Committee and all horses were treated according to South African Veterinary Council ethical standards.

Six Thoroughbred horses (GrA (control), which were the same horses wherein the feasibility of dGEMRIC in the horse metacarpophalangeal joint was first reported[16]) were prospectively recruited from a local welfare unit for horses. Study inclusion criteria were as follows: age 3-6 years, any gender, no signs of lameness and no history of recent corticosteroid or proteoglycan treatments. Horses meeting inclusion criteria underwent a clinical examination to confirm absence of lameness. Immediately following the examination, horses were shot intra-cranially and all four limbs were removed at the middle portions of the Mc3/Mt3 diaphyses. Limbs were kept cool and transported to an MRI facility. Another six horses (GrB) were treated identically, except that a randomly selected forelimb and hind limb of each horse was kept for 48 hours at a household fridge temperature of 5º (GrBchill) and the other two

limbs frozen (GrBfrozen) from 60 to 90 days at a household freezer temperature of -20º. After these two time periods, the limbs of GrBfrozen were thawed and both GrBfrozen and GrBchill limbs were allowed to return to room temperature.

A vitamin E oil capsule was taped to the lateral aspect of each metacarpo/metatarsophalangeal joint and each limb was positioned with the dorsum facing downward and the toe facing into the gantry. A clinical 1.5 T MRI scanner (Avanto, Siemens Healthcare. Erlangen, Germany) was used with a 12-channel head and neck receive-only coil was used. The forelimbs were first scanned in random order followed by the hind limbs also in random order. All limbs were scanned at room temperature (20℃). For each joint, T1 weighted images were acquired in the sagittal plane (TR 557 ms, time to echo (TE) 23 ms, field of view (FOV) 100x100 mm, matrix 256x256, slice thickness 3 mm, receiver band-width 130 Hz/pix). Seventeen slices were acquired with the central slice positioned in the middle of the distal Mc3/Mt3 sagittal ridge. (Fig.7.1 A).

For each lateral and medial midcondylar slice, pre-contrast T1 relaxation time was measured using single slice inversion recovery spin echo sequences (TR 3000 ms, TE 13 ms, six TIs between 100 and 2800 ms, FOV 140x140 mm, matrix 256x256 mm, slice thickness 3 mm, receiver band-width 130 Hz/pix). Subsequently, joint fluid was aspirated from each joint and Gd-DTPA^{2-} (Magnevist®, gadopentetate dimeglumine, Bayer Health Care Pharmaceuticals) was injected using a dose of 0.05 ml in 5 ml saline (0.025 mmol/joint). Joints were manually flexed at one flexion per second for 5 minutes. Using the same mid-condylar slice locations as those used for the pre-contrast scans, T1 relaxation time measurements were repeated at 30, 60, 120, and 180 minutes post-injection as previously reported.[16] Following the MRI examinations, joints were evaluated using radiography and computed tomography. Joints with gross abnormalities were excluded from further analyses.

Five sites were analysed for each mid-condylar slice and each scan. Site 1 was defined using a 25° dorsal angle from a point in the center of the rotation of the joint; Site 2 was defined as the distal aspect of a line drawn down the axis of the diaphysis of Mc3/Mt3 and corresponding to the

transverse ridge. Site 3 was defined using a 35° palmar/plantar angle from a point in the center of the rotation of the joint. The ROIs for sites 1-3 were drawn 3 degrees dorsal to and 3 degrees palmar/plantar to sites 1-3. Sites 4 and 5 were where the cartilage was clearly seen at the most palmar/planter and dorsal locations where Mc3 and Mt3 cartilage could be clearly distinguished from adjacent first phalanx cartilage (Fig.7.1 B). Often site 3 was partially or totally included within site 4.

Following imaging, each Mc3 and Mt3 bone was dissected away from the rest of the limb and the distal condylar cartilage surface was evaluated macroscopically before and after 3-5 minute staining with India ink (Parker Quink Ink, Post Net Suite #283, Private Bag X1005, Claremont, 7735, South Africa). All cartilage and synovial tissues were examined, and gross abnormalities recorded. The cartilage was also graded using the Neundorf grading system.[24] Only joints with Grade 1 cartilage were used for further analyses. Grade 1 was defined using the following criteria: no gross abnormalities, minimal loss of reflectance, minimal cartilage hypertrophy at the joint margins, minimal partial thickness wear lines, minimal thinning of cartilage, minimal thickening of cartilage, and no enlarged synovial fossae. Mid-portions of the medial and lateral condyles of Mc3 and Mt3 were sectioned into 3-5 mm thick slices in a sagittal plane. The samples were fixed and decalcified in an 8% nitric acid made up in 10% buffered formalin solution. Sites 1, 2 and 3 were identified using a sagittal template of the corresponding lateral and medial condyles (Fig.7.1B). Each cut block was processed and stained using standard hematoxylin and eosin. The cartilage at sites 1-3 for each mid-condylar slice was evaluated for pathology using a modification of an Osteoarthritis Research Society International (OARSI) microscopic cartilage grading system.[24] Only cartilage with a grade less than 2 was used for further analyses.[25]

7.3.1 **dGEMRIC Data Analysis**

Full-thickness regions of interest (ROIs) were placed on sites 1-3 by one of the authors (AC). Each ROI extended 3°on either side of the template lines. Each ROI was manually positioned between the cartilage bone interface and the articular surface at site 3. The ROIs for sites 1 and 2 were

positioned adjacent to the bone-cartilage interface of phalanx 1 since the cartilage surface could not be positively identified in most of the limbs at these sites. Larger regions of interest were segmented at sites 4 and 5 from the bone-cartilage interface to the articular surface of Mc3/Mt3 which was clearly visible at these sites (Fig.7.1 B). Regions of interest of the entire cartilage for each specimen were also segmented (Fig.7.1 C). T1 maps were created by fitting the respective data into mono-exponential relaxation equations using an in-house MATLAB application (MATLAB, MathWorks Inc., Natick, MA, USA). Mean values for each ROI were calculated.

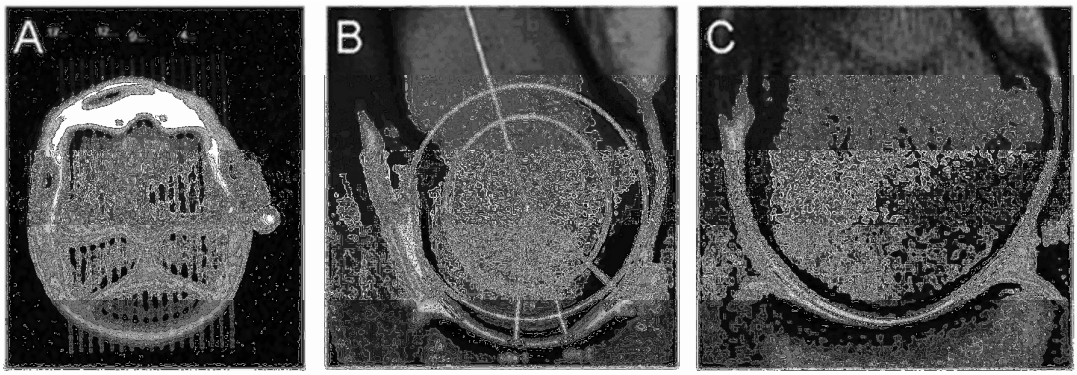

Figure 7.1 (A) Transverse MRI image of a distal Mt3 with a 17 line template with the central slice 9 placed sagitally over the distal sagittal ridge, slice 1 positioned on the lateral and slice 17 positioned on the medial epicondyle cortices. Note the hyperintense vitamin E oil capsule on the lateral epicondylar surface. (B) Parasagittal mid-condylar MRI image of a distal Mt3 with representation of the translucent template illustrating concentric circles placed “best-of-fit” over the Mt3 condyle with a line transecting midline of Mc3/Mt3 diaphysis/distal metaphysis. Regions of interest sites are outlined in black. Sites 1-3 are identified. Site 4 is where cartilage is clearly defined at the edges of the plantar articulation and Site 5 is where cartilage is clearly defined at edges of dorsal articulations. (C) Parasagittal mid-condylar MRI image of a distal Mc3 illustrating the segmentation of the entire distal Mc3 cartilage including the proximal phalanx cartilage where the 2 surfaces cannot be distinguished. The region of interest is outlined in black.

7.3.2 **Statistical analysis**

All statistical tests were selected and performed by Mrs J Jordaan, data analyst, Department of Statistics, University of Pretoria. Since the sample sizes are small, non-parametric tests - which are more robust - were conducted. Unfortunately, small sample sizes result in low power for statistical

tests, hence we reported exact p-values where possible. The Kruskall-Wallis test, which is analogous to an ANOVA, (SPSS. Version 20, 2012, IBM, New Orchard Road, Armonk, New York 10504) was conducted, where the data of the pooled limbs of the three different independent groups, respectively, were compared across the three groups per site and per relaxation time. The same was done for the combined five sites and the full cartilage ROIs. In the case of significant differences, Mann-Whitney U tests were performed *post hoc* to determine which relaxation times differed. Non-parametric Friedman tests were used to compare T1 relaxation times for pooled limbs across the five time periods for each of the three groups. For comparisons with significant differences from these tests, Wilcoxon signed rank tests were performed *post hoc*. The level of significance, α, was specified at 0.05. The evaluator was not blinded to the group.

7.4 RESULTS

For GrA, twenty of the 24 limbs met the inclusion criteria and four limbs were excluded, two for OA, one for synovitis, and one for an osseous cyst-like lesion. For GrB, thirteen limbs met the inclusion criteria and eleven limbs were excluded, for excessive cartilage wearlines, osteochondritis dissecans lesions, and palmar/plantar osteoarthritis, resulting in GrBchill with 8 limbs and GrBfrozen with 5 limbs. The presence of osteoarthritis could only be detected after the macroscopic and microscopic grading, hence the disparate numbers in the two B groups. Figures 7.2 and 7.3 demonstrate a representative set of dGEMRIC color maps for groups A, Bchill and Bfrozen for the entire segmented cartilage and at each of the 5 sites, respectively.

Using the current measurement setup the cartilage of distal Mc3/Mt3 at sites 1 and 2 could not be differentiated from the cartilage of the adjacent P1, therefore the ROIs drawn there were a combination of the two adjacent cartilages and the thin layer of fluid between them, as reported previously.[16,17]

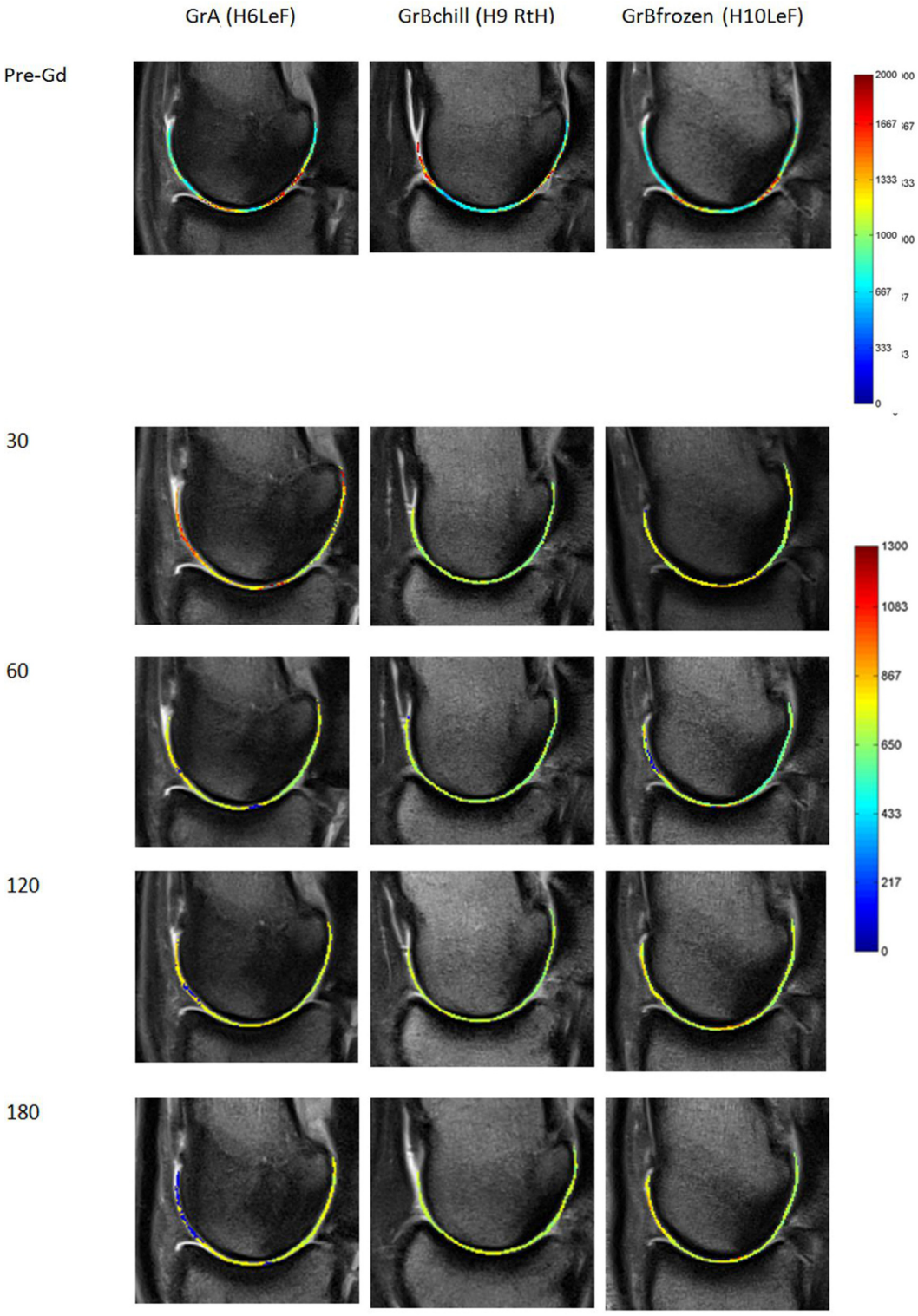

Figure 7.2 Comparative representative dGEMRIC maps of the mid condyles (either forelimb or hind limb), illustrating the colour-coded relaxation times (in ms) for each of the regions of interest for full cartilage segmentation for GrA (control), GrBchill and GrBfrozen. Note the colour inhomogeneity of the pre gadolinium images, likely a.r.o the combined distal Mc3/Mt3-proximal phalanx at sites 1 and 2, resulting in partial volume averaging of the synovial fluid between the cartilages.

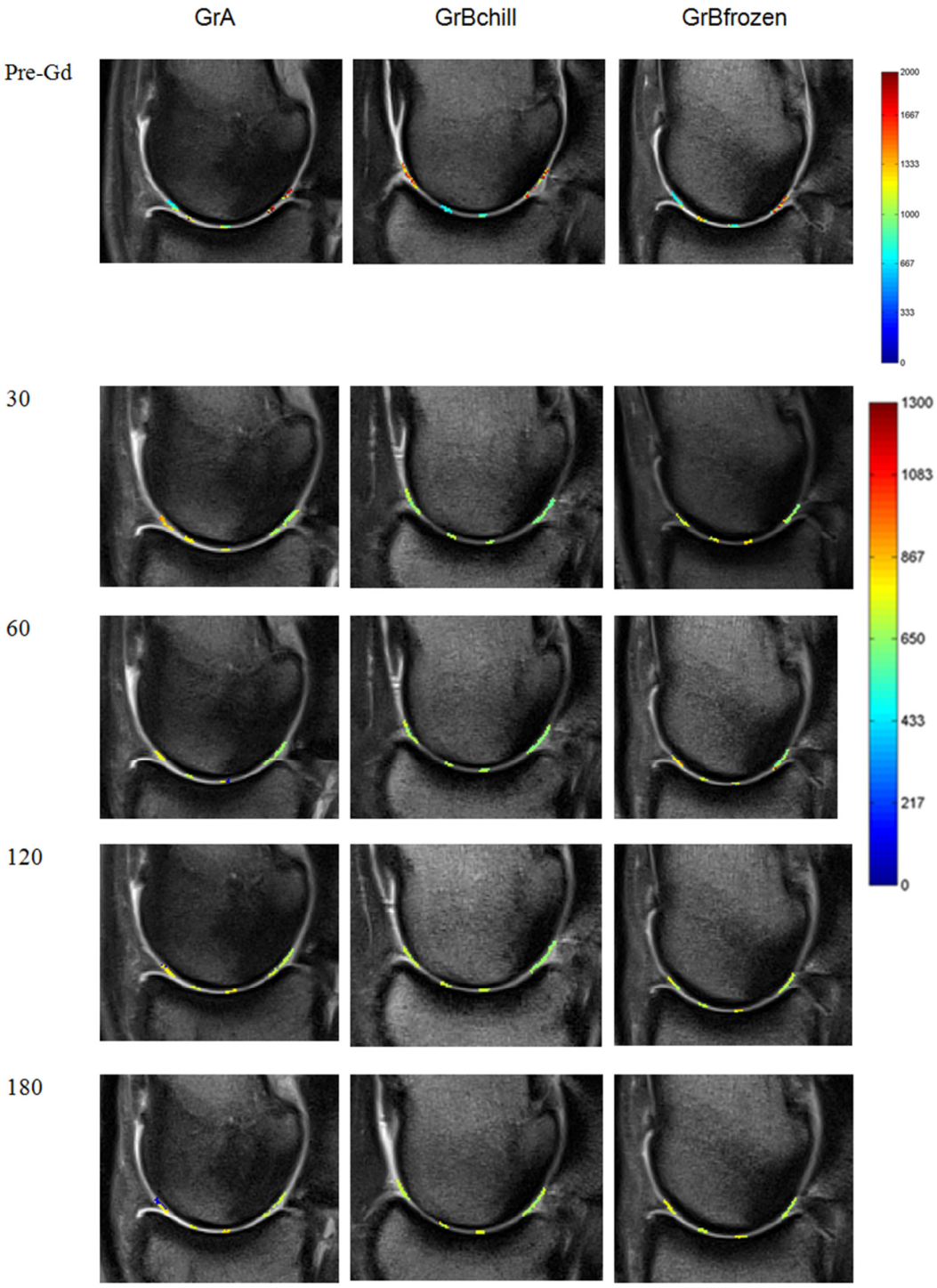

Figure 7.3 Comparative representative dGEMRIC maps of the mid condyles (either forelimb or hind limb), illustrating the colour-coded relaxation times (in ms) for each of the regions of interest for Sites 1-5 cartilage segmentation for GrA (control), GrBchill and GrBfrozen. Note the colour inhomogeneity of the pre gadolinium images, likely a.r.o the combined distal Mc3/Mt3-proximal phalanx at sites 1 and 2, resulting in partial volume averaging of the synovial fluid between the cartilages.

One can visually appreciate the substantial difference caused by the intra-articular injection of Gd-DTPA^{2-} between the pre-gadolinium (relatively high initial T1 relaxation time) and post gadolinium time periods (lower T1 relaxation time. Both the pre-gadolinium series had an inhomogenous appearance.

Tables 7.1 and 7.2 summarize relaxation times measured at each time interval for all 5 cartilage sites and the combined five sites, and full cartilage, respectively, and the results of the Kruskall-Wallis and Mann-Whitney U tests. There was no difference in the T1 relaxation time between the groups at any of the scanning times for the full cartilage or the sum of the sites, and only a difference between the groups at site 2 pre-gadolinium and at site 3 at 30 minutes post gadolinium injection.

TABLE 7.1. Kruskall-Wallis and Relevant Mann-Whitney U Tests for Independent Variables Showing Mean and Standard Deviation of T1 Relaxation Time of GrA, GrBchill and GrBfrozen of Distal Mc3/Mt3 (in ms) at Sites 3-5 and Combined with the Proximal Phalanx at Sites 1-2.

	Site 1			Site 2			Site 3			S4		S5	
Time (min)		T1 rel time (ms)	K-W	T1 rel time (ms)	K-W	M-W	T1 rel Time (ms)	K-W	M-W	T1 rel time (ms)	K-W	T1 rel Time (ms)	K-W
Pre-	c	1012.1 ±233.9	0.14 (33)	855.0 ±154.6	0.03 (33)	c vs ch 0.26	1370.7 ±264.8	0.79 (33)		1474.1 ±111.7	0.6 (33)	990.5 ±265.9	0.24 (33)
	ch	903.2 ±277.7		785.2 ±106.0		c vs fr 0.04	1453.0 ±205.5			1450.3 ±145.6		1076.0 ±304.6	
	fr	1148.9 ±195.4		1078.3 ±252.8		ch vs fr 0.011	1367.5 ±93.0			1429.3 ±74.8		1248.9 ±368.9	
30	c	701.3 ±143.7	0.31 (32)	667.9 ±191.7	0.72 (32)		682.7 ± 44	0.03 (32)	c vs ch 0.004	662.1 ±72.6	0.10 (32)	685.9 ±179.8	0.25 (32)
	ch	708.3 ±32.3		717.2 ±34.1			641.3 ±18.2		c vs fr 1.00	635.1 ±21.5		694.2 ±17.7	
	fr	656. 5 ±111.3		718.8 ±144.0			648.7 ±108.7		ch vs fr 0.22	649. 5 ±75.6		688.4 ±119.5	
60	c	674.3 ±156.8	0.54 (33)	668.7 ±209.1	0.86 (33)		673.6 ±115.2	0.1 (33)		667.4 ±140.3	0.15 (33)	642.3 ±191.8	0.07 (33)
	ch	709.8 ±34.2		748.1 ±47.9			662.2 ±27			660.0 ±24.3		689.5 ±13.4	
	fr	743.3 ±52.1		758.1 ±44.6			721.2 ±55.2			697.6 ±50.8		745.4 ±45.9	
120	c	670.6 ±201.4	0.79 (31)	668.0 ±205.2	0.88 (31)		652.3 ±144.5	0.11 (31)		661.3 ±147.8	0.06 (31)	646.3 ±210.0	0.97 (31)
	ch	728.8 ±29.3		731.9 ±34.5			675.2 ±29.6			670.1 ±24.5		730.1 ±29.5	
	fr	735.7 ±38.4		732.3 ±78.8			722.4 ±33.3			716.2 ±35.4		719.8 ±97.0	
180	c	700.7 ±199.9	0.52 (32)	725.8 ±230.0	0.38 (33)		685.6 ±213.9	0.24 (33)		683.0 ± 209.0	0.2 (33)	630.7 ±213.3	0.56 (33)
	ch	740.1 ±28.8		743.6 ±32.8			695.2 ±34.1			694.4 ±28.5		730.6 ±24.6	
	fr	733.6 ±85.2		692.2 ±137.4			741.7 ±44.5			741.9 ±45.6		684.1 ±126.4	

Footnote : T1 rel time, T1 relaxation time ; c, control ; ch, chilled ; fr, frozen ; min, minutes; ms, milliseconds; KW, Kruskall-Wallis test; M-W, Mann-Whitney U Test; underlined *P*-values, significant difference ($P<0.05$).

TABLE 7.2. Kruskall-Wallis Tests for Independent Variables Showing Mean and Standard Deviation of T1 Relaxation Time of GrA, GrBchill and GrBfrozen of Distal Mc3/Mt3 in ms at Sites1-5 Combined and Full Cartilage.

		Sites 1-5		Full cartilage	
Time (min)		T1 rel time (ms)	K-W	T1 rel time (ms)	K-W
Pr-Gd	c	1140.5±129.1	0.178	1027.0 ± 121.6	0.244
	ch	1133.5±157.1		1029.8 ± 93.1	
	fr	1254.6±108.0		1105.3 ± 95.7	
30	c	680.0±100.1	0.217	675.9 ± 137.7	0.332
	ch	679.2±15.0		687.7 ± 7.3	
	fr	672.4±107.9		677.4 ± 103.9	
60	c	665.3±139.8	0.152	664.5 ± 140.5	0.796
	ch	693.9±22.7		700.5 ± 11.1	
	fr	733.1±41.8		660.5 ± 113.6	
120	c	660.0±167.7	0.482	642.6 ± 165.8	0.729
	ch	707.2±24.8		716.9 ± 17.3	
	fr	725.3±36.4		707.9 ± 58.2	
180	c	689.6±208.9	0.880	662.9 ± 203.1	0.543
	ch	720.8±26.2		730.8 ± 14.5	
	fr	718.7±41.7		691.3 ± 70.0	

Footnote : T1 rel time, T1 relaxation time ; c, control ; ch, chilled ; fr, frozen ; min, minutes; ms, milliseconds; KW, Kruskall-Wallis test; *, significant difference *(P*<0.05).

Figures 7.4 and 7.5 illustrate graphic representations of Tables 7.1 and 7.2. They illustrate the marked decrease in T1 relaxation time after gadolinium administration as has been previously reported.[16] Table 7.3 shows the results of Friedman and Wilcoxon signed rank tests for repeated measures of the full cartilage measurements of the T1 relaxation time of GrA, GrBchill and GrBfrozen of Distal Mc3/Mt3. All the groups showed significant decrease in T1 relaxation time between pre-gadolinium injection and the later scan times and only differences between the later scan times for GrBchill. Figure 7.5 illustrates Table 7.3's contents graphically.

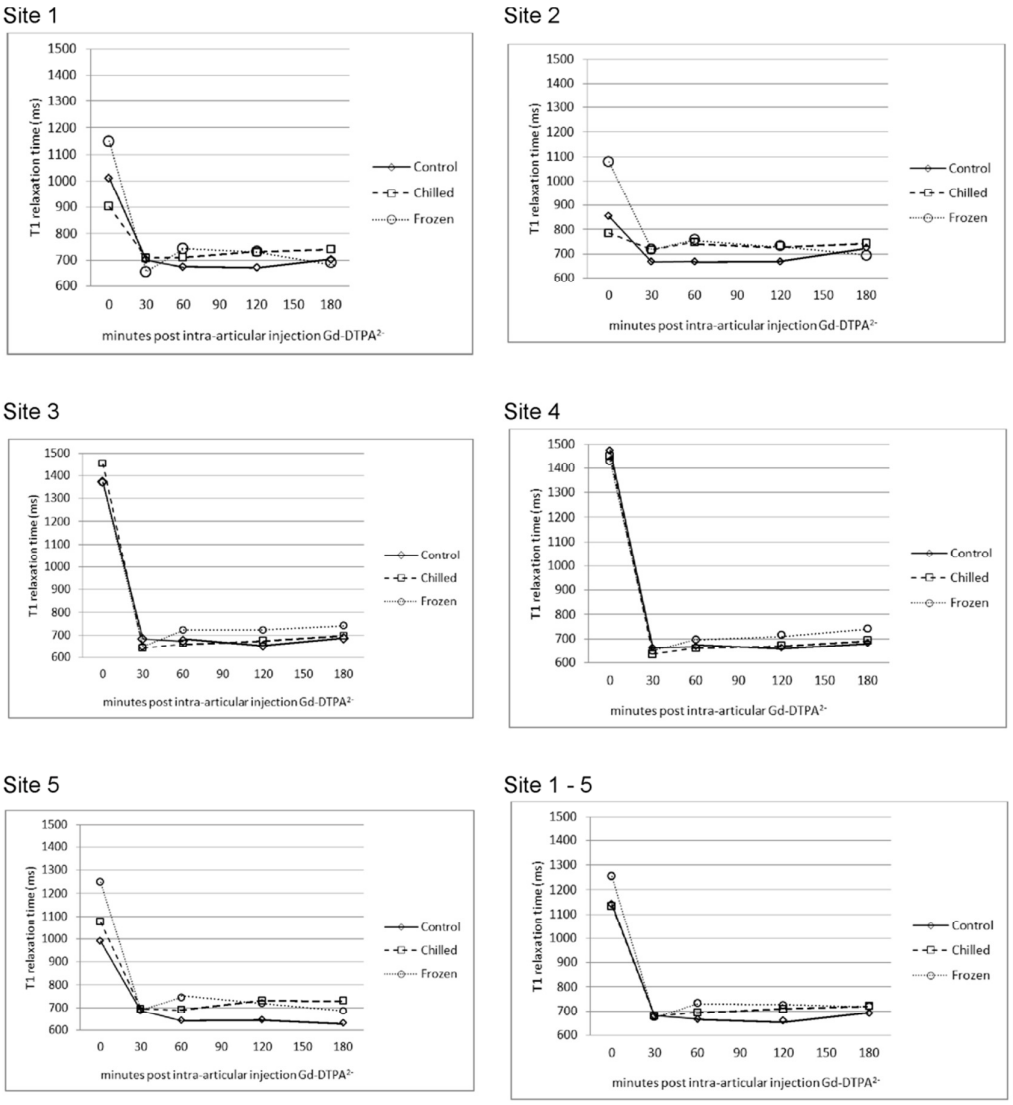

Figure 7.4 Mean of T1 relaxation times of GrA (control), GrBchill and GrBfrozen sites 1-5, and sites 1-5 combined of the cartilage of distal Mc3/Mt3. For standard deviations see Tables 7.1 and 7.2.

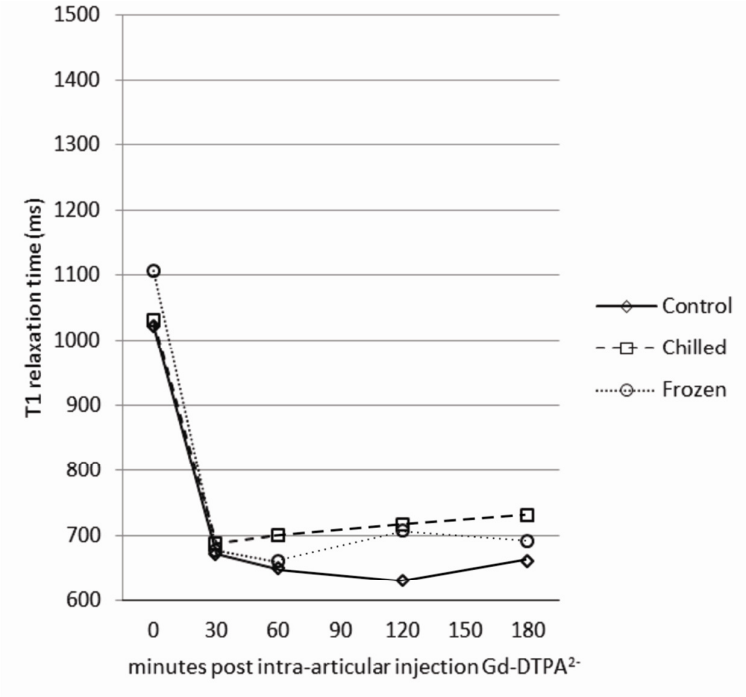

Figure 7.5 Mean of T1 relaxation times of the full cartilage of distal Mc3/Mt3 of GrA (control), GrBchill and GrBfrozen. For standard deviations see Table 7.3.

TABLE 7.3. Friedman and Wilcoxon Signed Rank Tests for Repeated Measures of the Full Cartilage Measurements Showing Mean and Standard Deviation of T1 Relaxation Time of GrA, GrBchill and GrBfrozen of Distal Mc3/Mt3 (in ms).

			FT	W-SRT	W-SRT	W-SRT	W-SRT	W-SRT	W-SRT	W-SRT	W-SRT	W-SRT	W-SRT
Time (min)		T1 relax time (ms)		Pre-Gd vs 30 min	Pre-Gd vs 60 min	Pre-Gd vs 120 min	Pre-Gd vs 180 min	30 Vs 60 min	30 vs 120 min	30 Vs 180 min	60 Vs 120 min	60 vs 180 min	120 vs 180 min
Pr-Gd	c	1027.0 ± 121.6	<0.0001*	<0.0001*	<0.0001*	<0.0001*	<0.0001*	0.640	0.284	0.623	0.86	0.891	0.865
	c	676.0 ± 137.7									5		
60	c	664.5 ± 140.5											
120	c	642.6 ± 165.8											
180	c	662.9 ± 203.1											
Pr-Gd	ch	1030.0 ± 93.1	<0.0001*	0.008*	0.008*	0.008*	0.008*	0.016*	0.008	0.008	0.016*	0.008*	0.008*
30	ch	687.7 ± 7.3											
60	ch	700.5 ± 140.5											
120	ch	716.9 ± 17.3											
180	ch	730.8 ± 14.5											
Pr-Gd	fr	1105.3 ± 95.7	0.009*	0.063	0.063	0.063	0.063	1	1	1	0.31		0.313
30	fr	677.4 ± 103.9											
60	fr	660.5 ± 113.6											
120	fr	707.9 ± 58.2											
180	fr	691.3 ± 70.0											

Footnote : c, control ; ch, chilled ; fr, frozen ; min, minutes; ms, milliseconds; FT, Friedman test; W-SRT, Wilcoxon Signed Rank test; *, significant difference (P<0.05).

7.5 DISCUSSION

The most important findings in this study were that the T1 relaxation pattern of distal Mc3/Mt3 cartilage after intra-articular injection of Gd-DTPA^{2-} that has been chilled or frozen decreases in a similar fashion over 3 hours to that of control specimens. There is also no difference in the T1 relaxation times among the control, chilled and frozen cartilage, except at site 2 prior to Gd-DTPA^{2-} injection between the frozen and the chilled and control, and at site 3 at 30 minutes post Gd-DTPA^{2-} injection between chilled and control limbs.

We chose three to six-year-old Thoroughbred horses for our study because horses in this age group are used for active flat-racing and are most likely to have some degree of mild osteoarthritis in their metacarpo/metatarso-phalangeal joints and this group would most benefit from the knowledge gleaned from this work. The modified Neundorf and OARSI scoring systems used a set of parameters that was easy to evaluate and should be repeatable within and among observers for future studies.[24,25] We excluded limbs from our study if gross abnormalities were present, or if there was minimal macroscopic (Grade 1) or microscopic (<Grade 2) cartilage damage at sites 1-3 of the condyles.

Since the cartilage of distal Mc3/Mt3 at sites 1 and 2 could not be differentiated from the cartilage of the adjacent P1, the ROIs drawn there were a combination of the two adjacent cartilages and the thin layer of fluid between them.[16,17] The distal Mc3 and Mt3 cartilage is approximately 1 mm thick (0.90±0.17 mm),[26] resulting in the resolution of the MR images being on the limit of the measurement setup used. MR measurement of horse carpal articular cartilage using a 1.5T machine has been reported with significant correlations found between MRI and histological measurements.[27]

The inhomogenous appearance of pre-contrast T1 was initially contrary to expectation. This is likely as result of the combined distal Mc3/Mt3 and proximal phalanx evaluation where some synovial fluid will inevitably be within the ROI, resulting in partial volume averaging. The thin cartilage also results in the segmentation of the ROI not always being precisely on the borders of the cartilage, thereby either including more or less of the synovium at each

area segemented. Even though the thickness of the fluid layer is so thin compared to the voxel size, its totally different relaxation properties would dominate in that voxel with red indicating synovial fluid inside the ROI. T1 relaxation time has been reported to correlate well with water content.[28]

Even though the numbers of the chilled and frozen specimens are lower than those of the control specimens, there appears to be minimal difference in the pattern of T1 relaxation seen among the 3 groups. The pattern of T1 relaxation time of the chilled and frozen specimens is similar to that seen in a previous report of fresh cadaver specimens (where only GrA T1 relaxation times were investigated.[16] The only difference found between the sites were at site 2 on the pre-gadolinium series where the control and chilled specimens differed from the frozen, which may be explained by the co-segmentation of the distal Mc3/Mt3 and proximal phalanx cartilage, again likely as result of partial volume averaging, and at site 3 where the control differed from the chilled cartilage. The differences found in the chilled group between the 30, 60, 120 mins vs all later times, is interesting and currently cannot be explained by the researchers. On visual inspection of the graphs, however, this difference does not appear remarkable.

Excluding the differences at the 2 sites, it is encouraging that minimal differences in T1 relaxation times are present in the remaining sites, the combined sites 1-5 and for the full cartilage, leading us to conclude that if limbs are to be stored using chilling or freezing prior to MRI T1 mapping, the resultant T1 maps and relaxation times are credible.

Cryopreservation of cartilage in humans is done for research and allografts[29] to preserve the specimen for the former until an optimal time for the MRI scan, and until transplantation for the latter. For research purposes it is done either by refrigeration or freezing, for allografting currently by refrigeration.

Freezing of cartilage can have marked effect on its tissue structure and composition,[30,31] after freezing and thawing, partially caused by enzymatic degradation may be involved[32] e.g. metalloproteinases destroying collagen,[33] stromolysin degradation of the core and link proteins in aggrecan,[34] and the polysaccharide components of aggrecan by hyaluronidase, chondroitinase

and other glycosidases.[35] The mechanical destruction that occurs by the expansion of water turning to ice is likely also involved.

Freeze-drying of cartilage decreases its water content, affecting T1 relaxation times, which have been shown to be linearly dependent on the solid-to-water ratio and inversely to the water content, but also dependent on the amount of free and loosely-bound water and percentage of GAG content.[20] In the current study no attempt was made to determine the difference in water content of the cartilage between the control and GrB specimens. Dessication may have had an effect on the results, but it appears minimally so, judging from the few differences among the specimens.

The greatest limitation to this study was the low numbers of specimens, in the cryopreserved groups and particularly that of the frozen specimens, leading to a low power of the statistical tests. The more robust non-parametric techniques used, resulted in some significant differences indicating that the results are valid. Other limitations include the relatively poor spatial resolution of the thin distal Mc3/Mt3 cartilage, which could be improved with the use of a dedicated surface coil, higher magnet field strength and a decreased FOV. The fact that the temperature of the limbs was not measured prior to scanning may have affected the results since they were not allowed to acclimatize to room temperature for at least 24 hours prior to scanning for logistical reasons, and it is well recognised that temperature of the sample affects T1 relaxation time;[36,37] however since samples were treated relatively similarly in this study it is unlikely to have had a significant effect on the results.The use of traction to separate the two cartilage surface can also be considered to improve visibility of articular surfaces.[38] In spite of these limitations, the results show that T1 relaxation times of the distal Mc3/Mt3 full cartilage after intra-articular injection of Gd-DTPA^{2-} differ minimally after chilling or freezing, implying specimens can be preserved until a later date and results after scanning will likely be reliable. The T1 relaxation pattern of distal Mc3/Mt3 cartilage that has been chilled or frozen decreases in a similar fashion over 3 hours to that of control specimens. Future research should address whether a difference in T1 post- Gd-DTPA^{2-} will occur due to the presence of osteoarthritis.

Delayed gadolinium enhanced MRI of the horse distal Mc3/Mt3 is feasible after chilling and freezing of the specimens and follows a similar

pattern of decreased T1 relaxation time as fresh specimens. The chilled and frozen cartilage T1 relaxation times differ little from fresh specimens, except at the transverse ridge, between frozen and control and chilled limbs, and at a site immediately palmar/plantar to the transverse ridge between chilled and frozen limbs.

ACKNOWLEDGMENTS

No author has any conflict of interest related to this work. The study was jointly financed by the University of Pretoria Veterinary Faculty Research Fund, the Department of Companion Animal Clinical Studies and a grant to Prof RM Kirberger from the National Research Foundation of South Africa. Thanks go to Faerie Glen Hospital MR Trust for the use of the MRI machine and their radiographers as well as to the OVAH radiographers. Thank you to the staff of the Highveld Horse Care unit, and Mrs J C Jordaan for the data analysis.

REFERENCES

1. Bailey CJ, Reid SW, Hodgson DR, Bourke JM, Rose RJ. Flat, hurdle and steeple racing: Risk factors for musculoskeletal injury. Equine Vet J 1998;30:498-503.

2. Dyson PK, Jackson BF, Pfeiffer DU, Price JS. Days lost from training by two- and three-year-old Thoroughbred horses: A survey of seven UK training yards. Equine Vet J 2008;40:650-657.

3. Perkins NR, Reid SW, Morris RS. Profiling the New Zealand Thoroughbred racing industry. 2. conditions interfering with training and racing. N Z Vet J 2005;53:69-76.

4. Anonymous. A comparison of the economic costs of equine lameness, colic, and equine protozoal myeloencephalitis (EPM) in the United States. Animal and Plant Health Inspection service. 2001. Available at http://www.aphis.usda.gov/animal_health/nahms/equine/downloads/equine98/Equine98_is_Colic.pdf. (accessed May 2011).

5. Wilsher S, Allen WR, Wood JL. Factors associated with failure of Thoroughbred horses to train and race. Equine Vet J 2006;38:113-118.

6. McIlwraith CW. General pathology of the joint and response to injury. In: McIlwraith CW, Trotter GW, editors. Joint disease in the horse. Philadelphia: WB Saunders; 2006. p. 40-70.

7. Smith KJ, Bertone AL, Weisbrode SE, Radmacher M. Gross, histologic, and gene expression characteristics of osteoarthritic articular cartilage of the metacarpal condyle of horses. Am J Vet Res 2006;67:1299-306.

8. Barr ED, Pinchbeck GL, Clegg PD, Boyde A, Riggs CM. Post mortem evaluation of palmar osteochondral disease (traumatic osteochondrosis) of the metacarpo/metatarsophalangeal joint in Thoroughbred racehorses. Equine Vet J 2009;41:366-371.

9. Goldring MB, Goldring SR. Osteoarthritis. J Cell Physiol 2007;213:626-634.

10. Javaid MK, Lynch JA, Tolstykh I, Guermazi A, Roemer F, Aliabadi P, et al. Pre-radiographic MRI findings are associated with onset of knee symptoms: The most study. Osteoarthritis Cartilage 2010;18:323-328.

11. Roemer FW, Eckstein F, Guermazi A. Magnetic resonance imaging-based semiquantitative and quantitative assessment in osteoarthritis. Rheum Dis Clin North Am 2009;35:521-555.

12. Crema MD, Roemer FW, Marra MD, Burstein D, Gold GE, Eckstein F, et al. Articular cartilage in the knee: Current MR imaging techniques and applications in clinical practice and research. Radiographics 2011;31:37-61.

13. Baldassarri M, Goodwin JS, Farley ML, Bierbaum BE, Goldring SR, Goldring MB, et al. Relationship between cartilage stiffness and dGEMRIC index: Correlation and prediction. J Orthop Res 2007;25:904-912.

14. Gray ML, Burstein D, Kim YJ, Maroudas A. 2007 elizabeth winston lanier award winner. Magnetic resonance imaging of cartilage glycosaminoglycan: Basic principles, imaging technique, and clinical applications. J Orthop Res 2008;26:281-291.

15. Menendez MI, Clark DJ, Carlton M, Flanigan DC, Jia G, Sammet S, et al. Direct delayed human adenoviral BMP-2 or BMP-6 gene therapy for bone and cartilage regeneration in a pony osteochondral model. Osteoarthritis and Cartilage 2011;19:1066-1075.

16. Carstens A, Kirberger RM, Velleman M, Dahlberg LE, Fletcher L, Lammentausta E. Feasibility for mapping cartilage T1 relaxation times in the distal metacarpus3/metatarsus3 of Thoroughbred racehorses using delayed gadolinium-enhanced magnetic resonance imaging of cartilage (dGEMRIC): Normal cadaver study. Vet Radiol US 2013. DOI:10-111/vru.12030.

17. Carstens A, Kirberger RM, Dahlberg LE, Prozesky L, Fletcher L, Lammentausta E. Validation of delayed gadolinium-enhanced magnetic resonance imaging of cartilage and T2 mapping for quantifying distal

metacarpus/metatarsus cartilage thickness in Thoroughbred racehorses. Vet Radiol Ultrasound 2013;54:139–148.

18. Reiter DA, Lin PC, Fishbein KW, Spencer RG. Multicomponent T2 relaxation analysis in cartilage. Magn Reson Med 2009;61:803-809.

19. Laouar L, Fishbein K, McGann LE, Horton WE, Spencer RG, Jomha NM. Cryopreservation of porcine articular cartilage: MRI and biochemical results after different freezing protocols. Cryobiology 2007;54:36-43.

20. Damion RA, Pawaskar SS, Ries ME, Ingham E, Williams S, Jin Z, et al. Spin-lattice relaxation rates and water content of freeze-dried articular cartilage. Osteoarthritis Cartilage 2012;20:184-190.

21. Widmer WR, Buckwalter KA, Hill MA, Fessler JF, Ivancevich S. A technique for magnetic resonance imaging of equine cadaver specimens. Vet Radiol Ultrasound 1999;40:10-4.

22. Bolen G, Haye D, Dondelinger R, Busoni V. Magnetic resonance signal changes during time in equine limbs refrigerated at 4 degrees C. Vet Radiol Ultrasound 2010;51:19-24.

23. Bolen GE, Haye D, Dondelinger RF, Massart L, Busoni V. Impact of successive freezing-thawing cycles on 3-T magnetic resonance images of the digits of isolated equine limbs. Am J Vet Res 2011;72:780-790.

24. Neundorf RH, Lowerison MB, Cruz AM, Thomason JJ, McEwen BJ, Hurtig MB. Determination of the prevalence and severity of metacarpophalangeal joint osteoarthritis in Thoroughbred racehorses via quantitative macroscopic evaluation. Am J Vet Res 2010;71:1284-1293.

25. McIlwraith CW, Frisbie DD, Kawcak CE, Fuller CJ, Hurtig M, Cruz A. The OARSI histopathology initiative - recommendations for histological assessments of osteoarthritis in the horse. Osteoarthritis Cartilage 2010;18 Suppl 3:S93-105.

26. Olive J, D'Anjou MA, Girard C, Laverty S, Theoret C. Fat-suppressed spoiled gradient-recalled imaging of equine metacarpophalangeal articular cartilage. Vet Radiol Ultrasound 2010;51:107-115.

27. Murray RC, Branch MV, Tranquille C, Woods S. Validation of magnetic resonance imaging for measurement of equine articular cartilage and subchondral bone thickness. Am J Vet Res 2005;66:1999-2005.

28. Berberat JE, Nissi MJ, Jurvelin JS, Nieminen MT. Assessment of interstitial water content of articular cartilage with T1 relaxation. Magn Reson Imaging 2009;27:727-732.

29. Williams RJ,3rd, Ranawat AS, Potter HG, Carter T, Warren RF. Fresh stored allografts for the treatment of osteochondral defects of the knee. J Bone Joint Surg Am 2007;89:718-726.

30. Fishbein KW, Canuto HC, Bajaj P, Camacho NP, Spencer RG. Optimal methods for the preservation of cartilage samples in MRI and correlative biochemical studies. Magn Reson Med 2007;57:866-873.

31. Zheng S, Xia Y, Bidthanapally A, Badar F, Ilsar I, Duvoisin N. Damages to the extracellular matrix in articular cartilage due to cryopreservation by microscopic magnetic resonance imaging and biochemistry. Magn Reson Imaging 2009;27:648-655.

32. Ellis AJ, Curry VA, Powell EK, Cawston TE. The prevention of collagen breakdown in bovine nasal cartilage by TIMP, TIMP-2 and a low molecular weight synthetic inhibitor. Biochem Biophys Res Commun 1994;201:94-101.

33. Kozaci LD, Buttle DJ, Hollander AP. Degradation of type II collagen, but not proteoglycan, correlates with matrix metalloproteinase activity in cartilage explant cultures. Arthritis Rheum 1997;40:164-174.

34. Bottomley KM, Borkakoti N, Bradshaw D, Brown PA, Broadhurst MJ, Budd JM, et al. Inhibition of bovine nasal cartilage degradation by selective matrix metalloproteinase inhibitors. Biochem J 1997;323 (Pt 2):483-488.

35. Shikhman AR, Brinson DC, Lotz M. Profile of glycosaminoglycan-degrading glycosidases and glycoside sulfatases secreted by human articular chondrocytes in homeostasis and inflammation. Arthritis Rheum 2000;43:1307-1314.

36. Petren-Mallmin M, Ericsson A, Rauschning Wea. The effect of temperature on MR relaxation times and signal intensities for human tissues. Magn Reson Mater Phys Biol Med 1993;1:176-184.

37. Reiter DA, Peacock A, Spencer RG. Effects of frozen storage and sample temperature on water compartmentation and multiexponential transverse relaxation in cartilage. Magn Reson Imaging 2011;29:561-567.

38. Nakanishi K, Tanaka H, Nishii T, Masuhara K, Narumi Y, Nakamura H. MR evaluation of the articular cartilage of the femoral head during traction. correlation with resected femoral head. Acta Radiol 1999;40:60-63.

CHAPTER 8

GENERAL DISCUSSION

The specific research hypotheses as pertaining to the distal cadaver Thoroughbred horse Mc3/Mt3 (where Mc3/Mt3 is not adjacent to P1):

Could not disprove H_0 :

1. dGEMRIC mapping measurement parameters result in the same cartilage thickness as histomorphometric (gold standard) parameters.
2. T2 mapping measurement parameters result in the same cartilage thickness as histomorphometric (gold standard) parameters.
3. dGEMRIC mapping of 5 ROIs of the cartilage can be performed.
4. dGEMRIC mapping of the entire cartilage can be performed.

Could not prove H_0:

5. The optimal time of scanning cartilage for dGEMRIC mapping after intra- articular injection of Gd-DTPA^{2-} is 30 minutes.

Could not disprove H_0:

6. T2 mapping of 5 ROIs of the cartilage can be performed.
7. T2 mapping of the entire cartilage can be performed.
8. Chilling/freezing does not affect T2 mapping of 5 ROIs of the cartilage.
9. Chilling/freezing does not affect T2 mapping of the entire cartilage.
10. Chilling/freezing does not affect dGEMRIC mapping of 5 ROIs of the cartilage.
11. Chilling/freezing does not affect dGEMRIC mapping of the entire cartilage.

Delayed gadolinium enhanced magnetic resonance imaging of cartilage (dGEMRIC) and T2 mapping can be performed in the distal Mc3/Mt3 of the horse cadaver limb and the results have been discussed in depth in the specific preceding chapters. However, as in all research, aspects have been identified that need to be addressed to further evaluate the use of these techniques *in vitro* as well as *in vivo*.

To determine whether the cartilage that was visualised with the dGEMRIC and T2 mapping segmentations was in fact representative of the true distal Mc3/Mt3 cartilage, an initial study was done to determine whether cartilage thicknesses measured by the mapping techniques and histomorphometric measurements were similar. It was found to be so, although the MRI measurement parameters were not optimized for use in very thin (only 1 mm thick) cartilage being less than two pixel widths, resulting in a relatively crude approximation of cartilage thickness. When equine carpus cartilage was evaluated, MRI measurements did not differ significantly from histological measurements, but the cartilage was approximately 1.4 mm thick. [1] Distal Mc3/Mt3 cartilage measurements were also reported with good precision and moderate correlation of cartilage thickness between MRI measurements (using a three-dimensional spoiled gradient-recalled echo with fat saturation), but it was found that the ability of MRI to detect full thickness cartilage erosions was only moderate although the specificity was high. [2] Early work done on the comparison between MRI and histological measurements in human cartilage states the reliability of cartilage thickness measurements depends on the absolute thickness of the cartilage layer, and that the correlation of cartilage less than 2 mm thick is only 0.73. Therefore MRI measurements are more accurate in cartilage thicker than 2 mm, implying that measurements of 1 mm thick cartilage of the distal Mc3/Mt3 with the measurement techniques used may not be totally accurate. [3]

The used imaging resolution also results in volume averaging, which additionally results in less reliable consistent relaxation times and in turn less reliable mapping.

Another point to consider is that tissue shrinkage occurs with histological fixation which could have affected the measurements, although buffering was performed which decreases this shrinkage effect. [4, 5] At sites 1 and 2 where articular surface to Haversian canal cartilage thickness (BC) measurement was the least reliable, the histological measurement was larger than the MRI measurements (P = 0.031), but at site 3 where cartilage was relatively well visualized, histological and MRI measurements were similar (0.1 mm absolute difference (P = 0.69). This further enforces the significance of resolution as a limitation in the present study.

Within these limitations, however, using MRI and histology the cartilage was measured to be approximately 1 mm thick in the current study and the previously reported study. [2] Therefore it is assumed that the mapping techniques did in fact reflect the distal Mc3/Mt3 cartilage where it did not overlap with the proximal phalanx cartilage. This overlapping occurred at the most distal aspect of the Mc3/Mt3. Similar overlapping occurs in human joints such as the coxofemoral joint. Adapted mapping techniques purposefully segmenting the combined adjacent cartilages have been reported with success in humans [6] and could be implemented in the horse where this occurs, particularly where the cartilage is as thin as it is in the distal Mc3/Mt3.

Once the cartilage visibility was established, the dGEMRIC mapping technique was investigated, firstly determining that T1 relaxation time decreased similarly to that in humans (both *in vitro* and *in vivo*) although the initial relaxation time (approximately 1500 ms) was higher than human cartilage. The second fact that was determined, was that the lowest relaxation time (approximately 650 ms) occurred between 60 and 120 minutes post intra-articular injection of Gd-DTPA^{2-} giving a one hour time period in which the procedure could reliably be performed. The relaxation time tended to increase slightly from just prior to 180 minutes post-injection indicating that a "washout" was taking place. It is likely that this washout would be accelerated in the live animal due to the presence of a blood supply and joint motion.

An interesting finding was the differences in T1 relaxation among most of the five sites prior to Gd-DTPA^{2-} administration, which could be due to the inherent differences in the cartilages, dorsally, distally and palmarly/plantarly, the combined segmentation of distal Mc3/Mt3 at sites 1 and 2, or a reflection of the poor spatial resolution. However, as the Gd-DTPA^{2-} diffused into the cartilage the difference between the sites decreased and become insignificant at 60 minutes post-injection, likely as result of the relatively high concentration of diffused Gd-DTPA^{2-} causing a relative equilibration within the cartilage resulting in similar relaxation times of the different areas.

The 12 minutes taken to perform one full dGEMRIC sequence, i.e. six different inversion recovery sequences, is a relatively long time if a horse is under general anaesthesia and four limbs need to be evaluated, probably resulting in a 60 minute scan time including repositioning of the horse. This

could be a limiting factor; a standing high field magnet would be ideal for solving this problem in future, but relatively low resolution, movement artefacts and longer scan time in the current low field standing magnets may preclude the use of dGEMRIC in these units. This needs to be investigated.

The T2 mapping resulted in good quality images, with the same cartilage overlapping limitations. There was marked pixel loss in the sloping palmar/plantar and less so dorsal condyles, due to the magic angle effect. This could be improved with higher field magnets, which are currently not readily available. Repositioning of the limb within the magnetic field to optimize the angle for visualizing certain parts of the cartilage should be considered. Control T2 relaxation times ranged from 50-143 ms. This generally higher T2 relaxation time, in comparison to humans, may be as result of higher water content, lower collagen concentration, and differing mechanical properties of the horse cartilage in comparison to that of normal human cartilage. On chilling and freezing of the cartilage and allowing thawing and returning to room temperature, few significant differences were seen. Those that were seen were at one site where the adjacent cartilages overlapped. No differences were seen where the full cartilage was mapped and compared. Another limitation of this study was the fact that limbs' temperatures were not determined at the time of scanning which may have affected the results somewhat, [7] albeit all limbs were treated in a similar fashion minimizing the risk that temperature differences would have had an impact on results.

The study comparing the dGEMRIC control, chilled and frozen limbs resulted in minimal differences between the groups at particular sites at particular time periods post Gd-DTPA^{2-} injection and none where the combined cartilage or full cartilages were segmented. There were, as expected, significant decreases in T1 relaxation time between pre- Gd-DTPA^{2-} and all post gadolinium times for the control, chilled and frozen limbs full cartilage segmentations, but additionally differences among all the post gadolinium times for the chilled limbs. This was an unexpected finding and has as yet to be explained. Possible reasons could include differences in limb temperature at the time of scanning, inherent differences in the specific joints

(although unlikely due to the stringent inclusion criteria) and the low number of limbs used.

The common limitation for all parts of this study was the relatively low number of limbs utilized, which relates to the decision making of cost-effectiveness between tissue sampling and power of experiments. This was particularly evident in the chilled and frozen limbs. I feel quite confident that the number of limbs studied gives sufficient evidence that both mapping techniques are reliable in the cadaver distal Mc3/Mt3 in fresh, chilled and frozen specimens, given the limitation of the spatial resolution.

Statistical analysis on this low number of limbs, necessitated the use of non-parametric tests, with the Friedman test for repeated dependent variables utilized in the comparisons of T1 relaxation times before and after Gd-DTPA^{2-} injection. If differences were found, these were than tested using the Wilcoxon signed rank tests. For independent variables, such as the different sites, non-parametric tests such as the Kruskal-Wallis test (analogous to the analysis of variance) was used, and in the case of significance, Mann-Whitney U tests were performed to see which parameters differed from one another. Since significant differences were found using these relatively insensitive tests, the non-parametric tests were deemed as acceptable and reliable tests. If more limbs had been available for testing, parametric tests would have been utilized.

Due to logistical, time and costing reasons, unblinded tests were not performed, although this would have ensured non-bias in the evaluation of the data. Neither intra-observer nor inter-observer validations of the measurements were performed in the dGEMRIC or T2 mapping relaxation studies. This was not deemed necessary since the technique has been well-proven in human studies to have very good inter- and intra-observer repeatability, and there was no reason to believe this would not be valid in equine cartilage. [8-10] However, since the distal Mc3/Mt3 cartilage is so much thinner than the cartilage measured in the human studies, this may need to be addressed if results are not consistent in future studies.

To particularly improve the poor spatial resolution factors it would be useful to repeat these studies using higher field magnets, thinner slices, and

increased fields of view, but also to evaluate equine joints with thicker cartilage.

The findings in the current study lay the foundation for evaluation of the technique in the live horse, and once reference values are established, to compare the results of the cadaver and live horse normal limbs with those of horses with osteoarthritis. Dividing the osteoarthritic limbs into different classes of severity would be useful in determining a trend in progression of cartilage damage. It would also be interesting to correlate the severity of clinical signs and joint pain to the amount of cartilage damage identified by the mapping techniques. Correlation of the cartilage mapping findings in osteoarthritis with the condition of the underlying subchondral bone and trabeculae would also add information as to the interaction between cartilage and subchondral bone in the pathogenesis of osteoarthritis

Ultimately this information will be invaluable in early diagnosis of osteoarthritis in the fetlock, providing guidance as to appropriate therapy and monitoring progression of the disease as well as response to therapy.

REFERENCES

1. Murray RC, Branch MV, Tranquille C, Woods S. Validation of magnetic resonance imaging for measurement of equine articular cartilage and subchondral bone thickness. Am J Vet Res 2005;66:1999-2005.

2. Olive J, D'Anjou MA, Girard C, Laverty S, Theoret C. Fat-suppressed spoiled gradient-recalled imaging of equine metacarpophalangeal articular cartilage. Vet Radiol Ultrasound 2010;51:107-115.

3. Kladny B, Bail H, Swoboda B, Schiwy-Bochat H, Beyer WF, Weseloh G. Cartilage thickness measurement in magnetic resonance imaging. Osteoarthritis Cartilage 1996;4:181-186.

4. Bahr GF, Bloom G, Friberg U. Volume changes of tissues in physiological fluids during fixation in osmium tetroxide or formaldehyde and during subsequent treatment. Exp Cell Res 1957;12:342-355.

5. Penttila A, McDowell EM, Trump BF. Effects of fixation and postfixation treatments on volume of injured cells; J Histochem Cytochem 1975;23:251-270.

6. Lattanzi R, Petchprapa C, Glaser C, Dunham K, Mikheev AV, Krigel A, et al. A new method to analyze dGEMRIC measurements in femoroacetabular impingement: Preliminary validation against arthroscopic findings. Osteoarthritis Cartilage 2012;20:1127-1133.

7. Reiter DA, Peacock A, Spencer RG. Effects of frozen storage and sample temperature on water compartmentation and multiexponential transverse relaxation in cartilage. Magn Reson Imaging 2011;29:561-567.

8. Multanen J, Rauvala E, Lammentausta E, Ojala R, Kiviranta I, Hakkinen A, et al. Reproducibility of imaging human knee cartilage by delayed gadolinium-enhanced MRI of cartilage (dGEMRIC) at 1.5 Tesla. Osteoarthritis Cartilage 2009;17:559-564.

9. Koff MF, Parratte S, Amrami KK, Kaufman KR. Examiner repeatability of patellar cartilage T2 values. Magn Reson Imaging 2009;27:131-136.

10. Glaser C, Mendlik T, Dinges J, Weber J, Stahl R, Trumm C, et al. Global and regional reproducibility of T2 relaxation time measurements in human patellar cartilage. Magn Reson Med 2006;56:527-534.

CHAPTER 9

CONCLUSIONS

The results of this study provide information on the technique of dGEMRIC and T2 mapping in the distal metacarpus3/metatarsus3 cartilage of the normal Thoroughbred horse cadaver. Values reported can serve as reference for further studies utilizing MRI to identify early cartilage matrix changes in horse lameness. Limitations of the used technique were identified. The main inferences from this study confirmed that:

1. Inversion recovery sequences utilizing STIR fat signal suppression are accurate techniques, within the limitations of spatial resolution, for measuring distal Mc3/Mt3 cartilage thickness at locations where the cartilage is not in direct contact with that of the proximal phalanx.
2. Proton density weighted sequences are accurate techniques, within the limitations of spatial resolution, for measuring distal Mc3/Mt3 cartilage thickness at locations where the cartilage is not in direct contact with that of the proximal phalanx.
3. dGEMRIC, using intra-articular Gd-DTPA^{2-} is a feasible technique for measuring and mapping changes in T1 relaxation times of the distal Mc3/Mt3 where the cartilage is not in direct contact with that of the proximal phalanx.
4. The optimal time of scanning the distal Mc3/Mt3 cartilage for dGEMRIC after intra-articular injection of Gd-DTPA^{2-} is 60-120 minutes.
5. T2 mapping in the horse cadaver distal Mc3/Mt3 where the proximal phalanx cartilage is not immediately adjacent, can be conducted after chilling and freezing of the limbs with minimal effect on T2 relaxation time and mapping images except where the magic angle effect predominates.
6. dGEMRIC mapping in the horse cadaver distal Mc3/Mt3 where the proximal phalanx cartilage is not immediately adjacent, can be conducted

after chilling and freezing of the limbs with minimal effect on T1 relaxation time and dGEMRIC mapping images.

Further studies that should be conducted include evaluation of:

1. distal Mc3/Mt3 cartilage using higher field magnets
2. other equine joints with thicker cartilage
3. intravenous *vs* intra-articular administration of Gd-DTPA^{2-}
4. dGEMRIC and T2 mapping in live horses
5. the effect of exercise on dGEMRIC and T2 mapping in live horses
6. dGEMRIC and T2 mapping on horse metacarpo/metatarsophalangeal joints with differing degrees of osteoarthritis and lameness in order to relate cartilage degeneration to symptoms, pain and the condition of the overlying subchondral bone and trabeculae.

APPENDICES- published/submitted articles

Article 1 Validation of delayed gadolinium-enhanced magnetic resonance imaging of cartilage and T2 mapping for quantifying distal metacarpus/metatarsus cartilage thickness in Thoroughbred racehorses

Publication attached (Vet Radiol Ultrasound 2013;54:139-148)

VALIDATION OF DELAYED GADOLINIUM-ENHANCED MAGNETIC RESONANCE IMAGING OF CARTILAGE AND T2 MAPPING FOR QUANTIFYING DISTAL METACARPUS/METATARSUS CARTILAGE THICKNESS IN THOROUGHBRED RACEHORSES

ANN CARSTENS, ROBERT M. KIRBERGER, LEIF E. DAHLBERG, LEON PROZESKY, LIZELLE FLETCHER, EVELIINA LAMMENTAUSTA

The purpose of this study was to determine whether delayed gadolinium-enhanced magnetic resonance imaging of cartilage (dGEMRIC) and T2 mapping are accurate techniques for measuring cartilage thickness in the metacarpus3/metatarsus3 (Mc3/Mt3) of Thoroughbred racehorses. Twenty-four Mc3/Mt3 cadaver specimens were acquired from six healthy racehorses. Cartilage thickness was measured from postintra-articular Gd-DTPA^{2-} images acquired using short tau inversion recovery (STIR), and proton density weighted (PDw) sequences, and compared with cartilage thickness measured from corresponding histologic images. Two observers performed each histologic measurement twice at three different sites, with measurement times spaced at least 5 days apart. Histologic cartilage thickness was measured at each of the three sites from the articular surface to the bone–cartilage interface, and from the articular surface to the mineralized cartilage interface (tidemark). Intra-observer repeatability was good to moderate for dGEMRIC where Mc3/Mt3 cartilage was not in contact with the proximal phalanx. Where the Mc3/Mt3 cartilage was in contact with the proximal phalanx cartilage, dGEMRIC STIR and T2 mapping PDw cartilage thicknesses of Mc3/Mt3 could not be measured reliably. When measured from the articular surface to the bone–cartilage interface, histologic cartilage thickness did not differ from STIR or PDw cartilage thickness at the site where the Mc3/Mt3 cartilage surface was separated from the proximal phalanx cartilage ($P > 0.05$). Findings indicated that dGEMRIC STIR and T2 mapping PDw are accurate techniques for measuring Mc3/Mt3 cartilage thickness at locations where the cartilage is not in direct contact with the proximal phalanx cartilage. © 2012 *Veterinary Radiology & Ultrasound.*

Key words: cartilage, dGEMRIC, horse, MRI, T2 mapping, validation.

Introduction

LAMENESS IS THE PRIMARY cause of poor performance and wastage in horses.[1–6] This decrease in athletic ability has been estimated to cost the performance horse industry in North America an estimated $1 billion annually, with an incidence of 8.5% to 13.7%.[7] In studies performed at racetracks throughout the world, the most common source of lameness is the distal limb.[5,8–13] Twenty five percent of racing Thoroughbreds experience metacarpophalangeal and metatarsophalangeal joint pain,[5] with this joint being the most commonly affected by traumatic and degenerative lesions of the appendicular skeleton resulting in osteoarthritis.[6,10,14–16] Osteoarthritis is characterized by matrix fibrillation, the appearance of fissures, and ulceration and full-thickness loss of the cartilage.[17–20]

Magnetic resonance imaging, including the use of gadolinium (Gd-DTPA^{2-}) has been used in human studies to visualize osteoarthritis early in the disease process.[21–25] Parametric mapping of cartilage entails postprocessing of images to give relaxation time-associated color-maps that provide a visual interpretation of the specific area's relaxation times. This has been described in T2, T2*, and delayed gadolinium enhancement of MR in cartilage (dGEMRIC)) techniques.[26] T2 mapping is a noninvasive

From the Section of Diagnostic Imaging, Department of Companion Animal Clinical Studies (Carstens, Kirberger), and the Department of Pathology (Prozesky), Faculty of Veterinary Science, and the Department of Statistics (Fletcher), University of Pretoria, South Africa; the Joint and Soft Tissue Unit, Department of Clinical Sciences, Lund University, and Department of Orthopaedics, Malmö University Hospital, Malmö, Sweden (Dahlberg, Lammentausta); and Department of Diagnostic Radiology, the Oulu University Hospital, Oulu, Finland (Lammentausta).

Supported by the University of Pretoria Veterinary Faculty Research Fund, the Department of Companion Animal Clinical Studies, and a grant to Professor R.M. Kirberger from the National Research Foundation of South Africa.

Address correspondence and reprint requests to Ann Carstens, at the above address. E-mail: ann.carstens@up.ac.za

Received May 25, 2012; accepted for publication September 26, 2012.
doi: 10.1111/vru.12002

technique that can characterize hyaline articular cartilage and repair tissue.[27] In dGEMRIC, the negatively charged Gd-DTPA^{2-}, injected either intra-articularly or intravenously, penetrates hyaline cartilage in an inverse relationship to the proteoglycan concentration of the cartilage. When proteoglycan concentration is decreased due to cartilage degradation, as seen in osteoarthritis, the penetration of Gd-DTPA^{2-} is increased due to a relative decrease in negative charge of the proteoglycan-depleted cartilage. Delayed gadolinium enhanced MR in cartilage has been shown to be an excellent indicator of early degenerative cartilaginous changes in humans.[24] The MRI parameter maps for T2 and dGEMRIC can be made by freehand drawing of cartilage regions of interest (ROIs). Signal intensity can be then fitted pixel by pixel into mono-exponential relaxation equations using image analysis software (MATLAB Mathworks Inc., Natick, MA, USA). Results of these calculations yield a relaxation time value for each pixel. A mean of the relaxation time values for pixels within a ROI can be then used to characterize the cartilage within each ROI.

To ensure that the bone–cartilage interface and the cartilage surface of the dGEMRIC and T2-mapping sites are consistent with true anatomical areas, previous validation studies have compared MRI measurements to histological measurements as the gold standard. A study validating MRI imaging measurements of equine carpal cartilage thickness found a significant correlation between gradient echo and spoiled gradient echo, and spoiled gradient echo and histologic measurements.[28] The same study found that, when calcified cartilage was excluded from the histologic measurement, MRI measurements were significantly greater than histologic measurements.[28]

Another previous human study reported good repeatability for cartilage thickness measurements using a 7T scanner, with a coefficient of variation of 1.13%.[29] Good repeatability of MRI cartilage thickness measurements was also found in a study of asymptomatic human hip joints.[30] Inter-rater and intra-rater reliability of human cadaver femoral head cartilage thickness measurements from 3D-spoiled gradient echo pulse sequences have been found to be very high (<0.98)[31] and high-resolution MRI cartilage thickness evaluation was also found to have good correlation with direct imaging analysis of surgically removed cartilage.[32] For accurate determination of highly curved and thin articular cartilage volume and thickness three dimensionally, a 3D gradient echo sequence with selective water excitation acquisition can be used together with semi-automatic segmentation using a spline Snake algorithm.[33]

Previous studies have also validated MRI cartilage measurement techniques for assessing progression of osteoarthritis. In one previous study, MRI detected a 1–2% decrease in cartilage thickness annually in human patients with some identifiable risk factors.[24] Another study reported that MRI cartilage thickness and volume measurements decrease in patients with symptomatic knee osteoarthritis.[34] In an experimental study using a guinea pig meniscectomy model, MRI cartilage thickness measurement precision (repeatability) was good, with positive agreement and a significant partial correlation between measurements.[35] Cartilage thickness changes were also seen in serial MRI examinations of guinea pig stifle joints after meniscectomy.[36] Computer-aided methods for quantifying cartilage thickness and volume changes using MRI have also been validated.[37] In a computer-aided technique where measurements were tested and re-tested (paired imaging analysis), improved precision of cartilage segmentation for articular surfaces of the femur, tibia, and patella was found.[38] Using MRI-based 3D cartilage models, the thickness of cartilage was overestimated in regions where cartilage thickness was less than 2.5 mm and correctly predicted in regions where the cartilage was greater than 2.5 mm.[39]

In a study comparing a standard MRI knee protocol and T2 mapping, T2 mapping was found to be feasible in a clinical setting and also revealed cartilage lesions not visible with standard clinical MRI protocols.[40] Day-to-day repeatability of the dGEMRIC measurements has also been reported at different knee joint surfaces of healthy humans, and has been found to be good for small, deep, or superficial segments, for full thickness ROIs and for bulk ROIs.[41]

The purpose of the current study was to validate T2 mapping and dGEMRIC techniques for measuring cartilage thickness in Thoroughbred racehorses, using three selected sites of the distal Mc3/Mt3 condyle of normal Thoroughbred cadaver specimens. The first objective of the study was to determine intra- and inter-observer agreement for histomorphometrical measurements of cartilage thickness for the three sites, measured from the articular surface to the most superficial bone Haversian canals (bone–cartilage interface) and to the most superficial aspect of mineralized cartilage (tidemark (mineralized cartilage interface)). The second objective was to determine intra-observer agreement for measurements of cartilage thickness for the three sites and for two MRI techniques, the TI = 200 ms (hereafter referred to as the STIR) images during dGEMRIC-mapping and the TE = 16.7 ms (hereafter referred to as PDw (proton density weighted)) images during T2 mapping. The third objective was to compare histologic measurements of bone–cartilage interface and mineralized cartilage interface to cartilage surface with measurements of cartilage thickness from the STIR images in dGEMRIC mapping and the PDw images in T2 mapping. The last objective was to compare cartilage thickness measurements from the STIR images in dGEMRIC mapping to measurements from the PDw images in T2 mapping.

Materials and Methods

This was a prospective cross-sectional study using 24 cadaver limbs of six clinically sound Thoroughbred horses. The project (V067/10) was approved by the Animal Use and Care Committee of the Faculty of Veterinary Science University of Pretoria and all horses were treated according to South African Veterinary Council ethical standards. Inclusion criteria were that the horses were to be Thoroughbreds aged between 3 and 6 years, of any gender, with no pain on flexion of the metacarpophalangeal or metatarsophalangeal joints and no signs of lameness at a walk or trot. There had to be no clinically apparent signs of marked appendicular skeletal abnormalities and no history of corticosteroid or glycosaminoglycan treatments in the past week. The horses were obtained from a welfare horse care organization where racing Thoroughbreds are sent for adoption or euthanasia.

The horses were shot intracranially and the limbs removed at the middiaphyses of the third metacarpal or metatarsal bones. The limbs were wrapped in cling plastic, identified, placed in a cool bag, and transported to an MRI facility (Pretoria MR Trust, Faerie Glen Branch, Pretoria, South Africa) with a Siemens Avanto 1.5 T MRI machine with A B17 Software upgrade (Siemens Healthcare, Erlangen, Germany). The scanning took place with the limbs at room temperature (20°C) approximately 6 h post-euthanasia. A vitamin E oil capsule was taped to the lateral aspect of every Mc3/Mt3 specimen. The limbs were placed on the scanner table with the dorsal surface facing down and with the toe facing into the gantry. A head and neck 12-channel receiver coil combination was used. The forelimbs were randomly selected and scanned, followed by those of the randomly selected hind limbs. A leapfrog time schedule was used to ensure optimal time use, with the four metacarpo-/metatarsophalangeal joints' scans finishing approximately 8 h after commencement of the scans. The T1-weighted images were acquired using turbo spin-echo sequences in the sagittal plane with TR: 557 ms; TE: 23 ms; FOV: 100 × 100; matrix: 256 × 256; and receiver bandwidth: 130 Hz/pix. The T2-mapping images were acquired using multi-slice multi-echo spin-echo sequences with TR: 2170 ms; six TEs at between 16.7 and 116.9 ms; FOV: 140 × 140; matrix: 256 × 256; slice thickness: 3 mm; and kHz receiver bandwidth: 130 Hz/pix. A 17-line software template was used on a transverse localizer of the distal Mc3/Mt3 to identify the midlateral Mt3 condyle and the midmedial Mc3 condyle (Fig. 1A).

To acquire the parasagittal images for dGEMRIC T1 relaxation time calculation, six precontrast inversion recovery sequences were performed on the mid lateral condyle for the hindlimb and the midmedial condyle for the forelimb, respectively. As much synovial fluid as possible was aspirated from the palmar/plantar recess of the metacarpo-/metatarsophalangeal joints to minimize dilution of the Gd-DTPA^{2-} and minimize fluid-related sources of variability. Gadolinium-DTPA^{2-} (Magnevist®, gadopentetate dimeglumine, Bayer Health Care

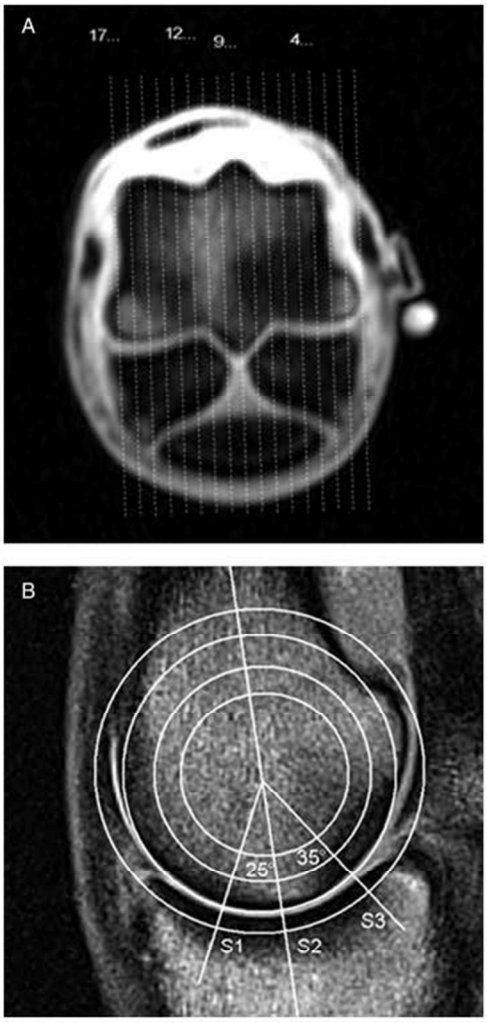

FIG. 1. (A) Transverse pilot MRI image of the distal third metatarsal bone of a normal Thoroughbred horse, demonstrating how MRI slices were marked for histologic comparisons. A 17-line template has been placed on the slice and centered over the distal sagittal ridge. Slice 1 is positioned on the lateral epicondyle cortex and slice 17 is positioned slightly axial to the medial epicondyle cortex. A hyperintense vitamin E oil capsule has been used as a marker for the lateral metatarso-phalangeal joint surface. (B) Lateral midcondylar parasagittal PDw (of T2 mapping) MRI image with a representation of the translucent template illustrating concentric circles placed using a "best-of-fit" method over the third metacarpal condyle and with a line transecting the midline of the Mc3 distal metaphysis. Sites 1–3 are also identified (S = site).

Pharmaceuticals, Isando, Gauteng, South Africa) was injected at 0.05 ml in 5 ml saline (0.025 mmol/joint). The joints were manually flexed at approximately one flexion per second for 5 min to ensure adequate contrast distribution in all parts of the joint. The same six inversion recovery T1 sequences as those used for precontrast images were repeated at 30, 60, 120, and 180 min postinjection and at the same midcondylar areas. The joint fluid was examined cytologically the following day and the balance aliquoted and frozen at −80° for later further analysis. Three distal articulation sites of Mc3/Mt3 were identified for histological and MRI measurements. Site 1 was defined based on a 25° dorsal angle and from a point in the center of the rotation of the joint. Site 2 was defined as the distal aspect of a line drawn down the axis of the diaphysis of Mc3/Mt3 and corresponding to the transverse ridge. Site 3 was defined based on a 35° palmar/plantar angle from a point in the center of the rotation of the joint and using the sagittal template of slices 5 and 13 (Fig. 1B). The palmar site location was chosen based on the site where cartilage injury has been previously reported, most often in conjunction with subchondral sclerosis and signs of fatigue condylar fractures.[42,43] The locations of sites 1–3 were chosen to be the same as sites previously evaluated by researchers studying stages of condylar fatigue fractures.[42]

The metacarpo-/metatarsophalangeal joints were radiographed and scanned with computed tomography and limbs discarded from this study if there were overt signs of pathology, such as osteochondritis dissecans or osteoarthritis changes with osteophytes larger than 2 × 2 mm. Metacarpus 3 and Mt3 were dissected loose from the rest of the limb and the midmedial and midlateral condyles of Mc3 and Mt3, respectively, were identified using the transverse MRI template and sectioned into 3–5 mm thick slices using a band saw. The dorsal and medial aspects of each bone section were marked and the sample was placed into an 8% nitric acid made up in 10% buffered formalin solution for fixation and decalcification. The solution was replaced every week to optimize demineralization until the bone floated in the solution. Sites 1, 2, and 3 were identified using the sagittal template of the midmedial and midlateral distal condyles of Mc3 and Mt3, respectively, the cut blocks processed, embedded into paraffin wax, sectioned on a rotary microtome and stained using standard Hematoxylin and Eosin. Sections were then mounted with Entellan (Merck Chemicals, Darmstadt, Germany).

For cartilage thickness measurement analysis, the stained sections were viewed with a Nikon (Centurion, South Africa) light microscope equipped with an Axio Cam camera (Axiovision VS40V4.8.1.0 Carl Zeiss Imaging Solutions GmbH). Two observers measured cartilage thickness from the articular surface to the first Haversian canal (bone–cartilage interface) and from the articular surface to the mineralized cartilage interface (tide mark) if visible (Fig. 2).

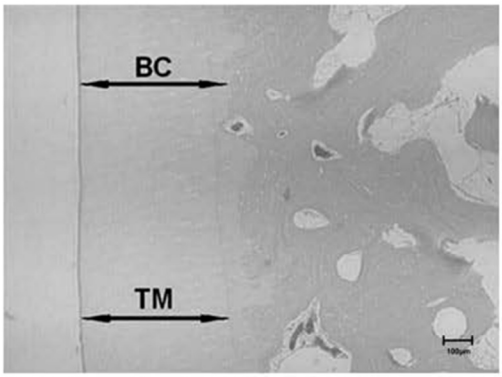

FIG. 2. Hematoxylin and eosin histology slide indicating how measurements were made for the distance between the articular surface and the beginning of the Haversion canal system (BC, bone–cartilage interface), and the distance between the articular surface and the beginning of the mineralized cartilage interface (TM, calcified cartilage tide mark).

Three measurements were made at each site and the mean determined. Each set of metacarpo-/metatarsophalangeal measurements was acquired at least 5 days apart.

To determine whether ROIs to be mapped on the T2- and dGEMRIC-mapped images were representative of true cartilage dimensions, the histomorphometric thicknesses of cartilage at sites 1–3 were compared to measurements from MRI images[28] Cartilage thickness was measured using a Siemens SYNGO workstation (Siemens Healthcare, Erlangen, Germany). The optimal inversion recovery sequence for visualizing the surface of the cartilage was determined subjectively by the first author and based on an evaluation of all 600 inversion recovery series of the dGEMRIC mapping images (four limbs × five times (pre-Gd, 30, 90, 120, 180 min) × five sites (the extra two were not used in this study) × six different TIs = 600) of a randomly picked horse's distal Mc3/Mt3 (Horse 6). Each image was zoomed and panned into an optimal position where a translucent template (Fig. 1B) could determine the midline of the relevant condyle of Mc3/Mt3 and the center of rotation of distal Mc3/Mt3. The optimal window was found using the windowing tool in the software package and the sites determined where the cartilage surface and bone–cartilage interface could best be identified. The mineralized cartilage interface could not be visualized so no attempt was made to measure this. Based on results of these assessments, the TI = 200 ms IR (STIR) in the 180-min post Gd-DTPA^{2-} time series was chosen as the best for measuring all horses' Mc3/Mt3 using the Syngo electronic callipers (Fig. 3A). A similar procedure was used for the T2-mapping TEs (using all 24 limbs × five sites × six TE = 720 sites) and the TE of 16.7 ms (PDw) was subjectively deemed the best image for visualizing the cartilage surface (Fig. 3B). The thickness of

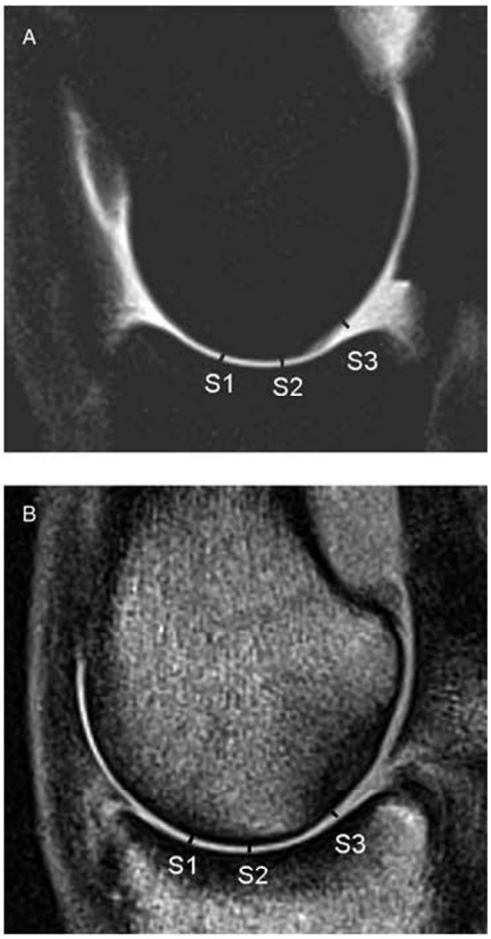

FIG. 3. (A) STIR image at 180 min post Gd-DTPA^{2-} demonstrating a parasagittal slice of the distal mid-Mt3 condyle for Horse 5 and locations where the hyperintense articular cartilage depth was measured at sites 1–3. Window width 1734; window level 964. (B) Proton density weighted image of the distal mid Mc3 condyle for Horse 4, demonstrating where the hyperintense articular cartilage depth was measured at sites 1–3. Window width 1445; window level 706. Note that since there is minimal synovial fluid within the joint and that this T2 image is prior to Gd injection. There is minimal fluid signal within the joint itself (S = site).

the articular cartilage was then measured for sites 1–3 for all the PDw and STIR images of all 24 limbs, respectively, three times and the mean determined for each site and MRI measurement. This measurement procedure was repeated at least 2 months later by the same observer. Histologic cartilage thicknesses were evaluated at Sites 1–3 by the same observer at least 3 months after the MRI measurements.

Statistical analyses were performed using SPSS software (version 19, SPSS Inc., Chicago, IL, USA). The selection and conduction of all statistical tests were made in collaboration with statisticians. The level of significance for all tests was set at $P < 0.05$. Repeatability for cartilage thickness measurements was determined using the intraclass correlation coefficient (ICC), which represents the error-free proportion of the intersubject score variation with a 95% confidence interval (CI). The ICC values above 0.75 were classified as good, values between 0.74 and 0.40 as moderate and values below 0.40 were deemed to have poor reliability[44] with a negative ICC also indicating low true intraclass correlation.[45]

Differences between cartilage thickness measurements were tested using Wilcoxon signed rank tests, performed post hoc. Forelimb and hindlimb cartilage thickness values (mm) recorded from histologic bone–cartilage interface, histologic mineralized cartilage interface, STIR and PDw were compared for sites 1, 2, and 3 separately as well as sites 1–3 combined using Wilcoxon signed rank tests.

Results

Twenty limbs met the inclusion criteria and four limbs were excluded, two for osteoarthritis, one for synovitis, and the other for an osseous cyst-like lesion. T2-mapping data was lost in Horse 1 right and left hindlimbs, and Horse 2's right hindlimb due to technical errors; therefore, 17 limbs were available for T2-mapping ROI tracing.

Means, standard deviations and intra and interobserver ICCs of cartilage thickness at sites 1–3 for bone–cartilage interface and mineralized cartilage interface, and combined sites 1–3, respectively, are summarized in Table 1. For histomorphometric cartilage thickness using the bone–cartilage interface, intraobserver repeatability for Observer A was good, with the least repeatable results at site 2 (ICC 0.80) and the most repeatable results at site 1 (0.97). Intraobserver repeatability for Observer B was good to moderate, with the most repeatable results at site 3 (0.85) and less repeatable results for site 2 (0.61). Repeatability based on means of Observer A1 and Observer A2 measurements and means of Observer B1 and Observer B2 measurements was good ($\geq$ 0.89) for sites 1 and 3 and sites 1–3, and moderate (0.66) for site 2.

For histomorphometric cartilage thickness using the mineralized cartilage interface, intraobserver repeatability for Observer A was good at sites 1 and 3, with least repeatability for site 2 (0.66) and most repeatability for site 1 (0.91). Observer B measurements were moderately repeatable for sites 1 and 2, but poorly repeatable for site 3 (0.10). The repeatability between means of Observer A1 and Observer A2 measurements, versus means of Observer B1 and Observer B2 measurements, was moderate for sites 1, 2, and 3, respectively, and poor for sites 1–3.

TABLE 1. Mean and Standard Deviation values for Histological Cartilage Thickness of Distal Metacarpal 3/Metatarsal 3 at Sites 1–3, Measured at Least 5 Days Apart by Observers A and B

	BC mm (SD)								
	Observer A				Observer B				
Site	1	2	ICC 1 vs. 2	Mean 1 and 2	1	2	ICC 1 vs. 2	Mean 1 and 2	ICC BC means of A1 and 2 vs. B1 and 2
1	0.87 (0.11)	0.88 (0.10)	0.97	0.87 (0.10)	0.88 (0.10)	0.86 (0.07)	0.67	0.87 (0.07)	0.89
2	0.98 (0.08)	1.00 (0.67)	0.80	0.99 (0.07)	0.99 (0.06)	1.02 (0.15)	0.61	1.00 (0.1)	0.66
3	0.79 (0.14)	0.77 (0.10)	0.87	0.79 (0.11)	0.77 (0.08)	0.74 (0.12)	0.85	0.76 (0.09)	0.95
1–3	0.88 (0.08)	0.89 (0.06)	0.89	0.88 (0.07)	0.88 (0.05)	0.87 (0.07)	0.61	0.88 (0.05)	0.92
	TM (SD)								
	Observer A				Observer B				
Site	1	2	ICC 1 vs. 2	Mean 1 and 2	1	2	ICC 1 vs. 2	Mean 1 and 2	ICC means of A (1 and 2) vs. B (1 and 2)
1	0.64 (0.1)	0.63 (0.09)	0.91	0.64 (0.09)	0.62 (0.10)	0.60 (0.08)	0.54	0.61 (0.07)	0.73
2	0.77 (0.09)	0.75 (0.09)	0.66	0.76 (0.07)	0.73 (0.08)	0.73 (0.24)	0.55	0.73 (0.14)	0.66
3	0.62 (0.12)	0.59 (0.06)	0.82	0.61 (0.09)	0.59 (0.05)	0.54 (0.11)	0.10	0.57 (0.06)	0.5
1–3	0.67 (0.07)	0.66 (0.05)	0.76	0.67 (0.05)	0.64 (0.05)	0.63 (0.08)	−0.21	0.63 (0.04)	0.37

BC: measurement from the articular surface to the beginning of the Haversian canals; TM: measurement from the articular surface to the beginning of the mineralized cartilage (tide mark); ICC = intraclass correlation coefficient; SD = standard deviation, mm = millimeters, Mc3 = metacarpal 3, Mt3 = metatarsal 3.

Means, standard deviations and intraobserver ICCs of cartilages thicknesses at sites 1–3, separately, and 1–3 combined, for the STIR images at 180-min post Gd-DTPA^{2-} and the PDw images are summarized in Table 2. For the STIR cartilage thickness measurements, Observer A showed good repeatability for site 3 (0.79), moderate repeatability for site 2 (0.58), and poor repeatability for Site 1 (0.11). For the PDw cartilage thickness measurements, Observer A showed good repeatability for site 1 (0.77), moderate repeatability for site 3 (0.69), and poor repeatability for site 2 (0.31).

Table 3 summarizes the Wilcoxon signed rank test results for cartilage thickness differences among histologic bone–cartilage interface, histologic mineralized cartilage interface, STIR, and PDw at sites 1–3 (separately and combined); and between STIR and PDw images at sites 1–3 (separately and combined). Histologic cartilage thickness measured using the bone–cartilage interface differed significantly from STIR and PDw measurements at sites 1 and 2 and at sites 1–3 combined, but not at site 3 ($P < 0.05$). Histologic cartilage thickness measured using the mineralized cartilage interface differed significantly from STIR and PDw measurements at site 2 and differed from PDw at site 3 and sites 1–3 combined ($P < 0.05$). Histologic cartilage thickness measured using the mineralized cartilage interface differed moderately from STIR cartilage thickness at sites 1 and 3 ($P = 0.063$).[46] Cartilage thickness from PDw did not significantly differ from STIR cartilage thickness

TABLE 2. Mean and Standard Deviation Values for Cartilage Thickness of Distal Metacarpal 3/Metatarsal 3, at Sites 1–3, Measured using a STIR Sequence at 180 min post Gd-DTPA^{2-} and a Proton Density weighted T2 Mapping Sequence, Repeated at Least 5 days Apart by Observer A

	STIR (SD) mm				PDw (SD) mm			
Site	1	2	ICC 1 vs. 2	Mean 1 and 2	1	2	ICC 1 vs. 2	Mean 1 and 2
1	0.56 (0.06)	0.53 (0.02)	0.11	0.54 (0.04)	0.54 (0.08)	0.56 (0.07)	0.77	0.55 (0.07)
2	0.51 (0.07)	0.54 (0.07)	0.58	0.52 (0.06)	0.44 (0.05)	0.51 (0.06)	0.31	0.47 (0.05)
3	0.87 (0.13)	0.80 (0.15)	0.79	0.84 (0.13)	0.77 (0.1)	0.86 (0.13)	0.69	0.81 (0.11)
1–3	0.65 (0.07)	0.62 (0.07)	0.48	0.63 (0.06)	0.71 (0.05)	0.74 (0.05)	0.47	0.72 (0.04)

STIR = short tau inversion recovery; PDw = proton density weighted; ICC = intraclass correlation coefficient; SD = standard deviation, mm = millimeters, Mc3 = metacarpal 3, Mt3 = metatarsal 3.

TABLE 3. Mean, Standard Deviation Values and Wilcoxon Signed Rank Evaluation of Mean Measurements of Cartilage Thickness of Distal Metacarpal 3/Metatarsal 3 Measured by Observer A, at Sites 1–3 using MRI and Histologic Techniques

	Histomorphometric (SD)				Wilcoxon signed rank test	
Site	BC mm	TM mm	STIR (SD) mm	PDw (SD) mm	Technique comparison	*P*
1	0.87 (0.10)	0.64 (0.09)	0.54 (0.04)	0.55 (0.07)	BC vs. STIR	0.031*
					BC vs. PDw	0.031*
					TM vs. STIR	0.063
					TM vs. PDw	0.063
					PDw vs STIR	0.563
2	0.99 (0.07)	0.76 (0.07)	0.52 (0.06)	0.47 (0.05)	BC vs. STIR	0.031*
					BC vs. PDw	0.031*
					TM vs. STIR	0.031*
					TM vs. PDw	0.031*
					PDw vs. STIR	0.688
3	0.79 (0.11)	0.61 (0.09)	0.84 (0.13)	0.81 (0.11)	BC vs. STIR	0.69
					BC vs. PDw	0.563
					TM vs. STIR	0.063
					TM vs. PDw	0.031*
					PDw vs. STIR	0.688
1–3	0.88 (0.07)	0.67 (0.05)	0.63 (0.06)	0.61 (0.04)	BC vs. STIR	0.031*
					BC vs. PDw	0.031*
					TM vs. STIR	0.688
					TM vs. PDw	0.031*
					PDw vs. STIR	0.563

STIR (short tau inversion recovery) = IR measured on TI = 200 msec at 180 min post Gd-DTPA^{2-} sequence; PDw (proton density weighted) = a T2-mapping sequence at TE = 16.7 ms; Wilcoxon signed rank test (two-tailed). Significant differences at $P < 0.05$ are marked with*. BC = articular surface to bone–cartilage interface; TM = articular surface to beginning of mineralized cartilage; SD = standard deviation, mm = millimeters, Mc3 = metacarpal 3, Mt3 = metatarsal 3.

at any sites. No differences were found between forelimb and hindlimb cartilage thickness values for all measurement methods; sites 1, 2, and 3 separately; and sites 1–3 combined using Wilcoxon signed rank tests and $P < 0.05$.

Discussion

The most important finding in this study was that the histological bone interface cartilage thickness and the STIR and PDw cartilage thicknesses of Mc3/Mt3 did not differ significantly when the distal Mc3/Mt3 was not in contact with the proximal phalanx, validating the STIR and PDw measurements for later studies using these sequences and particularly dGEMRIC and T2 mapping of articular cartilage of the distal Mc3/Mt3. It has previously been reported that cartilage thickness for dorsal and palmar sites of distal Mc3 in racehorses is approximately 0.79 ± 0.16 mm when measured histologically, and 0.90 ± 0.17 mm when measured using fat-suppressed spoiled gradient-recalled images.[47] The current study's mean histological cartilage thickness measurement was slightly higher, which could be a result of individual observer technique, e.g. Observer A and B's measurements did differ significantly at some sites. Overestimation of cartilage thickness when the actual thickness is less than 1 mm thick has been observed with MRI-based 3D cartilage models.[48] This is similar to findings in the current study where the STIR and PDw bone–cartilage interface measurements were larger than the histomorphometric dimensions at site 3 where the cartilage surface could be seen and less at sites 1 and 2 where the cartilage made contact with phalanx 1. For sites 1 and 2, when windowing the STIR and PDw images to attempt to identify the articular cartilage surface, partial volume averaging of the thin intra-articular space (often on the 1-pixel threshold) tended to determine the boundary between the articular surfaces of distal Mc3/Mt3 and proximal phalanx to be half way between them, resulting in a halving of the measured distance. In a previous human knee cartilage report, the weightbearing and central areas on each femoral and tibial condyle yielded more accurate measurements than boundary and nonweightbearing regions based on sagittal plane MR imaging.[8] However, the normal human knee cartilage is 1.3 to 2.5 mm thick vs. the approximately 1 mm thickness of the distal Mc3/Mt3 horse cartilage. Human knee cartilage also has a meniscus that is not present in the equine metacarpo/metatarsophalangeal joint, therefore similar comparisons with the equine Mc3/Mt3 joint cannot be made.[49] The use of traction to separate the two cartilage surfaces and better evaluate them has been described in human knees[50] and should therefore be considered in the future when evaluating the metacarpo/metatarsophalangeal cartilages using dGEMRIC and T2 mapping in the horse and in the clinical setting.

Histomorphometrically, the bone–cartilage interface measurements of cartilage thickness were consistently higher than the mineralized cartilage interface measurements. This finding was expected, since the tideline of

calcified cartilage is found in the articular cartilage between the Haversian canals and the cartilage surface. The amount of mineralized cartilage interface measurements that could be made with confidence were less than the bone–cartilage interface measurements, because the border of the mineralized cartilage could not be clearly ascertained in several of the slides.

Mineralized cartilage interface cartilage thicknesses were consistently found to be higher than STIR and PDw measurements at sites 1 and 2, but lower at site 3, likely for the same reason as for the bone–cartilage interface measurements. These findings support previously reported findings where MRI measurements of equine carpal cartilage were significantly greater than the histologic measurements.[28]

The subjective choice of STIR and PDw sequences as being the best for visualizing cartilage in the current study was supported by the fact that TI = 200 ms is quite close to STIR imaging at 1.5T (where TI = 150 ms), which means that the fat signal of the image is close to zero, and cartilage with relatively high water content can be well differentiated from its surroundings. For T2, the image with the shortest TE has the best signal-to-noise ratio and least T2 weighting, therefore closer to a proton density weighting, which yields a good contrast between cartilage and surrounding tissues. One possible limitation of the study was that only one horse's limb was used to determine the selection of these sequences. However, a very rigorous review process was followed for all the limbs to ensure the cartilage examined was as normal as possible. Also, the MRI properties of fat and water were expected to be constant and behave similarly when using a constant set of imaging parameters at a constant field strength.

It was encouraging that findings from the current study indicated that intraobserver repeatability of MRI measurements was good to moderate where cartilage was not in contact with other cartilage. This finding was similar to previously published findings.[29–31] One limitation of the current study was that no interobserver comparisons were made. However, previous studies have found good interobserver repeatability for MRI measurements.

Another limitation of the current study was that histomorphometric measurements were not measured at more sites away from adjacent cartilage. Histomorphometric cartilage thickness measurements of the dorsal and palmar aspects of distal Mc3 have not been found to differ in previous studies.[47] Therefore, it is reasonable to assume that measurements from these sites would be relatively similar to site 3's measurements.

If a higher field strength magnet had been used, higher resolution images could have resulted in superior cartilage thickness measurements as has been reported in a human study comparing 3T with 1.5T images. However, even in that study, correlation coefficients for values obtained at 3T and 1.5T were high.[51] Using thinner slices for MRI scans was considered for the current study, but this would have resulted in a lower signal-to-noise ratio and would have been more time consuming. The effect of slice thickness on assessment of human knee cartilage volume has been previously reported and findings indicated that there was little difference in human tibial cartilage volume as slice thickness increased from 1.5 to 7.5 mm.[52] Conclusions from the previous study were that increasing slice thicknesses could be used and that this would result in decreased acquisition and postprocessing times. However, since human knee cartilage thickness is much greater than that of the equine fetlock, this extrapolation may not be valid in equine fetlock joints. Cartilage curvature is another important factor to consider. If cartilage is very thin but not curved in the region being evaluated, thicker slices will also give reliable results. The small sites evaluated in the distal Mc3/Mt3 had very little curvature. Another limitation to this study was the relatively low number of horses and limbs used, decreasing the power of the findings.

In spite of these limitations, bone–cartilage interface histomorphometric cartilage thickness measurements did not differ from MRI measurements using a selected inversion recovery sequence for dGEMRIC mapping, and a selected time to echo image for T2 mapping in the palmaro/plantarodistal aspect of the distal Mc3/Mt3. This finding validates the use of dGEMRIC and T2 mapping for measuring cartilage thickness in locations where cartilage is not in close approximation to opposing adjacent cartilage in Mc3/Mt3 of Thoroughbred horses. Future studies are needed to evaluate these dGEMRIC and T2-mapping techniques in live horses with and without joint disease.

ACKNOWLEDGMENTS

The authors thank the Pretoria MR Trust for the use of the MRI machine and their radiographers who helped so ably; also the radiographers of the Onderstepoort Veterinary Academic Hospital, the entire staff of the Highveld Horsecare Unit, Meyerton, South Africa and Mrs Joyce Jordaan, data analyst from the Department of Statistics, University of Pretoria, South Africa.

REFERENCES

1. Dyson PK, Jackson BF, Pfeiffer DU, Price JS. Days lost from training by two- and three-year-old Thoroughbred horses: a survey of seven UK training yards. Equine Vet J 2008;40:650–657.

2. Perkins NR, Reid SW, Morris RS. Profiling the New Zealand Thoroughbred racing industry. 2. conditions interfering with training and racing. N Z Vet J 2005;53:69–76.

3. Parente EJ, Russau AL, Birks EK. Effects of mild forelimb lameness on exercise performance. Equine Vet J Suppl 2002;34:252–256.

4. Hernandez J, Hawkins DL. Training failure among yearling horses. Am J Vet Res 2001;62:1418–1422.

5. Bailey CJ, Reid SW, Hodgson DR, Bourke JM, Rose RJ. Flat, hurdle and steeple racing: risk factors for musculoskeletal injury. Equine Vet J 1998;30:498–503.

6. Olivier A, Nurton JP, Guthrie AJ. An epizoological study of wastage in Thoroughbred racehorses in Gauteng, South Africa. J S Afr Vet Assoc 1997;68:125–129.

7. A comparison of the economic costs of equine lameness, colic, and equine protozoal myeloencephalitis (EPM) in the United States. Animal and Plant Health Inspection service. 2001. Available at http://www.aphis.usda.gov/animal_health/nahms/equine/downloads/equine98/Equine98_is_EconCost.pdf (accessed May 2011).

8. Broster CE, Burn CC, Barr AR, Whay HR. The range and prevalence of pathological abnormalities associated with lameness in working horses from developing countries. Equine Vet J 2009;41:474–481.

9. de Grauw JC, van de Lest CH, van Weeren R, Brommer H, Brama PA. Arthrogenic lameness of the fetlock: synovial fluid markers of inflammation and cartilage turnover in relation to clinical joint pain. Equine Vet J 2006;38:305–311.

10. Wilsher S, Allen WR, Wood JL. Factors associated with failure of thoroughbred horses to train and race. Equine Vet J 2006;38:113–118.

11. Dabareiner RM, Cohen ND, Carter GK, Nunn S, Moyer W. Musculoskeletal problems associated with lameness and poor performance among horses used for barrel racing: 118 cases (2000–2003). J Am Vet Med Assoc 2005;227:1646–1650.

12. Rossdale PD, Hopes R, Digby NJ, Offord K. Epidemiological study of wastage among racehorses 1982 and 1983. Vet Rec 1985;116:66–69.

13. Bailey CJ, Reid SW, Hodgson DR, Rose RJ. Impact of injuries and disease on a cohort of two- and three-year-old Thoroughbreds in training. Vet Rec 1999;145:487–493.

14. Brommer H, van Weeren PR, Brama PA, Barneveld A. Quantification and age-related distribution of articular cartilage degeneration in the equine fetlock joint. Equine Vet J 2003;35:697–201.

15. Pool RR. Pathologic manifestations of joint disease in the athletic horse. In: McIlwraith CW, Trotter GW (eds): Joint disease in the horse. Philadelphia: W. B. Saunders Co., 1996;87–104.

16. McIlwraith CW. General pathology of the joint and response to injury. In: McIlwraith CW, Trotter GW (eds): Joint disease in the horse. Philadelphia: WB Saunders Co., 2006;40–70.

17. Martel-Pelletier J. Pathophysiology of osteoarthritis. Osteoarthr Cartilage 2004;12(Suppl A):S31–S33.

18. Pearle AD, Warren RF, Rodeo SA. Basic science of articular cartilage and osteoarthritis. Clin Sports Med 2005;24:1–12.

19. Rannou F, Sellam J, Berenbaum F. Pathophysiology of osteoarthritis: updated concepts. Presse Med 2010;39:1159–1163.

20. Goldring MB, Goldring SR. Osteoarthritis. J Cell Physiol 2007;213:626–634.

21. Gold GE, Burstein D, Dardzinski B, Lang P, Boada F, Mosher T. MRI of articular cartilage in OA: novel pulse sequences and compositional/functional markers. Osteoarthr Cartilage 2006;14(Suppl A):A76–A86.

22. Guermazi A, Burstein D, Conaghan P, et al. Imaging in osteoarthritis. Rheum Dis Clin North Am 2008;34:645–687.

23. Trattnig S, Domayer S, Welsch GW, Mosher T, Eckstein F. MR imaging of cartilage and its repair in the knee -a review. Eur Radiol 2009;19:1582–1594.

24. Roemer FW, Eckstein F, Guermazi A. Magnetic resonance imaging-based semiquantitative and quantitative assessment in osteoarthritis. Rheum Dis Clin North Am 2009;35:521–555.

25. Potter HG, Black BR, Chong le R. New techniques in articular cartilage imaging. Clin Sports Med 2009;28:77–94.

26. Domayer SE, Welsch GH, Dorotka R, et al. MRI monitoring of cartilage repair in the knee: a review. Semin Musculoskelet Radiol 2008;12:302–317.

27. Goodwin DW. Visualization of the macroscopic structure of hyaline cartilage with MR imaging. Semin Musculoskelet Radiol 2001;5:305–312.

28. Murray RC, Branch MV, Tranquille C, Woods S. Validation of magnetic resonance imaging for measurement of equine articular cartilage and subchondral bone thickness. Am J Vet Res 2005;66:1999–2005.

29. Zuo J, Bolbos R, Hammond K, Li X, Majumdar S. Reproducibility of the quantitative assessment of cartilage morphology and trabecular bone structure with magnetic resonance imaging at 7 T. Magn Reson Imaging 2008;26:560–566.

30. Naish JH, Xanthopoulos E, Hutchinson CE, Waterton JC, Taylor CJ. MR measurement of articular cartilage thickness distribution in the hip. Osteoarthr Cartilage 2006;14:967–973.

31. McGibbon CA. Inter-rater and intra-rater reliability of subchondral bone and cartilage thickness measurement from MRI. Magn Reson Imaging 2003;21:707–714.

32. Graichen H, von Eisenhart-Rothe R, Vogl T, Englmeier KH, Eckstein F. Quantitative assessment of cartilage status in osteoarthritis by quantitative magnetic resonance imaging: technical validation for use in analysis of cartilage volume and further morphologic parameters. Arthritis Rheum 2004;50:811–816.

33. Graichen H, Jakob J, von Eisenhart-Rothe R, Englmeier KH, Reiser M, Eckstein F. Validation of cartilage volume and thickness measurements in the human shoulder with quantitative magnetic resonance imaging. Osteoarthr Cartilage 2003;11:475–482.

34. Raynauld JP, Martel-Pelletier J, Abram F, et al. Analysis of the precision and sensitivity to change of different approaches to assess cartilage loss by quantitative MRI in a longitudinal multicenter clinical trial in patients with knee osteoarthritis. Arthritis Res Ther 2008;10:R129, doi:10.1186/ar2543.

35. Bolbos R, Benoit-Cattin H, Langlois JB, et al. Measurement of knee cartilage thickness using MRI: a reproducibility study in a meniscectomized guinea pig model of osteoarthritis. NMR Biomed 2008;21:366–375.

36. Bolbos R, Benoit-Cattin H, Langlois JB, et al. Knee cartilage thickness measurements using MRI: a 4(1/2)-month longitudinal study in the meniscectomized guinea pig model of OA. Osteoarthr Cartilage 2007;15:656–665.

37. Kauffmann C, Gravel P, Godbout B, et al. Computer-aided method for quantification of cartilage thickness and volume changes using MRI: validation study using a synthetic model. IEEE Trans Biomed Eng 2003;50:978–988.

38. Brem MH, Lang PK, Neumann G, et al. Magnetic resonance image segmentation using semi-automated software for quantification of knee articular cartilage-initial evaluation of a technique for paired scans. Skeletal Radiol 2009;38:505–511.

39. Koo S, Giori NJ, Gold GE, Dyrby CO, Andriacchi TP. Accuracy of 3D cartilage models generated from MR images is dependent on cartilage thickness: laser scanner based validation of in vivo cartilage. J Biomech Eng 2009;131:121004, doi:10.1115/1.4000087.

40. Hannila I, Nieminen MT, Rauvala E, Tervonen O, Ojala R. Patellar cartilage lesions: comparison of magnetic resonance imaging and T2 relaxation-time mapping. Acta Radiol 2007;48:444–448.

41. Multanen J, Rauvala E, Lammentausta E, et al. Reproducibility of imaging human knee cartilage by delayed gadolinium-enhanced MRI of cartilage (dGEMRIC) at 1.5 Tesla. Osteoarthr Cartilage 2009;17:559–564.

42. Firth EC, Doube M, Boyde A. Changes in mineralised tissue at the site of origin of condylar fracture are present before athletic training in Thoroughbred horses. NZ Vet J 2009;57:278–283.

43. O'Brien T, Baker TA, Brounts SH, et al. Detection of articular pathology of the distal aspect of the third metacarpal bone in Thoroughbred racehorses: comparison of radiography, computed tomography and magnetic resonance imaging. Vet Surg 2011;40:942–951.

44. Bland JM, Altman DG. Measurement error and correlation coefficients. BMJ 1996;313:41–42.

45. Taylor PJ. An introduction to intraclass correlation that resolves some common confusions. 2011 Available at http://faculty.umb.edu/pjt/9b.pdf (accessed July 21, 2011).

46. Albright SC, Winston WL, Zappe CJ. Statistical inference. In: Albright SC, Winston WL, Zappe CJ (eds): Data analysis and decision making, 4th ed. Australia: South-Western Cengage Learning, 2010;503.

47. Olive J, D'Anjou MA, Girard C, Laverty S, Theoret C. Fat-suppressed spoiled gradient-recalled imaging of equine metacarpophalangeal articular cartilage. Vet Radiol Ultrasound 2010;51:107–115.

48. Koo S, Gold GE, Andriacchi TP. Considerations in measuring cartilage thickness using MRI: factors influencing reproducibility and accuracy. Osteoarthr Cartilage 2005;13:782–789.

49. Eckstein F, Reiser M, Englmeier KH, Putz R. In vivo morphometry and functional analysis of human articular cartilage with quantitative

magnetic resonance imaging-from image to data, from data to theory. Anat Embryol 2001;203:147–173.

50. Nakanishi K, Tanaka H, Nishii T, Masuhara K, Narumi Y, Nakamura H. MR evaluation of the articular cartilage of the femoral head during traction. Correlation with resected femoral head. Acta Radiol 1999;40:60–63.

51. Eckstein F, Charles HC, Buck RJ, et al. Accuracy and precision of quantitative assessment of cartilage morphology by magnetic resonance imaging at 3.0T. Arthritis Rheum 2005;52:3132–3136.

52. Cicuttini F, Morris KF, Glisson M, Wluka AE. Slice thickness in the assessment of medial and lateral tibial cartilage volume and accuracy for the measurement of change in a longitudinal study. J Rheumatol 2004;31:2444–2448.

Article 2 Feasibility for mapping cartilage T1-relaxation times in the distal metacarpus3/metatarsus3 of Thoroughbred racehorses using delayed gadolinium enhanced magnetic resonance imaging of cartilage (dGEMRIC): normal cadaver study.

Publication attached (Vet Radiol Ultrasound 2013;DOI:10.111/vru.12030)

FEASIBILITY FOR MAPPING CARTILAGE T1 RELAXATION TIMES IN THE DISTAL METACARPUS3/METATARSUS3 OF THOROUGHBRED RACEHORSES USING DELAYED GADOLINIUM-ENHANCED MAGNETIC RESONANCE IMAGING OF CARTILAGE (DGEMRIC): NORMAL CADAVER STUDY

ANN CARSTENS, ROBERT M. KIRBERGER, MARK VELLEMAN, LEIF E. DAHLBERG, LIZELLE FLETCHER, EVELIINA LAMMENTAUSTA

Osteoarthritis of the metacarpo/metatarsophalangeal joints is one of the major causes of poor performance in horses. Delayed gadolinium-enhanced magnetic resonance imaging of cartilage (dGEMRIC) may be a useful technique for noninvasively quantifying articular cartilage damage in horses. The purpose of this study was to describe dGEMRIC characteristics of the distal metacarpus3/metatarsus3 (Mc3/Mt3) articular cartilage in 20 cadaver specimens collected from normal Thoroughbred horses. For each specimen, T1 relaxation time was measured from scans acquired precontrast and at 30, 60, 120, and 180 min post intraarticular injection of Gd-DTPA^{2-} (dGEMRIC series). For each scan, T1 relaxation times were calculated using five regions of interest (sites 1–5) in the cartilage. For all sites, a significant decrease in T1 relaxation times occurred between precontrast scans and 30, 60, 120, and 180 min scans of the dGEMRIC series ($P < 0.0001$). A significant increase in T1 relaxation times occurred between 60 and 180 min and between 120 and 180 min post Gd injection for all sites. For sites 1–4, a significant increase in T1 relaxation time occurred between 30 and 180 min postinjection ($P < 0.05$). Sites 1–5 differed significantly among one another for all times ($P < 0.0001$). Findings from this cadaver study indicated that dGEMRIC using intraarticular Gd-DTPA^{2-} is a feasible technique for measuring and mapping changes in T1 relaxation times in equine metacarpo/metatarsophalangeal joint cartilage. Optimal times for postcontrast scans were 60–120 min. Future studies are needed to determine whether these findings are reproducible in live horses. © 2013 *Veterinary Radiology & Ultrasound.*

Key words: Cartilage, dGEMRIC, horse, metacarpus, metatarsus, MRI, T1 mapping

Introduction

LAMENESS IN HORSES is the primary cause of poor performance and wastage.[1–3] Costs to the horse industry in North America were an estimated $1 billion in 1998.[4] The fetlock (metacarpo/metatarsophalangeal) joint is commonly affected by trauma, degeneration,[5] and osteoarthritis.[6] Lesions often involve both lateral and medial condyles of distal metacarpus3/metatarsus3.[7,8] Osteoarthritis is defined as degeneration of articular cartilage and is characterized by matrix fibrillation, fissures, ulceration, and full-thickness loss of cartilage.[9] Diagnosis of osteoarthritis in the metacarpo/metatarsophalangeal joints of horses is based on clinical evaluation, perineural or intraarticular nerve blocks, and combinations of radiography, ultrasonography, computed tomography, scintigraphy, and magnetic resonance imaging (MRI). Many of these modalities detect disease only after the degenerative process has become advanced.[10,11]

From the Section Diagnostic Imaging, Department of Companion Animal Clinical Studies, Faculty of Veterinary Science, University of Pretoria, Private Bag X04 Onderstepoort 0110 (Carstens, Kirberger), Pretoria South Africa; Little Company of Mary Hospital, George Storrar Ave. (Velleman), Pretoria South Africa; Joint and Soft Tissue Unit, Department of Clinical Sciences, Malmö, Lund University, Department of Orthopaedics, Malmö University Hospital, SE-205 02 (Dahlberg, Lammentausta), Malmö Sweden; Department of Statistics, University of Pretoria (Fletcher), Pretoria South Africa; Department of Diagnostic Radiology, Oulu University Hospital, POB 50, FI-90029 OYS (Lammentausta), Oulu, Finland.

Portions of this study were presented at the European Association Veterinary Diagnostic Imaging Congress, London, UK, 1–3 September, 2011.

This manuscript represents a portion of a thesis to be submitted by Prof. Carstens to the Department of Companion Animal Clinical Studies, Faculty of Veterinary Science, University of Pretoria, South Africa, as partial fulfillment of the requirements for a Ph.D. degree.

Supported by University of Pretoria Veterinary Faculty Research Fund, the Department of Companion Animal Clinical Studies, and a grant to Prof. R. M. Kirberger from the National Research Foundation of South Africa.

Address correspondence and reprint requests to Ann Carstens, at the above address. E-mail: ann.carstens@up.ac.za

Received May 29, 2012; accepted for publication February 8, 2013.
doi: 10.1111/vru.12030

Magnetic resonance imaging has been previously established as a method for visualizing early articular cartilage pathology in human studies.[12,13] In delayed gadolinium-enhanced MRI of cartilage (dGEMRIC), negatively charged Gd-DTPA^{2-} is injected either intraarticularly or intravenously. The contrast agent penetrates hyaline cartilage and distributes in an inverse relationship to the proteoglycan content of the cartilage. When the proteoglycan concentration is decreased as a result of cartilage degradation, as seen in osteoarthritis, the gadolinium uptake is increased as result of the relative decrease in negative charge of the proteoglycan-depleted cartilage. This dGEMRIC technique has been described as an excellent indicator of degenerative cartilaginous changes and has been found to correlate with mechanical properties of cartilage such as cartilage stiffness.[14,15] Parametric mapping of cartilage can be accomplished by postprocessing dGEMRIC images and creating relaxation time color maps. These maps provide a visual representation of relaxation times within specific cartilage locations.

The use of dGEMRIC has been reported once in a group of ponies, where it was used to test effects of administered bone morphogenic protein in experimentally created femoral condyle lesions.[16] The adjacent noninjured cartilage had significantly lower dGEMRIC T1 relaxation times than lesion repair tissue at 12 weeks post lesion creation. At 52 weeks, dGEMRIC T1 relaxation times were lower in both the lesion and the adjacent cartilage. Authors proposed that these findings could have been due to early osteoarthritis or because the bone morphogenic protein caused cartilage degeneration. Other proposed theories were that changes were caused by immobilization and unloading of the cartilage because of pain. Other experimental animal studies and dGEMRIC studies have found that unloaded cartilage has a lower dGEMRIC T1 relaxation time after compression.[17]

The purposes of the current study were to determine the feasibility of dGEMRIC mapping in the metacarpo/metatarsophalangeal joint of horses and optimal imaging times post intraarticular administration of Gd-DTPA^{2-} into the same joint. Our hypothesis was that T1 relaxation times for five sites within the articular cartilage of distal metacarpus3/metatarsus3 would decrease after intraarticular injection of Gd-DTPA^{2-}.

Methods

This project was approved by the Animal Use and Care Committee of the Faculty of Veterinary Science University of Pretoria and all horses were treated according to South African Veterinary Council ethical standards. Six Thoroughbred horses were prospectively recruited from the Highveld Horsecare Unit, Meyerton, South Africa. Study inclusion criteria were as follows: age 3–6 years, any gender, no signs of lameness, and no history of recent corticosteroid or proteoglycan treatments. Horses meeting inclusion criteria underwent a clinical examination to confirm absence of lameness. Immediately following the examination, horses were shot intracranially and all four limbs were removed at the mid metacarpus3/metatarsus3 diaphyses. Limbs were kept cool and transported to an MRI facility. A vitamin E oil capsule was taped to the lateral aspect of each metacarpo/metatarsophalangeal joint and each limb was positioned with the dorsum facing downward and the toe facing into the gantry. A head and neck 12-channel radiofrequency coil was used. The forelimbs were first scanned in random order using a 1.5 Tesla MRI scanner (Avanto, Siemens Healthcare, Erlangen, Germany). The hindlimbs were then scanned in random order using the same scanner. All limbs were scanned at room temperature (20°C). For each joint, T1 weighted images were acquired in the sagittal plane (TR 557 ms, TE 23 ms, field of view 100 × 100 mm, matrix 256 × 256, slice thickness 3 mm, receiver bandwidth 130 Hz/pixel). Seventeen slices were acquired with the central slice positioned in the middle of the distal metacarpus3/metatarsus3 sagittal ridge (Fig. 1A).

For each lateral and medial midcondylar slice, precontrast T1 relaxation time was measured using single slice inversion recovery spin echo sequences (TR 3000 ms, TE 13 ms, six TIs between 100 and 2800 ms, field of view 140 × 140 mm, matrix 256 × 256 mm, slice thickness 3 mm, receiver bandwidth 130 Hz/pixel). Subsequently, joint fluid was aspirated from each joint and Gd-DTPA^{2-} (Magnevist®, gadopentetate dimeglumine, Bayer Health Care Pharmaceuticals, Bayer Pty. Ltd., Isando, South Africa) was injected using a dose of 0.05 ml in 5 ml saline (0.025 mmol/joint). Joints were manually flexed at one flexion per second for 5 min. Using the same midcondylar slice locations as those used for the precontrast scans, T1 relaxation time measurements were repeated at 30, 60, 120, and 180 min postinjection. Following MRI examinations, joints were evaluated using radiography and computed tomography. Joints with gross abnormalities were excluded from further analyses.

Five sites were analyzed for each midcondylar slice and each scan. Site 1 was defined using a 25° dorsal angle from a point in the center of the rotation of the joint. Site 2 was defined as the distal aspect of a line drawn down the axis of the diaphysis of metacarpus3/metatarsus3 and corresponding to the transverse ridge. Site 3 was defined using a 35° palmar/plantar angle from a point in the center of the rotation of the joint. Sites 4 and 5 were defined as the most palmar/planter and dorsal locations where metacarpus3 and metatarsus3 cartilage could be clearly distinguished from adjacent first phalanx cartilage (Fig. 1B). Often site 3 was partially or totally included within site 4. Immediately following imaging, each metacarpus3 and metatarsus3 bone was dissected away from the rest of the limb and the

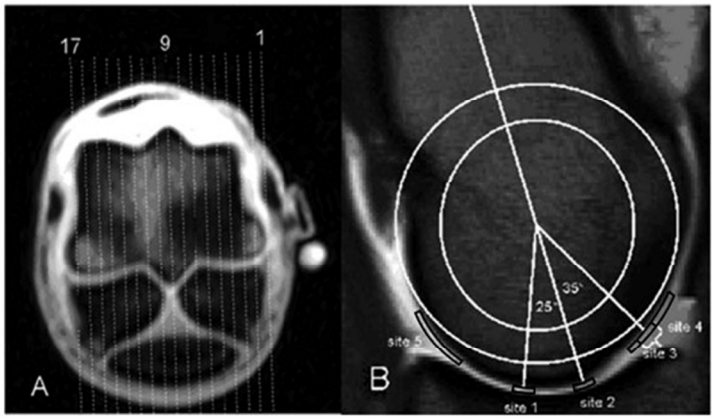

FIG. 1. (A) Transverse magnetic resonance imaging (MRI) image of a distal Mt3 with a 17 line template with the central slice 9 placed sagitally over the distal sagittal ridge, slice 1 positioned on the lateral, and slice 17 positioned slightly beyond the medial epicondyle cortices. Note the hyperintense vitamin E oil capsule on the lateral epicondylar surface. (B) Parasagittal midcondylar MRI image of distal Mc3/Mt3 with representation of the translucent template illustrating concentric circles placed "best-of-fit" over the condyle with a line transecting the midline of Mc3/Mt3 diaphysis/distal metaphysis. Region-of-interest sites are outlined. Sites 1–3 are identified. Site 4 is where cartilage is clearly defined at the edges of palmar/plantar articulations and site 5 is where cartilage is clearly defined at the edges of dorsal articulations.

distal condylar cartilage surface was evaluated macroscopically before and after 3- to 5-min staining with India ink (Parker Quink Ink, Claremont, South Africa). All cartilage and synovial tissues were examined, and gross abnormalities recorded. The cartilage was also graded using the Neundorf grading system.[18] Only joints with Grade 1 cartilage were used for further analyses. Grade1 was defined using the following criteria: no gross abnormalities, minimal loss of reflectance, minimal cartilage hypertrophy at the joint margins, minimal partial thickness wear lines, minimal thinning of cartilage, minimal thickening of cartilage, and no enlarged synovial fossae. Midportions of the medial and lateral condyles of metacarpus3 and metatarsus3 were sectioned into 3- to 5-mm-thick slices in a sagittal plane. The samples were fixed and decalcified in an 8% nitric acid made up in 10% buffered formalin solution. Sites 1, 2, and 3 were identified using a sagittal template of the corresponding lateral and medial condyles (Fig. 1B). Each cut block was processed and stained using standard hematoxylin and eosin. The cartilage at sites 1–3 for each midcondylar slice was evaluated for pathology using a modification of an Osteoarthritis Research Society International (OARSI) microscopic cartilage grading system.[19] Only cartilage with a grade less than 2 was used for further analyses.

dGEMRIC Data Analysis

Full-thickness regions of interest (ROIs) were placed on sites 1–3 by one of the authors (A.C.) Each ROI extended 3° on either side of the template lines. Each ROI was manually positioned between the cartilage bone interface and the articular surface at site 3. The ROIs for sites 1 and 2 were positioned adjacent to the bone–cartilage interface of phalanx 1 since the cartilage surface could not be positively identified in most of the limbs at these sites. Larger ROIs were segmented at sites 4 and 5 from the bone–cartilage interface to the articular surface of metacarpus3/metatarsus3, which was clearly visible at these sites (Fig. 1B). T1 maps were created by fitting the respective data into mono-exponential relaxation equations using an in-house matrix laboratory application (MATLAB, MathWorks Inc., Natick, MA). Mean values for each ROI were calculated.

Statistical Analysis

All statistical tests were selected and performed by a statistician. Nonparametric Friedman tests (SAS. Version 9.2, 2011, SAS Institute, Cary, NC) were used to compare T1 relaxation times for pooled limbs across the five time periods. For comparisons with significant differences from these tests, Wilcoxon signed rank tests were performed post hoc. The level of significance for all tests was defined as $P < 0.05$. An effect size (r) was calculated for significant results. A small effect was defined as $0.1 < r < 0.3$; medium effect $0.3 < r < 0.5$; and large effect $r \geq 0.5$.

Results

Of the 24 limbs collected, 20 met all inclusion criteria and 4 were excluded. Two were excluded for osteoarthritis, one for an osseous cyst-like lesion and one for synovitis. It

took 12 min per limb to acquire the six inversion recovery images required for T1 mapping analyses.

Figure 2 demonstrates a representative set of color maps at sites 1–5 prior to injection of Gd-DTPA^{2-} and at 30, 60, 120, and 180 min postinjection. A higher relaxation time range was set for the precontrast series (0–2000 ms) than the postcontrast series (0–1300 ms). Table 1 summarizes T1 relaxation times measured at each time interval for all five cartilage sites and results of the Friedman tests. The T1 relaxation times measured at the five sites are graphically displayed in Fig. 3. A significant decrease in T1 relaxation time occurred at sites 1–5 between precontrast and 30, 60, 120, and 180 min dGEMRIC series ($P \leq 0.0001$; Friedman ANOVA). All sites had a significant increase in T1 relaxation time between 60 and 180 min, and between 120 and 180 min postcontrast. For sites 1–4, a significant increase in T1 relaxation time occurred between 30 and 180 min postinjection (Table 2). For all sites, the effect size was large between precontrast and all dGEMRIC series (between $r = 0.5$ and $r = 0.88$). For sites 1, 3, and 4, the effect size was large between 60 and 180 min, and between 120 and 180 min ($r = 0.52$ and $r = 0.73$). For site 2, the effect size was medium between 60 and 180 min ($r = 0.47$). Results of Wilcoxon signed rank test comparisons among sites and time periods are summarized in Table 3.

Table 4 summarizes means and standard deviations of T1 relaxation times for the combined sites 1–5 for the different limbs as well as for the combined sites for all four limbs. The T1 relaxation times differed between the time periods for the left forelimb, right hind limb, and left hind limb (P-values < 0.05; Friedman test). Differences were not significant in the right forelimb ($P = 0.06$).[20]

Discussion

We chose 3- to 6-year-old Thoroughbred horses for our study because horses in this age group are used for active flat-racing and are most likely to have some degree of mild osteoarthritis in their metacarpo/metatarsophalangeal joints. The modified Neundorf and OARSI scoring systems used a set of parameters that was easy to evaluate and should be repeatable within and among observers for future studies.[18,19] We excluded limbs from our study if gross abnormalities were present, or if there was minimal macroscopic (Grade 1) or microscopic (<Grade 2) cartilage damage at sites 1–3 of the condyles.

Regions of interest for T1 relaxation time measurements were constrained by the resolution of the 1.5 Tesla MRI scanner used in our study. The dGEMRIC measuring technique on distal horse metacarpus3/metatarsus3 cartilage has previously been validated by comparing histologic cartilage thickness measurements at site 3 with a single STIR sequence used in the dGEMRIC mapping technique,[21] as was done between MRI and histological measurements of horse carpal articular cartilage using a 1.5 T machine.[22] Distal metacarpus3 and metatarsus3 cartilage in normal horses is approximately 1 mm thick (0.90 ± 0.17 mm).[23] Since the cartilage of distal metacarpus3/metatarsus3 (Mc3/Mt3) at sites 1 and 2 could not be differentiated from the cartilage of the adjacent P1, the ROIs drawn were a combination of the two adjacent cartilages and the thin layer of synovial fluid between them. Combined analysis of articulating surfaces has been previously described as an acceptable method for dGEMRIC analysis of joints with thin cartilage, such as the human hip.[24] In future clinical dGEMRIC studies of horse joints with thin cartilage, this combined articular dGEMRIC ROI technique may also be helpful for scans acquired using relatively low field MRI machines.[24]

Both the lateral and medial condyles of metacarpus3/metatarsus3 are prone to palmar/plantar osteochondral disease.[8] As the joint is extended, the dorsal and palmar/plantar surfaces of the condyle become increasingly compressed.[25] With further acceleration, stress to the palmar/plantar surface of the metacarpal/metatarsal condyle can be more than twice that applied to the dorsal surface. These findings support the theory that biomechanics may play an important role in osteoarthritis pathogenesis.[26]

The 12 min needed to acquire the six inversion recovery images for T1 mapping was a relatively long period of time. In the clinical situation, a horse would be anesthetized and would have to be repositioned to ensure all limbs were placed within the iso-center of the gantry. However, repositioning times could be reduced by simultaneously imaging both forelimbs or both hind limbs, even though they would not then be within the iso-center of the gantry. Three-dimensional techniques are available that will shorten acquisition time even further, although these will unlikely be available for dedicated equine scanners in the near future.

The pattern of decreasing T1 relaxation times we observed over 120 min in our horse cadaver specimens was similar to that previously reported in human studies, where dGEMRIC series were acquired between 30 and 100 min.[27] Human cadaver results have been found to be similar to live patient results for dGEMRIC.[28] We assume that the same would apply in horses. A previous study in normal dog elbows found a mean T1 dGEMRIC value of 400 ± 47 ms at 30 min post intravenous injection of gadopentate dimeglumine, as opposed to the current study's post intraarticular injection mean value at site 3 of 682.7 ± 44 for the same time period.[29] This discrepancy could be due to the method of administering the contrast, cartilage thickness differences, or other inherent cartilage differences between the two species and joints.

Significant differences in T1 relaxation times between most of the precontrast sites were likely because of inherent

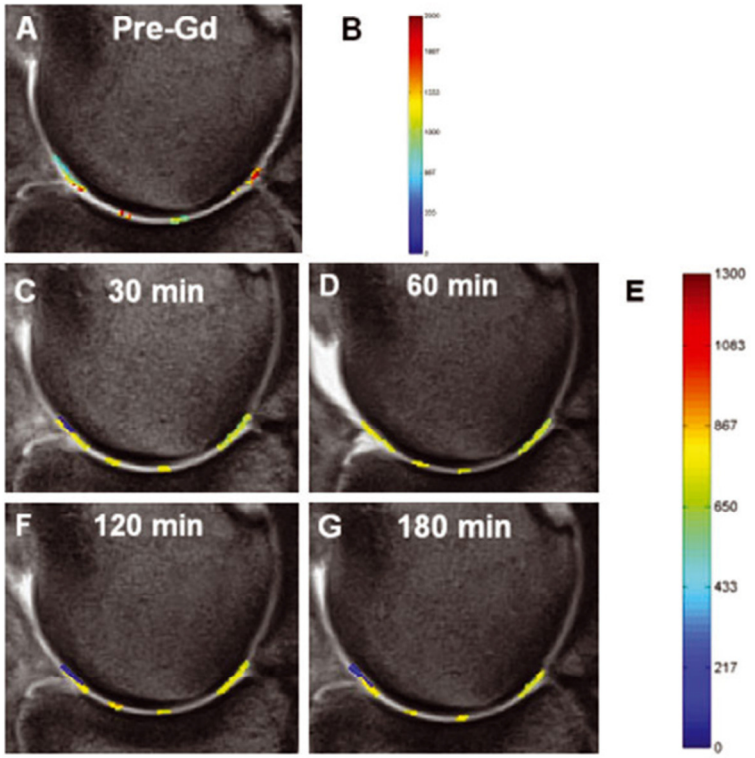

FIG. 2. Delayed gadolinium-enhanced magnetic resonance imaging of cartilage (dGEMRIC) maps of the mid medial condyle of the right forelimb of Horse 2, illustrating the color-coded relaxation times (in ms) for each of the regions of interest measured over times pre- and post-Gd-DTPA^{2-} intraarticular administration. Sites 3 and 4 overlap in this figure. (B) and (E) are the color keys for pre-Gd (A) and post Gd (C, D, F, G), respectively.

TABLE 1. Mean (and standard deviation) Delayed Gadolinium Enhanced Magnetic Resonance Imaging of Cartilage (dGEMRIC) T1-Relaxation Times (in ms) of the Distal Metacarpus3/Metatarsus3 Cartilage (sites 3–5) and Metacarpus3/Metatarsus3–Proximal Phalanx Combined Cartilage (sites 1–2) per Site and Time period

	Site 1		Site 2		Site 3		Site 4		Site 5		
Min	Mean	SD	Mean	SD	Mean	SD	Mean	SD	Mean	SD	Among sites
Pre	1012.1	233.9	855.0	154.6	1370.7	264.8	1474.1	111.7	990.5	265.9	$P < 0.0001$
30	701.3	143.7	667.9	191.7	682.7	44.0	662.1	72.6	685.9	179.8	$P < 0.0001$
60	674.3	156.8	668.7	209.1	673.6	115.2	667.4	140.3	642.3	191.8	$P = 0.006$
120	670.6	201.4	668.0	205.2	652.3	144.5	661.3	147.8	646.3	209.6	$P < 0.0001$
180	700.7	199.9	725.8	229.9	685.6	213.9	683.0	209.0	630.7	213.3	$P < 0.0001$
	$P < 0.0001$*		$P = 0.0001$*		$P = 0.0001$*		$P = 0.0001$*		$P = 0.0001$*		

*Significant differences at the 5% level. (P values - Friedman's ANOVA).
min, minutes; Pre, pre-Gd-DTPA^{2-} injection; SD, standard deviation.

differences in cartilage substrate, as has been previously seen in the human knee.[30] Differences in cartilage substrate could occur as an adaptation to the varying forces applied. There are more viable chondrocytes in palmar condyle cartilage than dorsal condyle cartilage in the equine fetlock and this finding has been correlated with proteoglycan content.[31,32] The number of sites with significant differences between them decreased to a minimum at 60 and 120 min post-Gd-DTPA^{2-} injection and then increased again at 180 min postinjection. This finding could have occurred because the gadolinium that was incorporated into the cartilage resulted in a more homogenous T1 relaxation

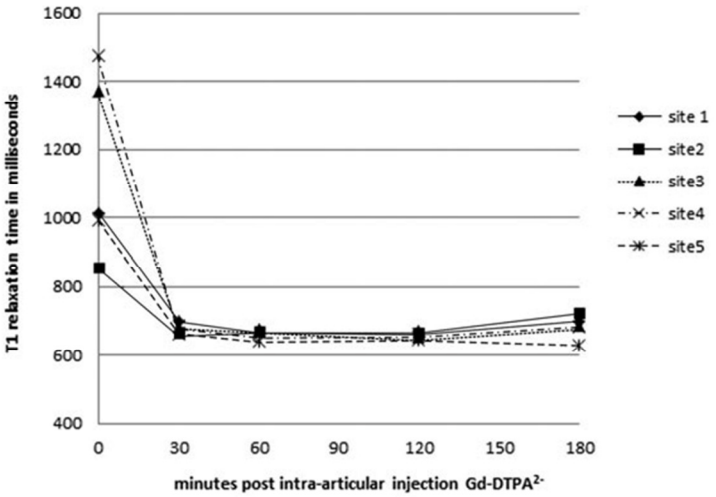

FIG. 3. Mean of T1 relaxation times of sites 1–5 of the cartilage of distal Mc3/Mt3 of 20 limbs of six horses. For standard deviations see Table 1.

TABLE 2. Wilcoxon Signed Rank Test Indicating Differences among T1- Delayed Gadolinium Enhanced Magnetic Resonance Imaging of Cartilage (dGEMRIC) Relaxation Times at Different Times Measured Pre- and Post Gd-DTPA^{2-} Administration

	Site 1	Site 2	Site 3	Site 4	Site 5
Pre vs. 30 (19)	$P < 0.0001^*$	$P < 0.0001^*$	$P < 0.0001^*$	$P < 0.0001^*$	$P < 0.0001^*$
Pre vs. 60 (20)	$P < 0.0001^*$	$P = 0.003^*$	$P < 0.0001^*$	$P < 0.0001^*$	$P < 0.0001^*$
Pre vs. 120 (18)	$P < 0.0001^*$	$P = 0.002^*$	$P < 0.0001^*$	$P < 0.0001^*$	$P < 0.0001^*$
Pre vs. 180 (19)	$P < 0.0001^*$	$P = 0.024^*$	$P < 0.0001^*$	$P < 0.0001^*$	$P < 0.0001^*$
30 vs. 60 (19)	$P = 0.798$	$P = 0.352$	$P = 0.104$	$P = 0.040^*$	$P = 0.096$
30 vs. 120 (17)	$P = 0.306$	$P = 0.243$	$P = 0.207$	$P = 0.040^*$	$P = 0.263$
30 vs. 180 (18)	$P = 0.043^*$	$P = 0.004^*$	$P = 0.018^*$	$P = 0.026^*$	$P = 0.182$
60 vs. 120 (18)	$P = 0.284$	$P = 0.702$	$P = 0.899$	$P = 0.865$	$P = 0.609$
60 vs. 180 (19)	$P = 0.006^*$	$P = 0.036^*$	$P = 0.021^*$	$P = 0.019^*$	$P = 0.898$
120 vs. 180 (17)	$P = 0.001^*$	$P = 0.014^*$	$P = 0.027^*$	$P = 0.021^*$	$P = 0.265$

*Significant differences at the 5% level.

time. Our study showed an increase in T1 relaxation time from 120 to 180 min in four of the five sites, indicating a wash-out from the cartilage. This finding was likely due to diffusion of the Gd-DTPA^{2-} from areas with high intraarticular and intracartilaginous concentration to areas with lower concentration.[29] This washout would likely occur even earlier in vivo, due to perfusion washout. Good correlation has been previously found between dGEMRIC in vivo and in vitro human studies after total knee replacement surgery.[28] It is likely that findings in this equine cadaver study will be similar to those in an equine in vivo study, but this would need to be confirmed. Previous studies have shown that dGEMRIC values are sensitive to mechanical cartilage stress.[34] Therefore, in the recumbent, non–weight-bearing joint, dGEMRIC values could differ from those of the weight-bearing cartilage, although the degree thereof is unknown. The dGEMRIC technique has been previously reported to have good day-to-day reproducibility in humans and is likely to be the same in the horse.[35]

The lack of a significant difference between T1 relaxation times of the right forelimb as opposed to significant differences among T1 relaxation times of the other limbs could be due to different loading and ambulating patterns of the right fore limb relative to the other limbs. This different loading could have an affect on the proteoglycan concentration of the cartilage. All these horses had recently come off the racetrack, where the inside limb would have been subjected to different forces compared to the outside limb.[36–38] This could have translated into different cartilage loading of distal metacarpus3/metatarsus3 in the right forelimb. However, this theory is only speculative and would require further investigation in a larger number of horses to confirm.

TABLE 3. Wilcoxon Signed Rank Test Indicating Differences between Delayed Gadolinium Enhanced Magnetic Resonance Imaging of Cartilage (dGEMRIC) T1- Relaxation Times at Different Sites 1–5

	Pre-Gd	30 min	60 min	120 min	180 min
S1 vs. S2	$P = 0.003^*$	$P = 0.738$	$P = 0.216$	$P = 1.000$	$P = 0.932$
S1 vs. S3	$P < 0.0001^*$	$P = 0.011^*$	$P = 0.154$	$P = 0.021^*$	$P = 0.007^*$
S1 vs. S4	$P < 0.0001^*$	$P = 0.008^*$	$P = 0.097$	$P = 0.130$	$P = 0.002^*$
S1 vs. S5	$P = 0.729$	$P = 0.441$	$P = 0.729$	$P = 0.702$	$P = 0.005^*$
S2 vs. S3	$P < 0.0001^*$	$P = 0.018^*$	$P = 0.123$	$P = 0.048^*$	$P = 0.001^*$
S2 vs. S4	$P < 0.0001^*$	$P = 0.018^*$	$P = 0.053$	$P = 0.142$	$P = 0.001^*$
S2 vs. S5	$P = 0.036^*$	$P = 0.275$	$P = 0.133$	$P = 0.212$	$P = 0.005^*$
S3 vs. S4	$P = 0.261$	$P = 0.016^*$	$P = 0.388$	$P = 1.000$	$P = 0.596$
S3 vs. S5	$P = 0.001^*$	$P = 0.020^*$	$P = 0.674$	$P = 0.246$	$P = 0.349$
S4 vs. S5	$P < 0.0001^*$	$P = 0.032^*$	$P = 0.475$	$P = 0.284$	$P = 0.388$

*Significant differences at the 5% level.
Pre, pre-Gd-DTPA^{2-} injection; S, site; min, minutes.

TABLE 4. Mean (and standard deviation) Delayed Gadolinium Enhanced Magnetic Resonance Imaging of Cartilage (dGEMRIC) T1-Relaxation times (in ms) of the Distal Metacarpus3/Metatarsus3 Cartilage (sites 3–5) and Metacarpus3/Metatarsus3–Proximal Phalanx Combined Cartilage (sites 1–2) per Limb and Time Period (min), also of all Limbs Tested Combined

Min	RF		LF		RH		LH		All limbs	
	Mean	SD	Mean	SD	Mean	SD	Mean	SD	Mean	SD
pre	1162.4	139.5	1162.8	98.9	1107.3	156.5	1118.3	161.6	1150.9	117.9
30	655.5	79.4	720.7	25.9	710.2	47.3	626.6	174.1	673.4	53.8
60	665.4	116.8	658.4	90.5	716.2	39.0	632.7	252.6	655. 4	76.8
120	626.0	204.5	727.8	18.7	712.0	40.1	564.4	275.9	647. 4	110.5
180	601.2	267.7	718.6	24.9	741.7	12.0	701.4	347.5	659.0	147. 8
	$P = 0.060$		$P = 0.004^*$		$P = 0.014^*$		$P = 0.035^*$		$P = 0.006^*$	

*Significant differences at the 5% level.
RF, right fore; LF, left fore; RH, right hind; LH, left hind; Pre, pre-Gd-DTPA^{2-} injection; Min, minutes.

Limitations of this study included the relatively poor spatial resolution of the thin distal metacarpus3/metatarsus3 cartilage, which could be improved in future studies with the use of a dedicated surface coil and decreased field of view. A higher field strength magnet would also improve resolution but since the highest field strength in general use currently is 1.5T, it is unlikely this adaptation will be in use soon. The setup used in the current study was chosen because it was realistic for in vivo studies and would allow a reasonable imaging time. The use of traction to separate the two cartilage surfaces could also be considered to improve visibility of articular margins.[39] The low number of limbs used in our study was also a limitation, although the nonparametric techniques used were able to detect significant differences. Another limitation was the lack of repeatability studies for intra- and interobserver evaluations. In spite of these limitations, results supported our hypothesis that T1 relaxation time in metacarpus3/metatarsus3 cartilage decreases significantly after Gd-DTPA^{2-} administration.

Future studies of the dGEMRIC technique in equine clinical patients will need to address the above-mentioned limitations. Standing MRI currently utilizes only low magnetic field strengths, for example, 0.27T, and the resolution may not be adequate for accurate dGEMRIC measurements of the thin cartilage in equine metacarpo/metatarsal joints. Before determining whether dGEMRIC could be applied in the clinical scenario, it should be also established that dGEMRIC can identify early cartilage degeneration in horses with varying degrees of osteoarthritis. Future research should address whether differences in T1 relaxation time post-Gd-DTPA^{2-} would be affected by the following factors: (1) chilling or freezing of cadaver limbs; (2) the administration route of Gd-DTPA^{2-}; (3) exercise or nonexercise post-Gd-DTPA^{2-} administration; or (4) the presence of osteoarthritis.

In conclusion, findings from this study indicated that dGEMRIC is a feasible technique for mapping cartilage T1 relaxation times in the equine distal metacarpus3/metatarsus3. Locations with thin cartilage in the fetlock joint may be measured using ROIs that combine analysis of adjacent articulating cartilages. For future studies, authors recommend that dGEMRIC scans in horse metacarpo/metatarsophalangeal joints be conducted 60–120 min post intraarticular Gd-DTPA^{2-} injection.

ACKNOWLEDGMENTS

The authors thank the Faerie Glen Hospital MR Trust for use of their MRI machine; A. Bester, A. Helberg, I. Martin, and S. Tarantino for MRI technical support; all the OVAH radiographers, and the staff of the Highveld Horse Care unit for radiographic technical support and case recruitment, respectively; and Mrs. J. C. Jordaan for statistical analysis.

REFERENCES

1. Dyson PK, Jackson BF, Pfeiffer DU, Price JS. Days lost from training by two- and three-year-old Thoroughbred horses: a survey of seven UK training yards. Equine Vet J 2008;40:650–657.

2. Perkins NR, Reid SW, Morris RS. Profiling the New Zealand Thoroughbred racing industry. 2. Conditions interfering with training and racing. NZ Vet J 2005;53:69–76.

3. Bailey CJ, Reid SW, Hodgson DR, Bourke JM, Rose RJ. Flat, hurdle and steeple racing: risk factors for musculoskeletal injury. Equine Vet J 1998;30:498–503.

4. A comparison of the economic cost of equine lameness, colic and equine protozoal myeloencephalitis (EPM) in the United States. Animal and Plant Health Inspection Services. 2001. Available at http://www.aphis.usda.gov/animal_health/nahms/equine/downloads/equine98/Equine98_is_EconCost.pdf (accessed May 2011).

5. Wilsher S, Allen WR, Wood JL. Factors associated with failure of Thoroughbred horses to train and race. Equine Vet J 2006;38:113–118.

6. McIlwraith CW. General pathology of the joint and response to injury. In: McIlwraith CW, Trotter GW (eds): Joint disease in the horse. Philadelphia: WB Saunders Co., 1996;40–70.

7. Smith KJ, Bertone AL, Weisbrode SE, Radmacher M. Gross, histologic, and gene expression characteristics of osteoarthritic articular cartilage of the metacarpal condyle of horses. Am J Vet Res 2006;67:1299–306 .

8. Barr ED, Pinchbeck GL, Clegg PD, Boyde A, Riggs CM. Post mortem evaluation of palmar osteochondral disease (traumatic osteochondrosis) of the metacarpo /metatarsophalangeal joint in Thoroughbred racehorses. Equine Vet J 2009;41:366–371.

9. Goldring MB, Goldring SR. Osteoarthritis. J Cell Physiol 2007;213:626–634.

10. Javaid MK, Lynch JA, Tolstykh I, , . Pre-radiographic MRI findings are associated with onset of knee symptoms: the most study. Osteoarthritis Cartilage 2010;18:323–328.

11. Butler JA, Colles CM, Dyson SJ, Kold S, Poulos P. General principles. In: Butler JA, Colles CM, Dyson SJ, Kold SE, Poulos PW (eds): Clinical radiology of the horse. Chichester, United Kingdom: Wiley-Blackwell, 2009;1–36.

12. Crema MD, Roemer FW, Marra MD, et al. Articular cartilage in the knee: current MR imaging techniques and applications in clinical practice and research. Radiographics 2011;31:37–61.

13. Roemer FW, Eckstein F, Guermazi A. Magnetic resonance imaging-based semiquantitative and quantitative assessment in osteoarthritis. Rheum Dis Clin North Am 2009;35:521–555.

14. Gray ML, Burstein D, Kim YJ, Maroudas A. 2007 Elizabeth Winston Lanier Award Winner. Magnetic resonance imaging of cartilage glycosaminoglycan: basic principles, imaging technique, and clinical applications. J Orthop Res 2008;26:281–291.

15. Baldassarri M, Goodwin JS, Farley ML, et al. Relationship between cartilage stiffness and dGEMRIC index: correlation and prediction. J Orthop Res 2007;25:904–912.

16. Menendez MI, Clark DJ, Carlton M, et al. Direct delayed human adenoviral BMP-2 or BMP-6 gene therapy for bone and cartilage regeneration in a pony osteochondral model. Osteoarthritis Cartilage 2011;19:1066–1075.

17. Mayerhoefer ME, Welsch GH, Mamisch TC, et al. The in vivo effects of unloading and compression on T1-gd (dGEMRIC) relaxation times in healthy articular knee cartilage at 3.0 Tesla. Eur Radiol 2010;20:443–449.

18. Neundorf RH, Lowerison MB, Cruz AM, Thomason JJ, McEwen BJ, Hurtig MB. Determination of the prevalence and severity of metacarpophalangeal joint osteoarthritis in Thoroughbred racehorses via quantitative macroscopic evaluation. Am J Vet Res 2010;71:1284–1293.

19. McIlwraith CW, Frisbie DD, Kawcak CE, Fuller CJ, Hurtig M, Cruz A. The OARSI histopathology initiative – recommendations for histological assessments of osteoarthritis in the horse. Osteoarthritis Cartilage 2010;18(Suppl 3):S93–S105.

20. Albright SC, Winston WL, Zappe CJ. Data analysis and decision making. Australia: South. Western/Cengage Learning, 2010;503.

21. Carstens A, Kirberger RM, Dahlberg LE, Prozesky L, Fletcher L, Lammentausta E. Validation of delayed gadolinium enhanced magnetic resonance imaging of cartilage and T2 mapping for quantifying distal metacarpus/metatarsus cartilage thickness in Thoroughbred racehorses. Vet Radiol Ultrasound 2013;54:139–148.

22. Murray RC, Branch MV, Tranquille C, Woods S. Validation of magnetic resonance imaging for measurement of equine articular cartilage and subchondral bone thickness. Am J Vet Res 2005;66:1999–2005.

23. Olive J, D'Anjou MA, Girard C, Laverty S, Theoret C. Fat-suppressed spoiled gradient-recalled imaging of equine metacarpophalangeal articular cartilage. Vet Radiol Ultrasound 2010;51:107–115.

24. Lattanzi R, Petchprapa C, Glaser C, et al. A new method to analyze dGEMRIC measurements in femoroacetabular impingement: preliminary validation against arthroscopic findings. Osteoarthritis Cartilage 2012;20:1127–1133.

25. Pool RR. Pathologic manifestations of joint disease in the athletic horse. In: McIlwraith CW, Trotter GW (eds): Joint disease in the horse. Philadelphia: W.B.Saunders Co., 1996;87–104.

26. Riggs CM, Whitehouse GH, Boyde A. Structural variation of the distal condyles of the third metacarpal and third metatarsal bones in the horse. Equine Vet J 1999;31:130–139.

27. Tiderius CJ, Jessel R, Kim YJ, Burstein D. Hip dGEMRIC in asymptomatic volunteers and patients with early osteoarthritis: the influence of timing after contrast injection. Magn Reson Med 2007;57:803–805.

28. Bashir A, Gray ML, Hartke J, Burstein D. Nondestructive imaging of human cartilage glycosaminoglycan concentration by MRI. Magn Reson Med 1999;41:857–865.

29. Wucherer KL, Ober CP, Conzemius MG. The use of delayed gadolinium enhanced magnetic resonance imaging of cartilage and T2 mapping to evaluate articular cartilage in the normal canine elbow. Vet Radiol Ultrasound 2012;53:57–63.

30. Krishnan N, Shetty SK, Williams A, Mikulis B, McKenzie C, Burstein D. Delayed gadolinium-enhanced magnetic resonance imaging of the meniscus: an index of meniscal tissue degeneration? Arthritis Rheum 2007;56:1507–1511.

31. Dykgraaf S, Firth EC, Rogers CW, Kawcak CE. Effects of exercise on chondrocyte viability and subchondral bone sclerosis in the distal third metacarpal and metatarsal bones of young horses. Equine Vet J 2008;178:53–61.

32. Rosenberg L. Chemical basis for the histological use of Safranin O in the study of articular cartilage. J Bone Joint Surg Am 1971;53:69–82.

33. Salo E-N, Nissi MJ, Kulmala KAM, Tiitu V, Töyräs J, Nieminen MT. Diffusion of Gd-DTPA^{2-} into articular cartilage. Osteoarthritis Cartilage 2012;20:117–126.

34. Tiderius CJ, Olsson LE, Leander P, Ekberg O, Dahlberg L. Delayed gadolinium-enhanced MRI of cartilage (dGEMRIC) in early knee osteoarthritis. Magn Reson Med 2003;49:488–492.

35. Multanen J, Rauvala E, Lammentausta E, et al. Reproducibility of imaging human knee cartilage by delayed gadolinium-enhanced MRI of cartilage (dGEMRIC) at 1.5 Tesla. Osteoarthritis Cartilage 2009;17:559–564

36. Beccati F, Pepe M, Di Meo A, Davanzo S, Moriconi F. Radiographic evaluation of changes in the proximal phalanx of Thoroughbreds in race training. Am J Vet Res 2011;72:1482–1488.

37. Firth EC, Rogers CW, Doube M, Jopson NB. Musculoskeletal responses of 2-year-old Thoroughbred horses to early training. 6. Bone parameters in the third metacarpal and third metatarsal bones. NZ Vet J 2005;53:101–112.

38. Davies HM, Merritt JS. Surface strains around the midshaft of the third metacarpal bone during turning. Eq Vet J 2004;36:689–692.

39. Nakanishi K, Tanaka H, Nishii T, Masuhara K, Narumi Y, Nakamura H. MR evaluation of the articular cartilage of the femoral head during traction: correlation with resected femoral head. Acta Radiol 1999;40:60–63.

Article 3 The effect of chilling and freezing on T2- mapping in the normal Thoroughbred horse cadaver distal metacarpus3/metatarsus3 cartilage.

(Submitted)

Article 4 The effect of chilling and freezing on dGEMRIC mapping in the normal Thoroughbred horse cadaver distal metacarpus3/metatarsus3 cartilage

(Submitted)